MASTER THESIS

Dynamic modelling of the physiology of breathing to improve mechanical ventilation

J. I. de Jong
s1727583

Faculty of Science and Technology
Biomedical Signals and Systems

EXAMINATION COMMITTEE
Prof.dr. L.M.A. Heunks
A. Jonkman, MSc.
Dr. E. Mos – Oppersma
Prof.dr.ir. P.H. Veltink

UNIVERSITY OF TWENTE.

Dynamic modelling of the physiology of breathing to improve mechanical ventilation

Date of publication: 05-07-2021
Author: J.I. de Jong
Student number: s1727583
Field of education: biomedical engineering
Examination committee: Prof.dr. L.M.A. Heunks, Drs. A. Jonkman, Dr. E. Mos – Oppersma, Prof.dr.ir. P.H. Veltink

Summary

Mechanical ventilation is the mainstay of supportive therapy in the intensive care unit for patients with respiratory failure. Although life-saving, mechanical ventilation may also cause secondary lung injury. Settings poorly adapted to the patient's physiology may result in poor outcome; however, finding the optimal settings for the individual patient is still an ongoing debate. As a result, the ventilation may not always be optimally adapted to the individual patient which may have negative effects on the patient's lungs and respiratory muscle function and may worsen clinical outcomes, including the increase of the duration of ventilation.

Our hypothesis was that a closed-loop mechanical ventilation system that is based on a model that considers a limited set of well-chosen aspects of the physiology of breathing may be able to improve these limitations. The aim of this thesis was to develop a simple but credible model that is aimed towards this objective. This model may be the initial step towards incorporating such a system in clinical practice and may provide a first insight in the clinical applicability in the context of the critically ill mechanically ventilated patient.

From the literature review and conversations with clinicians it resulted that a model of the gas exchange and the respiratory drive with low complexity could be of an improvement to current clinical practice by increasing the insight in the patient's respiratory parameters and variables and predicting patient responses to changes in ventilator settings.

A two-compartment model based on the gas exchange was developed of which the dynamical behaviour consists of a slow and a fast exponential component. The model reaches an equilibrium state that is dependent on the minute ventilation. For carbon dioxide, this behaviour complies with the behaviour found in an experimental study that was conducted in a healthy volunteer. Aggregated model parameter groups could be identified, and predictions could be made with the identified model that were qualitatively similar to the results of the experimental study. While the limited observability and resources limit the possibilities for extensive model validation, this gives an indication that the simple model may have the right structure to describe the gas exchange of carbon dioxide.

The developed model may be an addition to current clinical practice by improving the clinician's insight into the efficiency of the gas exchange of patients on mechanical ventilation. This may give the clinician an improved insight into the readiness of the patient for weaning and may make better-substantiated ventilator setting choices possible. Increased testing and experimental validation are required before clinical application is possible.

Table of contents

Glossary

name	definition
accessory muscles	The muscles that assist in breathing but do not play a primary role.
acute respiratory distress syndrome	A type of respiratory failure characterized by rapid onset of widespread inflammation in the lungs.
airway occlusion pressure	The pressure generated at the airways during a period of no airflow in the airways.
alveolar dead space	The sum of the volumes of the alveoli which have little or no blood flowing through their capillaries.
alveolar infiltration	A substance denser than air, e.g. blood or pus, which lingers within the lungs.
assisted ventilation	Mode of ventilation where the inspiratory efforts of the patient are detected and ventilatory assist is delivered accordingly.
blood gasses	Measurement of the concentration of pH, oxygen, carbon dioxide and several other components present in a sample of blood.
breathing effort	The energy-consuming activity of the respiratory muscles aimed at driving respiration.
controlled ventilation	A mode of ventilation in which the ventilator delivers the pre-set volume or pressure regardless of the patient's own inspiratory efforts.
dynamical analysis	An area of mathematics used to describe the behaviour of complex dynamical systems, usually through differential equations.
eigenvalue	A scalar that describes the relationship between the individual system state variables and their derivatives.
equilibrium state	The state of a system in which properties have constant values if external conditions are unchanged.
order of system	The number of independent energy storage elements in the system.
parameter identification	The determination of the most optimal combination of values of the model parameters.
patient-ventilator asynchrony	A mismatch between the patient’s respiratory system and the ventilator, regarding time, flow, volume, or pressure demands.
PEEP	The pressure in the lungs above atmospheric pressure at the end of expiration.
pulmonary fibrosis	A lung disease that occurs when lung tissue becomes scarred and damaged.
pulmonary shunt	The passage of venous blood through the lungs without participation in gas exchange.
respiratory mechanics	The mechanical properties of the pulmonary system; the airway pressures, airflow rate and lung volumes.
spontaneous breathing trial	A trial that assesses the patient's ability to breathe while receiving minimal or no ventilatory support.
time constant	the duration in seconds during which a variable rises of falls exponentially and becomes 63.2% of its final value.
observability	A measure of how well internal states of a system can be retrieved from measured outputs.
ventilation-perfusion mismatch	A condition in which one or more areas of the lung receive either no oxygenated air or no blood flow.
ventilator-induced lung injury	An acute lung injury that develops during mechanical ventilation.
weaning	The process of reducing ventilatory support, ultimately resulting in a patient breathing spontaneously and being disconnected from the ventilator.

1. Introduction

1.1. Background and research problem

It is probable that somewhere in the next decade patients and clinicians will arrive at the hospital in self-driving cars. This makes it hard to imagine that mechanical ventilation, which is the mainstay of supportive therapy in the intensive care unit for patients with respiratory failure, is still mainly manually operated. This clinician-in-the-loop system is labour-intensive and requires expert knowledge [1]. Settings poorly adapted to the patient's physiology may result in poor outcome; however, finding the optimal settings for the individual patient is still an ongoing debate. As a result, mechanical ventilation may not always be optimally adapted to the individual patient which may have negative effects on the patient's lungs and respiratory muscle function and may worsen clinical outcomes, including the increase of the duration of ventilation.

Closed-loop mechanical ventilation systems have been the subject of research for a long time. Closed-loop mechanical ventilation is in essence the automatic control of ventilator settings based on measured physiological variables. In figure 1 the workflow of simple closed-loop mechanical ventilation is presented schematically. In this example, the system has one physiological variable that is controlled. The clinician sets a desired value for this variable, and the variable is constantly measured with a sensor and compared to the desired value. The controller will determine the difference between the actual value and the desired value and give an appropriate adjustment of ventilator settings. This adjustment in ventilator settings should impose changes in patient ventilation that should bring the controlled physiological variable to the desired value. Since these desired values or target ranges of physiological variables depend on the initial parameters set by the clinician, it is of utmost important that these are programmed correctly for the individual patient.

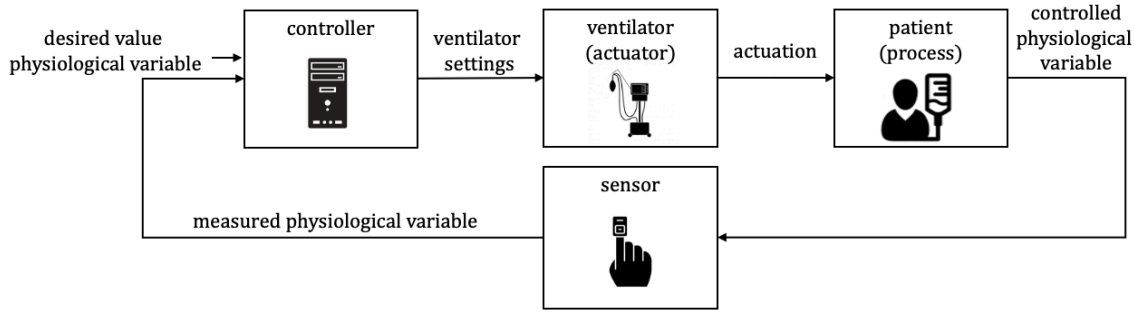

Figure 1 Schematic overview of closed-loop mechanical ventilation.

Closed-loop mechanical ventilation systems that involve the measurement of multiple variables to control multiple settings are able to mimic the response of real human physiology closely [2]. The controllers of these advanced closed-loop mechanical ventilation systems are often based on models that aim to describe the state of the patient being controlled.

In the recent years, several advanced closed-loop mechanical ventilation systems have been developed. An example is the automated system INTELLiVENT-adaptive support ventilation (ASV) [3, 4]. This system controls the respiratory rate, tidal volume, end-tidal carbon dioxide and oxygen saturation by automatic adaption of the ventilator settings. A limitation of automated modes, such as ASV, is that the patient's breathing effort is not measured directly. Proportional closed-loop mechanical ventilation systems do consider patient effort and adjust ventilatory support proportional to this effort. An example of a proportional system is neurally adjusted ventilatory assist (NAVA) that measures the electrical activity of the diaphragm (EAdi) via electrodes embedded on a nasogastric catheter to control the ventilator output [5].

Although the current closed-loop mechanical ventilation systems seem promising, there is room for further improvement. The closed-loop mechanical ventilation systems that are used in current practice mainly focus on the mechanics of breathing. For example, there are currently no commercially available closed-loop systems that consider the metabolism, efficiency of the gas exchange and the acid-base balance [6]. As a result, the clinician must set most of the ventilator settings manually. Choosing the optimal ventilator settings may be challenging because insight in certain parts of the physiological state of the patient may be low. Throughout the duration of mechanical ventilation, it is therefore often unknown what the optimal combination of ventilator settings is for the individual patient [1]. As a result, the ventilation may not be optimally adapted to the individual patient throughout the duration of mechanical ventilation. A stated before, this may have negative effects on the patient's lungs and respiratory muscle function and may worsen clinical outcomes, including the increase of the duration of ventilation.

Our hypothesis is that a closed-loop mechanical ventilation system that is based on a model that considers a limited set of well-chosen aspects of the physiology of breathing to determine the optimal ventilator settings may be able to improve these limitations. The physiological model, that forms the basis of the system, could provide insight in patient specific respiratory parameters and variables that cannot be directly obtained from current routine clinical measurements. This would provide constant insight into a patient's physiological state which may enable individualization and optimization of patient treatment [7, 8]. This may limit the negative consequences of mechanical ventilation on the patient's breathing function, and hence, it may reduce the time spent on mechanical ventilation, which is clinically and economically important [6, 9, 10].

1.2. Research questions

The aim of this thesis is to develop a simple but credible model of the physiology of breathing based on the difficulties encountered in current clinical practice. This model will be the initial step towards the use of a closed-loop system based on a model of the full physiology of breathing in clinical practice and will allow for a first insight in the clinical applicability.

The research questions of this thesis are:

- What is the state-of-the-art of closed-loop mechanical ventilation?
- How can model-based closed-loop mechanical ventilation be used to improve the current clinical practice of mechanical ventilation?
- What dynamic model of the physiology of breathing satisfies these requirements?
- What is the dynamic behaviour of the developed model?
- What relevant information about the dynamic behaviour of the real breathing system can be obtained from experimental measurements?
- How can this information be used to evaluate the model's ability to identify the respiratory parameters and predict the ventilatory responses?

1.3. Approach and outline of this thesis

To answer these questions, several actions were performed. First, a literature review of the current state-of-the-start was conducted. Parallel to this literature review, conversations with clinicians and a literature research were conducted to specify the possible improvements that a model of the physiology of breathing could add to current clinical practice. Subsequently, a model was developed aiming to satisfy these requirements. A dynamical analysis of the model was performed to identify the dynamic behaviour of the model. With the obtained knowledge, an experiment within practical limitations was created that could be used to obtain the relevant information about the dynamic behaviour of the real breathing system. This information was

used to assess the validity of the model structure and the identifiability of the respiratory parameters.

The overall structure of this thesis takes the form of six chapters. Chapter 2 begins by describing the state-of-the art and the possible improvements that can be achieved in current clinical practice by using model-based closed-loop mechanical ventilation. Chapter 3 describes the development and the dynamical analysis of the model. Chapter 4 describes the design of the experiment and the obtained experimental results. Chapter 5 contains a discussion about the implications and limitations of the presented concepts and results and suggestions for further research. The thesis finishes with a conclusion in chapter 6.

2. State-of-the-art of closed-loop mechanical ventilation and possible improvements.

Before the development of the model can start, it is crucial to determine what the desirable improvements in current clinical practice are. Subsequently, it can be determined what components and functions the model should encompass. To create a complete overview, the general workflow of mechanical ventilation is discussed briefly in section 2.1. In section 2.2. it is described what the current state-of-the-art of closed-loop mechanical ventilation is. In section 2.3. the possible improvements that can be obtained in clinical practice using a new model-based closed-loop mechanical ventilation system are described. In section 2.4. the most important results are summarized, interpreted and their implications for the development of the model are stated.

2.1 General overview of the workflow mechanical ventilation

The duration of mechanical ventilation can be roughly and globally divided into three global stages, but this may vary between patients according to the indication for mechanical ventilation. Each stage has different aims and conditions regarding to the monitoring of parameters and variables.

The first stage starts when a patient arrives at the ICU with respiratory failure and/or an indication to intubate and start mechanical ventilation. The patient is often sedated and is put on controlled mechanical ventilation. During controlled mechanical ventilation, the patient cannot breathe spontaneously. The main aim of this stage is to give the lungs time to repair. It is therefore very important to monitor the pressures and the volumes applied to the lungs which should stay low to prevent further injury and inflammation (e.g., ventilator-induced lung injury). The blood gases should stay between predetermined safe bounds. However, reaching optimal blood gasses comes second to the protection of the lungs. The clinician may for example allow permissive hypercapnia, where a very high carbon dioxide fraction in the blood is allowed for the sake of keeping the tidal volume and pressure low. It is assessed at least daily whether a patient on a controlled mode of ventilation can be switched to an assisted form of ventilation and sedation can be lowered.

When the lungs have mostly healed, the next stage of mechanical ventilation starts. The aim of this stage is to recover the breathing function of the patient. In this stage, the patient is on assisted ventilation, during which the ventilator detects inspiratory effort of the patient and delivers pressure assist accordingly. During this stage, the lungs can handle a larger range of pressures and volumes. As a result, the clinician can choose higher values for the applied tidal volume which may make it easier to reach the desired blood gasses. It is assessed regularly whether the level of ventilatory support can be reduced.

The last stage is the weaning stage and starts when the patient is still on the ventilator but seems to be able to breathe sufficiently with low support (PEEP <8, FiO_2<0.5). Weaning is the term used to describe the process of withdrawing the ventilatory support and eventually removing the patient from the ventilator. It is not always clear when a patient is ready for weaning. As a result, the clinician needs to trust in his own insight and experience. The patient will start a spontaneous breathing trial (SBT), during which the patient is not yet extubated but does not receive any support or a limited amount of ventilator support, allowing to test the readiness for weaning of the ventilator. Throughout the SBT, which usually takes 30 minutes, respiratory parameters and blood gases are monitored. If sufficient, the patient can be released from the ventilator. When the blood values are not sufficient or when the patient meets criteria for SBT failure at any time point during the SBT, ventilatory support will be resumed [29]. This is common, 25 percent of patients fail in the first spontaneous breathing trial [30]. On the other

hand, there are indications that weaning sometimes takes place later than strictly necessary [31].

The current closed-loop mechanical ventilation systems often only focus on one stage of mechanical ventilation. For example, there are several closed-loop systems that solely focus on the breathing mechanics and are only usable during the first stage. In the next section, the closed loop mechanical ventilation systems that are used in current clinical practice are described.

2.2. The state-of-the-art of closed-loop mechanical ventilation.

In this section, several examples of closed loop mechanical ventilation systems are given. The systems are categorized based on the controlled physiological variable or variables.

Closed-loop control based on gas exchange

Several closed loop models based on the control of oxygen have been developed. Most of these systems are focussed on neonates. The AVEA-CLiO2 is a commercially available system for neonates based on oxygenation control [11]. This system controls the oxygen saturation and maintains this variable within a target range by adapting the fraction of inspired oxygen. A study of Salverda et al. (2021) that included a total of 588 infants found that the use of the system did not lower the mortality or morbidity, but did reduce the duration of invasive ventilation [12].

No commercial systems that are solely based on the control of carbon dioxide have been developed thus far. In a study of Martinoni et al. (2004) a model-based control system was created that controls the end-tidal carbon dioxide fraction by adjusting the minute ventilation. The system is based on a model of Chiari et al. that consists of three compartments: lung, brain and body tissue [13]. The system was tested in clinical settings and the model-based controller seemed to meet the requirements for routine clinical application [14]. However, clinical implementation has never been achieved.

The former systems were based on either the control of carbon dioxide or oxygen. A recently developed system of Hermand et al. (2016) controls both the partial pressures of oxygen and carbon dioxide in the arterial blood. A mathematical model that mimics the central and peripheral chemoreceptor responses in humans uses the values of the partial pressures to adjust the minute ventilation. The model response matches with experimental data but the model has not been tested in clinical practice thus far [15].

A disadvantage of the closed-loop ventilation strategies presented in the former section, is that they focus only on the gas exchange and do not consider the lung mechanics. Achieving proper oxygenation and emission of carbon dioxide may require large tidal volumes or ventilator pressures, which may cause ventilator-induced lung injury (VILI). With clinical ventilation strategies becoming focused on protective ventilation that aims to prevent VILI, the lung mechanics are an important aspect to take into consideration [6].

Closed-loop control based on the respiratory mechanics

Most closed-loop mechanical ventilation systems used in current clinical practice are mainly based on the respiratory mechanics. An example is adaptive support ventilation (ASV) that controls the minute ventilation by finding the optimum combination of respiratory rate and tidal volume based on the respiratory mechanics of the patient. The respiratory mechanics consist of the lung compliance, airway resistance and expiratory time constant [4]. This principle is based on the Otis equation which states that there is an optimum respiratory rate that minimises the breathing effort [16].

Another example is SmartCare that adapts the delivered pressure support level to the patient's effort. The system continuously determines the patient's respiratory mechanics and patterns. The aim is to simulate clinical reasoning to avoid under- or over-assistance during mechanical ventilation by constantly adjusting the level of pressure support. These frequent adjustments in pressure support would be unrealistic if attempted by a clinician. The system also has an automated weaning protocol that consists of an automated reduction of pressure support level and thereafter an automated spontaneous breathing test.[17]

Closed-loop control based on the multiple components of the physiology

Recently, researchers and industry have presented automated systems which are based on a culmination of the categories described before. This encompasses maintaining optimal blood gasses, preventing VILI and improving patient-ventilator synchrony.

INTELLiVENT-ASV is a system based on ASV that provides automatic gradual decreases in inspiratory support levels to facilitate weaning of the patient from the ventilator [22]. This system controls the respiratory rate, tidal volume, end-tidal carbon dioxide and oxygen saturation by automatic adaption of the ventilator settings to reach target values set by the clinician. The ventilator setting that are adapted are the fraction of inspiratory oxygen, minute ventilation and positive end-expiratory pressure. The system has shown to be feasible and able to deliver protective ventilation in passive and spontaneously breathing patients with different lung conditions [23]. However, there are few experienced facilities where INTELLiVENT-ASV can be used, and therefore, its usage status and efficacy have not yet been reported [24]. One of the reasons for this is that the clinical situations in which INTELLiVENT-ASV should be used have not yet been clarified.

Other systems are developed but not yet commercialized. An example is the system of Schwaiberger et al. (2018). This system reacts protocol-driven to any measured change in respiratory mechanics or oxygenation. It controls the airway pressures, oxygen saturation and end-tidal carbon dioxide fraction by adjusting the tidal volume, PEEP, respiratory rate and the fraction of inspired oxygen accordingly. A pilot animal study showed promising results, but clinical trials have yet to be performed [25].

Closed-loop control based on breathing effort

The former described automated modes integrate closed-loop principles but do not directly measure patient effort. Proportional modes of ventilation are assisted modes of ventilation that measure patient effort and deliver assistance proportional to this effort [18].

Proportional assist ventilation with load-adjustable gain factors (PAV+) determines the inspiratory effort of the patient by measuring the volume and airflow being pulled in by the patient. End-inspiratory occlusions are used to determine the respiratory system resistance (R_{rs}) and elastance (E_{rs}) every couple of breaths. R_{rs} is the resistance of the respiratory tract to airflow and E_{rs} is the measure of the elastic properties of the lung and pleura. Using equation 1, the ventilator can calculate the total pressure that is delivered to the respiratory system (P_{total}). [4]

$$P_{total} = P_{vent} + P_{muscle} = (airflow \times R_{rs}) + (volume \times E_{rs}) \quad (1)$$

PAV+ is designed in a way that the work is shared between the patient and the ventilator. The total pressure is the sum of the pressure generated by the breathing muscles and the pressure generated by the ventilator. The clinician will determine what percentage of the total pressure should be accounted for by the ventilator. For example, if the clinician sets this level of assist at

70 percent, the ventilator will provide 70 percent of the calculated total pressure, the remaining being assumed by the patient's respiratory muscles [19].

Neurally adjusted ventilatory assist (NAVA) is an assisted ventilation mode that measures the electrical activity of the diaphragm (EAdi) via transoesophageal electromyography using a modified nasogastric catheter with electrodes at the level of the diaphragm [5]. The EAdi is used to control the ventilator: ventilator assist is provided proportional to the EAdi over the full inspiratory phase according to a gain (NAVA level, in cmH2O/uV) set by the clinician. Improved patient-ventilator synchrony for this system was shown by Piquilloud et al. [20]. Vahedi et al. showed positive staff experiences with the use of NAVA in clinical practice [21]. One drawback is that NAVA is only available on one ventilator brand, which hinders widespread implementation. NAVA can be used with both noninvasive and invasive mechanical ventilation. In addition, EAdi monitoring is available in other modes than NAVA as well, as a measure to monitor diaphragm activity and patient-ventilator interaction in order to further optimize ventilation management.

Model-based decision support systems

Systems have been created that computerize clinical protocols which medical staff use to adapt mechanical ventilator settings. These decision support systems are not able to make changes to the ventilator themselves but propose the changes to the clinician. Even though these systems are not closed-loop systems, they are described in this section because of their similarities with closed loop systems.

The INVENT system, recently commercialised as the Beacon Caresystem, is an open-loop system that combines a set of physiological models describing pulmonary gas exchange, lung mechanics, ventilation, the acid-base chemistry of blood, respiratory drive and metabolism [9, 26]. The Beacon Caresystem presents advice for ventilator adjustments and the physiological rationale behind this advice. A study by Spadaro et al. (2018) has shown that use of the Beacon Caresystem resulted in appropriate responses to changes in pressure support levels while acting to preserve respiratory muscle function [27, 28]. It is currently being researched if the use of the decision support system over the entire duration of ICU stay will reduce the time spent on mechanical ventilation and the difficulty of the weaning process [26].

Another decision support model that is currently being developed is the Lung and Diaphragm Protective Ventilation (LDPV) model, aiming to assist the clinician in adjusting mechanical ventilation settings toward target ranges that are considered safe for the lungs and the diaphragm. The model considers the respiratory drive, pharmacokinetics of propofol, acid–base homeostasis, ventilator settings and lung and respiratory muscle mechanics. It differs from existing mechanical ventilation models by focusing on output indicators that reflect lung and diaphragm safety. This model has not been tested in clinical settings, but initial simulations have produced results which demonstrate simulated physiological responses consistent with what is expected.[7]

Overview

In table 1 an overview is given of the closed loop systems described in this section. The model-based decision support systems are not included.

Table 1 Overview of the state-of-the-art systems described in this section.

system	**controlled variable**	**adapted variable**	**source**
Martinoni et al. (2004)	End-tidal CO_2	Minute ventilation	[14]
Hermand et al. (2016)	Partial pressure arterial CO_2 and O_2	Minute ventilation	[15]

AVEA-CLiO2	O_2 saturation	fraction of inspired O_2	[11]
ASV	Breathing effort	Tidal volume, respiratory rate	[4]
Dräger SmartCare	Respiratory rate, tidal volume, end-tidal CO_2	Pressure support level	[23]
PAV+	Airflow, volume	Pressure support level	[4]
NAVA	Electrical activity of the diaphragm	Triggering, level of inspiratory assist, cycle-off	[5]
INTELLiVENT-ASV	Respiratory rate, tidal volume, end-tidal CO_2, O_2 saturation	Respiratory rate, tidal volume, inspiratory time, PEEP, fraction of inspired O_2	[23]
Schwaiberger et al. (2018)	Airway pressures, tidal volume, end-tidal CO_2, O_2 saturation	Tidal volume, PEEP, respiratory rate, I:E-ratio and fraction of inspired O_2	[25]

2.3. Possible improvements of current clinical practice with a model-based closed-loop system

In the introduction the hypothesis was stated that model-based closed-loop mechanical ventilation systems could be of use by providing insight in the important patient's specific parameters. This would result in ventilator settings that are optimally adapted to the individual patient. To improve the specification of the clinical problem, we have spoken to an intensivist and a technical physician specialized in the respiratory system of the Amsterdam UMC and a respiratory physiologist of the Medisch Spectrum Twente. The questions that were asked during these conversations are presented in appendix 4. We have also searched in literature for the difficulties that are encountered in monitoring the important parameters and choosing the optimal ventilator settings. The possibilities for a system based on a model of the physiology of breathing to overcome these difficulties are described at the end of this section.

Monitoring the mechanical properties of the respiratory system

Accurate monitoring of the mechanical properties of the respiratory system is important to understand respiratory failure in patients on mechanical ventilation and to optimize mechanical ventilation settings [32]. There are several parameters that describe the mechanical properties of the respiratory system. The first is the respiratory system compliance which is the measure of the lung and chest wall's ability to stretch and expand. The compliance can be determined from the tidal volume (V_t), the plateau pressure (P_{plat}) and total positive end-expiratory pressure (PEEP).

$$C_{rs} = \frac{V_t}{P_{PLAT} - PEEP_{tot}} \quad (2)$$

The respiratory resistance is the resistance of the respiratory tract to airflow during inhalation and exhalation. Airway resistance can be measured by dividing the difference between the plateau pressure (P_{PLAT}) and the peak pressure (P_{PEAK}) by the airflow in liters per second (ϕ_{air}).

$$R_{rs} = \frac{P_{PEAK} - P_{PLAT}}{\phi_{air}} \quad (3)$$

During controlled modes of ventilation, a simple end-inspiratory occlusion maneuver is used to compute P_{PEAK} and P_{PLAT}, whereas an end-expiratory occlusion is performed for measurement of total PEEP. Resistance measurements can only be done with a constant flow condition such as in volume-controlled mode; compliance measurements can be performed during both pressure-controlled and volume-controlled modes.

During assisted ventilation, obtaining an inspiratory hold and measurement of pulmonary mechanics may be complicated because of the combination of both ventilator and respiratory muscle pressures during inspiration [32]. It may then be necessary to use an esophageal balloon catheter for dynamic rather than static measures of lung and chest wall mechanics. However, esophageal manometry is minimally invasive and may be complicated to perform [29].

Although several experts have confirmed that the measurement of C_{rs} and R_{rs} in spontaneously breathing patients is feasible and reliable, it is still rarely applied in the clinical practice [32, 33]. In addition, not all available mechanical ventilation systems allow occlusion maneuvers during assisted ventilation modes [29].

Monitoring the gas Exchange

The gas exchange describes the movement of oxygen and carbon dioxide between the alveoli and the capillaries in the lungs. An impaired gas exchange may have several causes, e.g. pulmonary shunt, ventilation-perfusion (V/Q) mismatch and alveolar dead space [34]. In clinical practice, description of the efficiency of the gas exchange is limited to two single lumped indices [9]. For oxygen, this is the ratio between the partial pressure of oxygen in the arterial blood and the fraction of inspired oxygen (P_aO_2/FiO_2) which primarily describes oxygenation abnormalities due to regions of the lung with pulmonary shunt and low V/Q ratio. For carbon dioxide, this is the ratio between the end-tidal carbon dioxide fraction and the partial pressure of carbon dioxide in the arterial blood ($EtCO_2/P_aCO_2$). It is used to approximate the effects of high V/Q ratio and alveolar dead space on CO_2-elimination [9].

These indices do not allow for separation of the causes of impaired gas exchange. There are indications that in patients with acute respiratory distress syndrome (ARDS), dead space has prognostic value and can be used to guide ventilator settings. Several studies have demonstrated that elevated dead space in patients with ARDS is associated with an increased risk of mortality [35-37]. However, dead space is seldom calculated in clinical practice because it requires the alveolar carbon dioxide fraction, which is difficult to measure or estimate [38].

Monitoring the breathing effort

Breathing effort is the energy-consuming activity of the respiratory muscles aimed at driving respiration. Maintaining patient breathing effort during mechanical ventilation has advantages and disadvantages. The positive effects of maintaining breathing effort are protection against respiratory muscle atrophy and improved oxygenation [39]. The potential negative effect of maintaining breathing effort is patient self-inflicted lung injury where intense effort may generate too large pressures that may be damaging to the lungs [40]. Finding the balance between the former named advantages and disadvantages remains a challenge in mechanical ventilation [41], especially in patients with excessive respiratory drive.

There is no specific diagnostic technique for the assessment of breathing effort. Physicians perform physical examination to assess breathing effort in clinical practice, like recruitment of accessory muscles or an increased respiratory frequency [42]. However, this does not allow for quantitative assessment of breathing effort.

For quantitative assessment of the breathing effort, the parameters work of breathing (WOB) and pressure-time product (PTP) are considered the gold standard. [42]. The WOB is the energy consumed for respiration, often expressed in joule per litre. The PTP is the integral of all pressures generated by the breathing muscles measured for one minute. For assessment of the WOB and PTP, it is necessary to perform pressure measurements which are difficult to interpret

and obtain. For this reason, quantitative assessment of the breathing effort is rarely performed in clinical practice and is limited to specialised research facilities [43].

Monitoring the respiratory drive

The respiratory drive describes the intensity of the output of the respiratory centers [44]. There is no technique that can measure the respiratory drive directly. As a result, the respiratory output is used to quantify the respiratory drive. The respiratory drive is often qualitatively assessed by clinical signs, e.g. dyspnea and the use of accessory respiratory muscles. Other examples of assessment are the electrical activity of the diaphragm (EAdi), the airway occlusion pressure and measurement of the esophageal and gastric pressures [44]. Pressure measurements for inspiratory effort only reflect the respiratory drive if both neural transmission and diaphragm function are functional.

EAdi records the electrical activity of the diaphragm with electrodes incorporated into a nasogastric tube [45]. This is the output that is closest to the output of the respiratory centers. It is easy the measure, minimally invasive and the activity represents the whole diaphragm. The limitation of EAdi is that there are no normal values because EAdi varies greatly between people. However, it can be useful to monitor changes in in the diaphragm activity within a patient over time [42].

The airway end-expiratory occlusion pressure is a noninvasive measurement that reflects the output of the respiratory control centre [46]. When an end-expiratory airway occlusion is applied, spontaneous respiratory effort by the patient during the occlusion will generate a negative pressure in the airway pressure that represents the respiratory muscle effort [32].

The esophageal or gastric pressure is measured via an air-filled balloon catheter inserted in the esophagus or stomach [47]. The esophageal pressure (Pes) indicates the level of effort for all inspiratory muscles, while the differential pressure (gastric pressure minus esophageal pressure = transdiaphragmatic pressure (Pdi)) indicates effort of the diaphragm only. Measurements are rarely done in clinical practice because they are challenging to perform and the results may be difficult to interpret for clinicians[29].

An important limitation of manometry in assessing the respiratory drive is that it is not possible to make a distinction between impairments in the breathing muscles and the neural drive. This imposes the risk of underestimating respiratory drive in patients with respiratory muscle weakness. In these patients, despite a high neural drive (EAdi), inspiratory effort (Pes, Pdi) might be low.

Monitoring the blood gases

Blood gas analysis during mechanical ventilation provides information that allows the assessment of oxygenation, ventilation and acid-base status. Modern blood gas machines measure the partial pressures of oxygen and carbon dioxide and the pH directly. These are then used to calculate the bicarbonate concentration, base excess and oxygen saturation. The blood gasses are measured multiple times per day but there is no standard protocol for the measurement of the blood gases, which can be a problem in understaffed intensive care units [29].

Possible improvements in monitoring parameters using a model-based closed-loop system

In the former paragraphs, it was described that in current clinical practice there is often limited insight in the important parameters relating to the physiological state of the patient. An improvement that a new model-based closed-loop mechanical ventilation system could provide

is the improved identification and observation of the important physiological parameters and variables. A model can provide insight in parameters and variables that cannot be directly obtained from measurements by using measured data to estimate the physiological parameters and variables.

An example of a model that could provide insight in patient specific parameters is the pressure reconstruction model that was developed by Damanhuri et al. (2016). This model was used to calculate how much breathing effort is exerted by the patient during reverse triggering, which is a specific from of patient-ventilator asynchrony in a sedated patient during fully controlled mechanical ventilation. The model's input were the airway pressures and flow, and no additional clinical protocols or invasive procedures were necessary [48]. It is unlikely that this model can be translated to the spontaneously breathing patient during assisted modes of ventilation, due to differences in airway pressure and flow waveform profiles; however, it would be interesting to further explore whether there are certain airway pressure and flow patterns or parameters that could predict the amount of patient effort in the spontaneously breathing patient.

The identification of parameters through perturbations in the system input may be an important technique to improve insight in the respiratory parameters. Jawde et al. (2020) described a model that can obtain the patient specific respiratory mechanics after application of perturbations in the breathing pattern. The system variates the respiratory rate and tidal volume breath-to-breath. From the measured change in airway pressures and airflows the model can determine the time-dependent respiratory resistance and elastance of the patient [49]. Both models have not yet been tested in clinical practice.

A system that could provide the automatic application of an end-inspiratory and end-expiratory occlusion manoeuvre could provide improved identification of the parameters that describe the respiratory mechanics. From the end-inspiratory occlusion manoeuvre, the respiratory resistance and compliance can be determined in controlled modes. In assisted modes, the respiratory resistance and compliance could be estimated using short occlusions and models, as is done in PAV+. Through the end-expiratory occlusion the airway occlusion pressure can be obtained which provides insight in the respiratory drive [44].

Measurements that are an addition to those available in routine clinical care may be included to the system to allow for identification of a greater number of parameters [1]. An example is the use of non-invasive sensors. In a study of Doorduin et al. (2016) it was found that the measurements of end tidal carbon dioxide with volumetric capnography could be used to determine the true Bohr dead space [38].
Continuous transcutaneous measurement of the pH and partial pressures of oxygen and carbon dioxide has been developing for many years, and it may prove useful in capturing respiratory and hemodynamic failures in critically ill patients [50].

Determination of the optimal ventilator settings

Choosing the optimal value for ventilator setting can be challenging because it is not always known what the optimal settings are in certain situations. An example is the pressure support level where there is a trade-off between beneficial and detrimental effects. When ventilating patients with pressure support, the clinical challenge is to determine the level of pressure support which reduces the risk of respiratory muscle atrophy and promotes weaning, without stressing or exhausting the patient and causing diaphragm fatigue, or introducing asynchrony between the patient and the ventilator [9].

Another example is setting the level of positive end-expiratory pressure (PEEP). PEEP has the advantage that is prevents the collapse of the alveoli. However, the disadvantage of PEEP is that it can lead to overstretching of other lung parts. This means that the value of PEEP should be

chosen as low as possible while still preventing alveolar collapse. The optimal level of PEEP is dependent on many factors, e.g. severity of lung damage, degree of recruitability. Studies comparing low and high PEEP in ARDS patients do not show an unequivocal answer. The choice of PEEP also proves subjective with high inter-clinician variability [51].

The last example given in this section is the level of the fraction of inspired oxygen (FiO_2). Breathing in air with sufficient oxygen is important to prevent hypoxia. However, there are also dangers to inspiring a high concentration of oxygen for a long duration of time. Examples are the suppression of the respiratory drive, alveolar infiltration and toxicity. Toxicity may cause inflammation and eventually, pulmonary fibrosis. It is not always possible to determine when the toxic level will be reached and it may therefore be difficult to determine what the optimal value of FiO_2 is. [52] A high FiO_2 also causes nitrogen washout. The oxygen molecules will replace the nitrogen molecules in the lungs. When the nitrogen concentrations lower, the alveoli will start to collapse. This may result in hypoxemia because fewer alveoli participate in the gas exchange.

Possible improvements in determination of the optimal ventilator settings using a model-based closed-loop system

In the former paragraphs, it was described that choosing the optimal ventilator settings can be challenging. The optimal ventilator settings often have significant inter-individual variability [1]. The ability of a model-based closed-loop system adapted to the individual patient to predict the response to changing ventilator settings would be a useful addition to clinical practice [53]. Accurate prediction of responses to changing ventilator settings may enable more personalised and efficient ventilation. This will minimise the risk of VILI and may reduce the duration of mechanical ventilation, which is clinically and economically important [10].

Morton et al. (2018) developed and validated a single compartment lung model that uses the information about the lung mechanics available at a low PEEP to predict the lung mechanics at a higher PEEP. The model could accurately predict peak inspiratory pressures after changes in PEEP and could improve clinician confidence in attempting potentially dangerous treatment strategies.[54]

These predictions can be further substantiated with artificial intelligence. With most data becoming digitized, it is plausible that in the future the data that describes the development of the state of the patient will be available to the ventilator [6]. Artificial intelligence may learn about the specific patient response to ventilator changes and can therefore provide predictions.

An example is the artificial neural network model developed by Kuo et al. (2015). This model receives a set of variables belonging to the subjects' characteristics and the breathing pattern and uses artificial intelligence to determine the chance of successful extubation. In clinical practice, this model could help clinicians to select the appropriate earliest weaning time. The downside of using a predictive model based on artificial intelligence compared to a regular predictive model is that the model is not transparent for clinicians and the reasoning behind decisions is not available [55]. These models are also solely based on routinely obtained 'standard' measurements, and not on in-depth physiology or patient effort.

2.4. Implications of the desirable improvements for the design of the model

The closed-loop mechanical ventilation systems that are used in current clinical practice mainly focus on the respiratory mechanics. In section 2.2. it was described that the systems that do encompass multiple aspects in their systems are perceived as complicated and non-transparent by clinicians and therefore their usage is low [21, 24]. The systems that are currently used also

do not consider the different stages of mechanical ventilation described in section 2.1 and are therefore not usable throughout the whole duration of mechanical ventilation.

In section 2.3. it was described that obtaining insight in important parameters that describe the physiological state of the patient is often challenging. During assisted ventilation, it is difficult to obtain insight in the respiratory mechanics, the breathing effort and the respiratory drive because of the combination of ventilator and patient efforts. Other parameters, like the physiological dead space, are useful to acquire but require difficult measurements.
It was also described that selecting ventilator settings can introduce a difficult balance between sufficient oxygenation, prevention of breathing function degeneration and prevention of ventilator-induced lung injury [56]. Throughout the duration of mechanical ventilation, it is often unknown what the optimal combination of ventilator settings is for the individual patient [1]. The chosen combinations of ventilator settings often vary among clinicians in similar situations [57].

In section 2.3. the possible improvements that a new model-based closed-loop ventilation system could add to current practice were described. The first improvement is the improved identification and observation of the important physiology parameters and variables that cannot be measured directly. A model could provide insight in parameters and variables that cannot be directly obtained from measurements by using measured data to estimate the values. When insight in the important parameters is obtained, the patient-specific model parameters can be identified, and it is possible to adapt the model to the individual patient. Measurements that are an addition to those available in routine clinical care may be included to allow for identification and observation of a greater number of parameters and variables [1]. Examples described in this section are the automatic periodic application of an end-inspiratory and end-expiratory occlusion manoeuvre, perturbations in the breathing pattern or the use of state-of-the-art non-invasive sensors [50, 58]. Periodically identifying the important parameters could provide better insight in the patient's physiological state and its development for the clinician.

This also induces the second improvement. The model that is adapted to the patient can predict patient responses to changes in ventilator settings. The ability to predict the response to changing ventilator settings would offer insight in the optimal ventilator settings that current care and equipment cannot provide [53]. This will minimise the risk of VILI and may reduce the duration of mechanical ventilation, which is clinically and economically important [10]. These predictions could be further substantiated through the use of artificial intelligence.

Our new model should focus on the two improvements that are described above. This pleads for a model that has low complexity but is adequately valid, so that all important parameters can be identified with limited information. Another benefit that this induces it that the model will be transparent and understandable for clinicians which may improve the usage. The model parameters should be adaptable to the individual patient to allow for model predictions of patient responses to changing ventilator settings. In the first stadium of development, this model could provide insight in respiratory parameters and variables that the clinician may use to choose the optimal ventilator settings. In a later stadium of development, this model could be the basis of a closed-loop mechanical ventilation system based on the physiology of breathing that can automatically adapt the ventilator settings.

The choice is made to mainly focus our model on the gas exchange and the respiratory drive. We are aware that gaining insight in the respiratory mechanics is, especially in the first stage of mechanical ventilation, of equal or even greater importance. However, the choice to focus on the other aspects of the physiology of breathing is made, because most commercialized systems already focus on the respiratory mechanics. It is suspected that a system that focusses on the gas exchange and the respiratory drive can also be very useful in clinical practice. Especially during

the later stages of mechanical ventilation when the patient comes near the weaning stage and assessment of the breathing function of the patient becomes of great importance.

It will likely not be possible to provide insight in all the important respiratory parameters and make elaborate predictions with the simple model that is developed in this thesis. However, before the creation of elaborate models, it is important to research what the base structure of these models should be. When the results of simulations with the model are qualitatively similar to the responses measured in an experimental study, we may be able to show the first signs of the use of such a model in clinical practice by identifying aggregated parameter groups and making simple predictions. In the next section, the development of the model is described.

3. Model development and analysis

In this section, the development and the subsequent dynamical analysis of the model are described. In section 2.4. it was described which requirements for the model followed from current clinical practice. The model should have low complexity and will mainly focus on the gas exchange and the respiratory drive. In section 3.1. the development of a model that meets these requirements is described. Since the model is created on a theoretical basis, it is necessary to find out if the mode has the right structure to accurately describe the real breathing system. With the dynamical analysis and subsequent simulations described in section 3.2, the dynamic behaviour of the model can be analysed and a hypothesis for the dynamic behaviour of the real breathing system can be stated. This hypothesis will later be tested with an experiment. In section 3.3. the most important results are summarized, interpreted and their implications for the experiment design are stated.

3.1. Model development

3.1.1. The schematic model

In the introduction the workflow of closed loop mechanical ventilation systems was briefly described. The human breathing system is in essence also a closed loop system. In this case, the sensor that measures a physiological variable is not an artificial sensor but are the central and peripheral chemoreceptors that measure the CO_2 and O_2 concentrations and the pH of the blood and the extracellular fluid (ECF). In the respiratory control centre (controller) that is located in the brain, the concentrations are compared to the desired value. In this case, the actuation is not a change in ventilator settings but a change in movement of the breathing muscles. The patient (process) may start ventilating more or less to obtain the desired blood gasses.

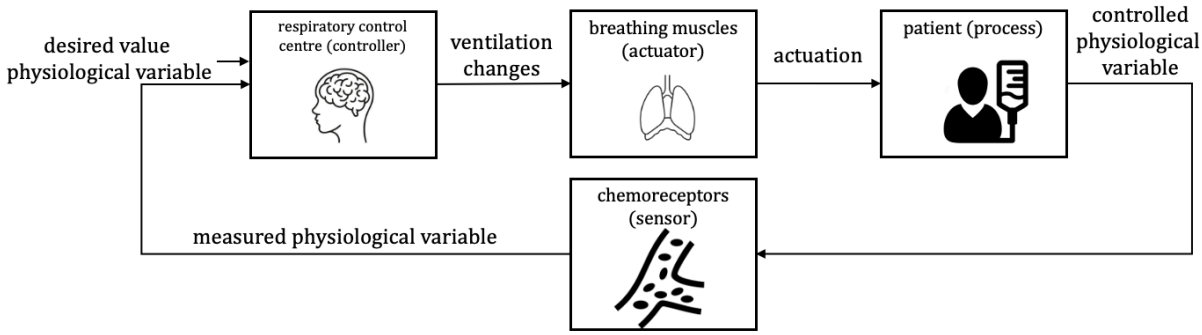

Figure 2 Schematic overview of the human ventilatory control function.

The development of the model will consist of three main steps:

- Creation of a schematic model
- Derivation of the mathematical equations
- Implementation in Simulink

The first step is the creation of a schematic model. In figure 3 this model is presented. The grey blocks in the schematic model represent the four general components of a closed loop system that were described in the previous paragraph: the process, the sensor, the controller and the actuator. The four components have different subsystems that are represented by the white coloured blocks. The arrows represent the information flow or the physiological interactions between the different subsystems. The values of the cursive variables belonging to the arrows are transferred from one subsystem to another. The receiving subsystem will use this

information to determine the value of other variables. For this, mathematical equations are used that are described in section 3.2.

In the process block there are three subsystems that can store CO_2 and O_2: the venous blood, the arterial blood and the alveolar air. In these subsystems, cursive variables are displayed, which represent the state variables. The state variables are variables that are not transported between subsystems but give information about the accumulation of CO_2 and O_2 in the storage blocks. In section 3.2. the content of each subsystem is described in detail.

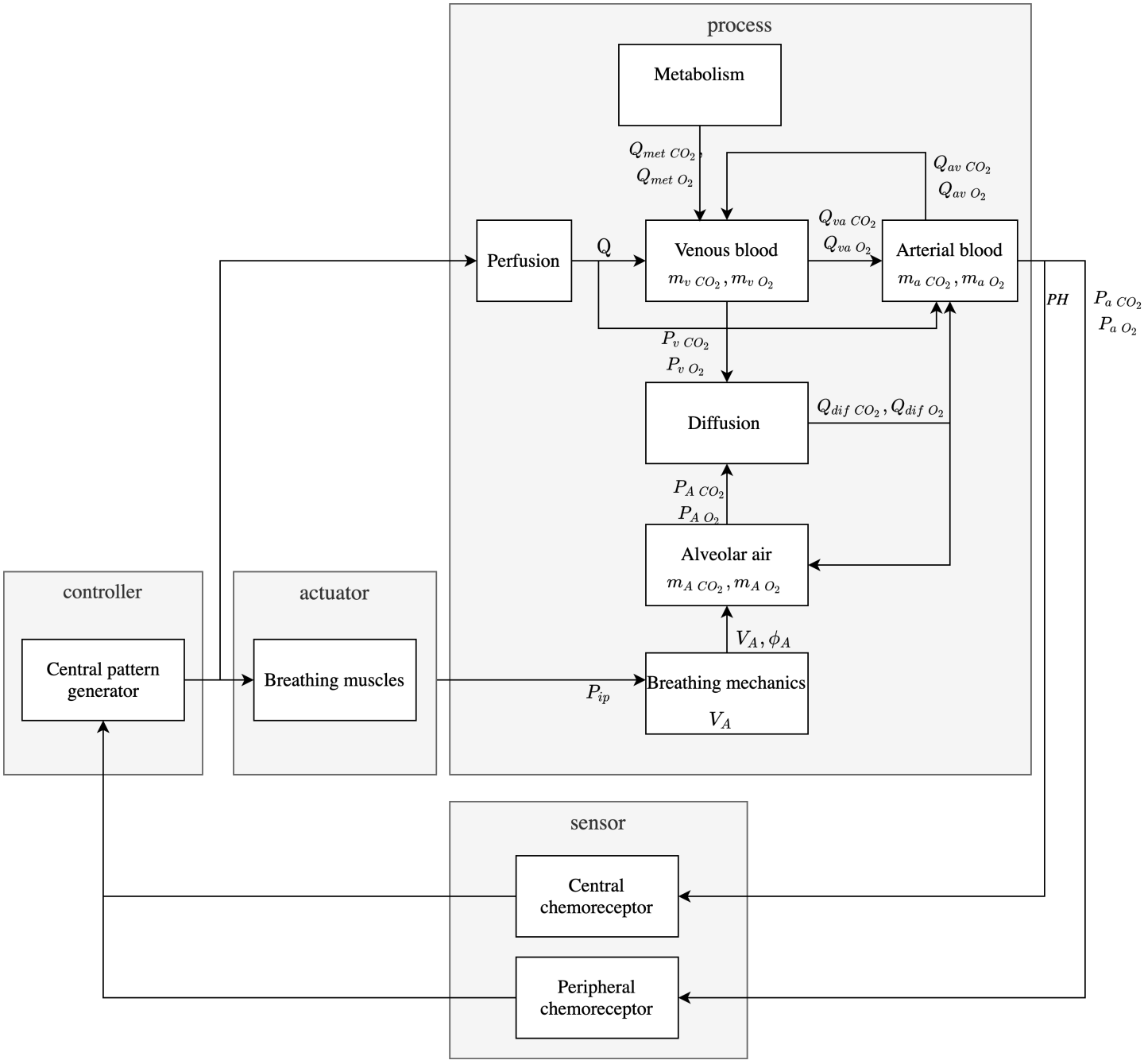

Figure 3 Schematic model of the physiology of breathing

3.1.2 Mathematical equations describing the relevant physiology

In the former section, an overview of the schematic model with the different subsystems was given. Each subsystem contains mathematical equations that are described in this section. To avoid repetition, only the equations for CO_2 will be described in this section of the report. In appendix 1 the equations for O_2 can be found.

Breathing mechanics

Since our model is not mainly focussed on the breathing mechanics, a simple first order system will be used to describe the beathing mechanics. The intrapleural pressure ($P_{IP}(t)$) is the pressure in the intrapleural space. Because the lungs and the chest wall pull away from each other on opposite sides of the intrapleural space, the intrapleural pressure is less than barometric pressure ($P_B(t)$). During inspiration, the inspiratory muscles expand the chest, making $P_{IP}(t)$ more negative. The lungs respond by expanding passively.

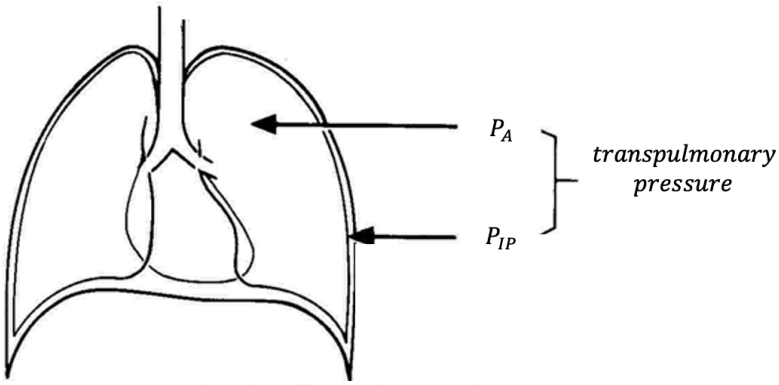

Figure 4 The transpulmonary pressure is equal to the difference between the alveolar pressure and the intrapleural pressure.

The alveolar pressure ($P_A(t)$)is equal to the pressure in the alveoli. The transpulmonary pressure ($P_{TP}(t)$) is the pressure across the alveolar wall. It is equal to the difference between the alveolar pressure and the intrapleural pressure.

$$P_{TP}(t) = P_A(t) - P_{IP}(t) \tag{4}$$

P_{TP} is also proportional to the difference between the alveolar volume ($\mathrm{V_A}(t)$) and the Functional residual capacity (V_{FRC}) and inversely proportional to the respiratory system compliance (C_{rs}).

$$P_{TP}(t) = \frac{\mathrm{V_A}(t) - V_{FRC}}{C_{rs}} \tag{5}$$

Airflow in the airways ($\phi_{AW}(t)$) is proportional to the pressure over the airways ($\Delta P_{AW}(t)$) and inversely proportional to total respiratory system resistance (R_{rs}). $P_{AW}(t)$ is equal to the difference between $P_A(t)$ and the ventilator-induced pressure at the mouth ($P_V(t)$). When the patient is not attached to a ventilator, $P_V(t)$ equals zero. All pressures have values relative to the atmospheric pressure.

$$\phi_{AW}(t) = \frac{P_{AW}(t)}{R_{rs}} = \frac{P_A(t) - P_V(t)}{R_{rs}} \tag{6}$$

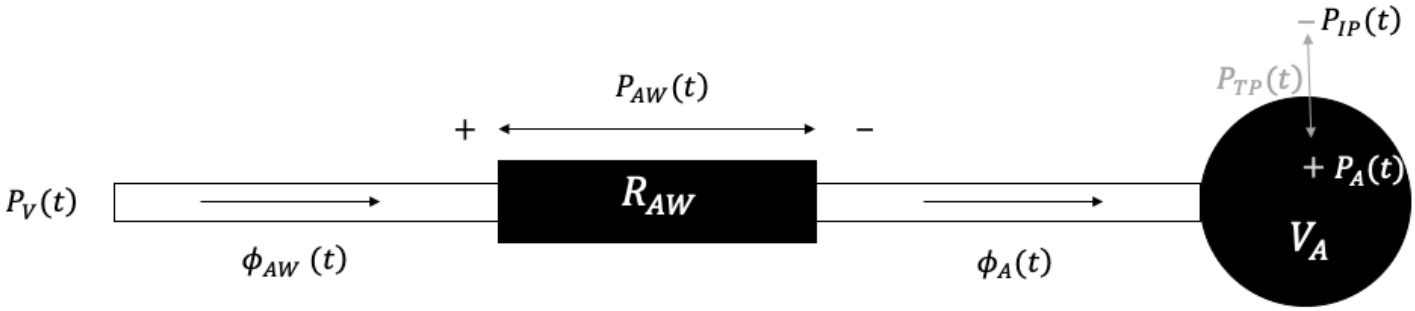

Figure 5 schematic overview of the respiratory mechanics.

In figure 5 a conceptual model of the breathing mechanics can be seen. Using Kirchhoff's law, it can be determined that the airflow in the airways ($\phi_{AW}(t)$) is equal to the airflow to the alveoli ($\phi_A(t)$). This flow is equal to the change in alveolar volume.

$$\phi_{AW}(t) = \frac{\mathrm{dV_A}(t)}{dt} \tag{7}$$

Kirchhoff's law also states that the sum of all the pressures in the conceptual model should be equal to zero.

$$P_V(t) - P_{AW}(t) - P_{TP}(t) - P_{IP}(t) = 0 \tag{8}$$

After combining the formed equations, equation 9 is obtained.

$$R_{rs} \cdot C_{rs} \cdot \frac{\mathrm{dV_A}(t)}{dt} + (\mathrm{V_A}(t) - V_{FRC}) = C_{rs} \cdot (P_V(t) - P_{IP}(t)) \tag{9}$$

Explanation: From this equation, the alveolar volume and airflow as a function of time can be determined when the pressures and resistance and compliance are known. The values of the alveolar volume and airflow will be transported to the subsystem 'the alveolar air' (figure 3). The system 'the alveolar air' will use its own equations to determine the value of other variables. These variables are in turn transported to other blocks. This is the global workflow of a mathematical model.

Alveolar air

The change in the number of CO_2 molecules in the alveolar air ($m_{A\,CO_2}(t)$) depends on the diffusion flow from the capillaries to the alveolar space ($\phi_{dif\,CO_2}(t)$) and the outflow of CO_2 from the body ($\phi_{AW\,CO_2}(t)$).

$$\frac{dm_{A\,CO_2}(t)}{dt} = \phi_{dif\,CO_2}(t) - \phi_{AW\,CO_2}(t) \tag{10}$$

The relation between the partial pressure of CO_2 in the alveolar air ($P_{A\,CO_2}$) and the concentration of CO_2 in the alveolar air is linear. The factor k_1 describes the linear relation between both variables.

$$P_{A\,CO_2}(t) = k_1 \cdot \frac{m_{A\,CO_2}(t)}{V_A(t)} \quad (11)$$

The flow of CO_2 in and out of the lungs ($\phi_{AW\,CO_2}(t)$) is dependent on the airflow ($\phi_{AW}(t)$) and during exhalation on the concentration of CO_2 in the lungs ($C_{A_{CO_2}}(t)$) or during inhalation on the concentration of CO_2 in the inspired air ($C_{atm_{CO_2}}(t)$).

Inhalation

$$\phi_{AW\,CO_2}(t) = C_{atm_{CO_2}}(t) \cdot \phi_{AW}(t) \quad (12)$$

Exhalation

$$\phi_{AW\,CO_2}(t) = C_{A_{CO_2}}(t) \cdot \phi_{AW}(t) \quad (13)$$

Diffusion between alveolar air and the pulmonary capillaries

The movement of CO_2 across the alveolar blood-gas barrier occurs by simple diffusion. Fick's law describes that the net flow is proportional to the difference in partial pressures of CO_2 in the alveolar air and the blood. The diffusion coefficient ($D_{L_{CO_2}}$) is dependent on the properties of both the barrier and the gas. If we assume that the alveolar air, blood-gas barrier and pulmonary capillary blood are uniform in space and time, then the net diffusion of CO_2 from the alveolar air to pulmonary capillary blood is described by equation 14.

$$\phi_{dif\,CO_2}(t) = D_{L_{CO_2}}\left(P_{v\,CO_2}(t) - P_{A_{CO_2}}(t)\right) \quad (14)$$

Arterial blood

The change of the total CO_2 mass in the arterial blood ($m_{a_{co_2}}(t)$) is equal to the sum of the flows that carry CO_2 in and out of the compartment. The outgoing flow consists of the diffusion flow and the flow of CO_2 molecules from the arterial blood to the venous blood ($\phi_{av\,CO_2}(t)$). The ingoing flow is the flow of CO_2 molecules from the venous blood to the arterial blood ($\phi_{va\,CO_2}(t)$)

$$\frac{dm_{a_{co_2}}(t)}{dt} = \phi_{va\,CO_2}(t) - \phi_{dif\,CO_2}(t) - \phi_{av\,CO_2}(t) \quad (15)$$

The flow of CO_2 from the venous to the arterial compartment ($\phi_{va\,CO_2}(t)$) and the flow of CO_2 from the arterial to the venous compartment ($\phi_{av\,CO_2}(t)$) are described by equation 16 and 17. The flows between the blood compartment are equal to the product of the blood flow in the compartment ($Q(t)$) and the concentration of CO_2 in the sending compartment.

$$\phi_{va\,CO_2}(t) = Q(t) \cdot \frac{m_{v_{CO_2}}(t)}{V_v} \quad (16)$$

$$\phi_{av\,CO_2}(t) = Q(t) \cdot \frac{m_{a_{CO_2}}(t)}{V_a} \quad (17)$$

The partial pressure of CO_2 in the arterial blood ($P_{a_{CO_2}}(t)$) is dependent on the mass concentration of CO_2 in the arterial blood ($C_{a_{CO_2}}(t)$). The carbon dioxide dissociation curve that describes the relationship between $P_{a_{CO_2}}(t)$ and $C_{a_{CO_2}}(t)$ is shown in figure 6. The curve is near-linear in the physiological range. Therefore, the constants k_2 and k_5 are introduced to describe this relation. The decreasing slope of the curve is likely caused by the buffering of CO_2 in bicarbonate. The buffering of CO_2 in bicarbonate will not be added to this first model to keep the model simple.

$$P_{a_{CO_2}}(t) = k_2 \cdot \frac{m_{a_{co_2}}(t)}{V_a} - k_5 \tag{18}$$

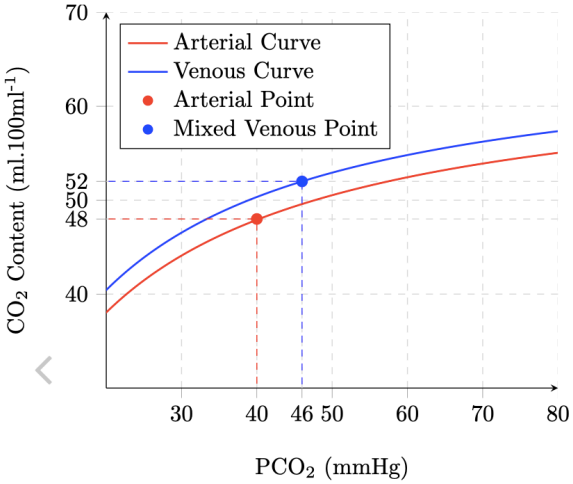

Figure 6 The dissociation curve of carbon dioxide. A tangent is added in the physiological range of the PaCO2.

Venous blood

The change of the total CO_2 mass in the venous blood ($m_{v_{co_2}}(t)$) is equal to the sum of the flows that carry CO_2 in and out of the compartment. The outgoing flow is the flow of CO_2 molecules from the venous blood to the arterial blood. The ingoing flow consists of the flow of CO_2 molecules from the arterial blood to the venous blood and the metabolic flow of CO_2 molecules ($\phi_{met\ CO_2}(t)$).

$$\frac{dm_{v_{co_2}}(t)}{dt} = \phi_{av\ CO_2}(t) + \phi_{met\ CO_2}(t) - \phi_{va\ CO_2}(t) \tag{19}$$

The partial pressure of CO_2 in the venous blood ($P_{v_{CO_2}}(t)$) is dependent on the mass concentration of CO_2 in the venous blood ($C_{v_{CO_2}}(t)$). The carbon dioxide dissociation curve that describes the relationship between $P_{v_{CO_2}}(t)$ and $C_{v_{CO_2}}(t)$ is shown in figure 6. The curve is near-linear in the physiological range. Therefore, the constants k_3 and k_4 are introduced to describe this relation. The constants k_3 and k_4 differ from k_2 and k_5 because the curve for the venous blood is shifted up compared to the arterial blood because of the Haldane effect. The Haldane effect describes the ability of haemoglobin to carry increased amounts of CO_2 in the deoxygenated state as opposed to the oxygenated state. As a result, a higher concentration of CO_2 is necessary in deoxygenated blood to reach a similar partial pressure.

$$P_{v_{CO_2}}(t) = k_3 \cdot \frac{m_{v_{CO_2}}(t)}{V_v} - k_4 \qquad (20)$$

A single blood compartment (simplification)

If the dynamical analysis of the original model proves impossible, a simplification should be applied. A simplification of the model is described here that turns the third order model in a second order model. The block for the arterial and the venous blood are merged into one single block that describes the total blood volume.

The change of the total CO_2 mass in the blood ($m_{b_{co_2}}(t)$) is equal to the sum of the flows that carry CO_2 in and out of the compartment. The outgoing flow is the flow of CO_2 molecules that diffuse to the lungs and the ingoing flow is the metabolic flow of CO_2 molecules.

$$\frac{dm_{b_{co_2}}(t)}{dt} = \phi_{met\ CO_2}(t) - \phi_{dif\ CO_2}(t) \qquad (21)$$

The partial pressure of CO_2 in the blood ($P_{b_{CO_2}}(t)$) is dependent on the mass concentration of CO_2 in the arterial blood. The constants k_6 and k_7 are used to describe the relation.

$$P_{b_{CO_2}}(t) = k_6 \cdot \frac{m_{b_{CO_2}}(t)}{V_b} + k_7 \qquad (22)$$

Metabolism

The metabolism encompasses all the chemical processes involved in energy production, energy release and growth. The metabolism requires a supply of O_2 and produces CO_2. The respiratory quotient (RQ) is the ratio of moles of CO_2 produced per moles of O_2 consumed at the tissue level.

$$\phi_{met\ CO_2}(t) = RQ \cdot \phi_{met\ O_2}(t) \qquad (23)$$

Perfusion

Perfusion ($Q(t)$) is the input variable for the subsystems 'arterial blood' and 'venous blood'. It represents the convective movement of blood that carries the dissolved gasses to and from the lung.

Central and peripheral chemoreceptors

The central and the peripheral chemoreceptors measure concentrations in the blood and the cerebrospinal fluid (CSF) and are the source of feedback for assessing the effectiveness of ventilation. When the $P_{a_{CO_2}}$ is too high or the $P_{a_{O_2}}$ is too low, the firing rate of the of the chemoreceptors will increase. This will in turn stimulate the breathing muscles and increase ventilation.

When the blood-gas parameters are nearly normal, the central chemoreceptors are of most importance. These receptors are sensitive to the pH of the cerebrospinal fluid (CSF) which is dependent on the $P_{a_{CO_2}}$ [44]. The central chemoreceptor response is slow, with a time constant in the range of 60 to 150 seconds [59].
The peripheral chemoreceptors are primarily sensitive to $P_{a_{O_2}}$, $P_{a_{CO_2}}$, and the pH of the arterial blood. Their contribution to respiratory drive in healthy subjects is modest. They are relevant in ventilated patients in whom hypoxemia, hypercapnia, and acidosis are more common [60]. The response of the peripheral chemoreceptors is fast, with a time constant of 10 to 30 seconds [59].

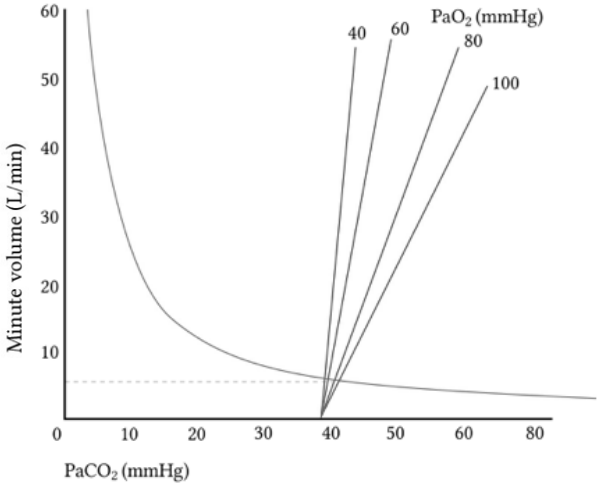

Figure 7 The minute volume induced by the ventilatory control centre is dependent on the partial pressure of carbon dioxide in the arterial blood. This figure presents the relationship in healthy subjects.

In figure 7 it is shown that the closed-loop relationship between $P_{a_{CO_2}}$ and the equilibrium value of the minute ventilation is linear when $P_{a_{CO_2}}$ increases above 40 mmHg (setpoint). When $P_{a_{CO_2}}$ decreases below 40 mmHg, the respiratory drive lowers gradually [61].

For now, the choice is made to only model the central chemoreceptors since these are of most importance in healthy subjects. In equation 24 the relation between the activity of the central chemoreceptors ($a_{ccr}\,(t)$) and the partial pressure of CO_2 in the arterial blood is presented. This relation is dependent on the desired value of the partial pressure of CO_2 in the arterial blood ($P_{a_{CO_2}\,desired}$), the activity of the central chemoreceptors in the normal situation (k_9) and the parameter k_8. The value of k_8 is likely dependent on $P_{a_{O_2}}$.

$$if\ P_{a_{CO_2}} > P_{a_{CO_2}\,setpoint}:$$

$$a_{ccr}(t) = \left(P_{a_{CO_2}}(t) - P_{a_{CO_2}\,desired}\right) \cdot k_8 + k_9 \qquad (24)$$

Central pattern generator

The central pattern generator (CPG) is located in the medulla and consists of the neurons that generate the respiratory rhythm. The CPG receives input from the central and peripheral chemoreceptors. In our model only the central chemoreceptors are considered and the relation between the activity of the central pattern generator (a_{cpg}) and the activity of the central chemoreceptors is described with the parameter k_{10}.

$$a_{cpg} = a_{ccr} \cdot k_{10} \qquad (25)$$

Breathing muscles

The muscles that produce a quiet inspiration are called the primary muscles of inspiration and include the diaphragm and the intercostal muscles. During inspiration, the muscles will create a decrease in the intrapleural pressure (P_{ip}) which makes air flow into the lungs. The size and frequency of the breaths are dependent on the output of the central pattern generator [62]. The central pattern generator can influence the frequency or the depths of the breaths. For this model, it is chosen to let the central pattern generator influence the intrapleural pressure that influences the depth of the breaths.

$$P_{ip}(t) = a_{cpg} \cdot k_{11} \tag{26}$$

In appendix 1 the implemented Simulink model and a table that contains the model variables and parameters, their abbreviations and their initial values is presented.

3.2. Dynamical analysis of the model

In this section, the dynamical analysis of the model is described. The model is created on a theoretical basis. Therefore, it is necessary to find out if the model that has been created, has the right structure to accurately describe the breathing system. With the dynamical analysis and subsequent simulations, we hope to analyse the dynamic behaviour of our model and state a hypothesis for the dynamic behaviour of the breathing system. In section 4 an experiment will be described that can be used to test this hypothesis.

The dynamic components that will be analysed are the equilibrium states, the eigenvalues and the time constants. When a system is stable and the system input is constant, all state variables of the system ($m_{A\,CO_2}(t), m_{a\,CO_2}(t)$ etc) will eventually reach a constant value which is called the equilibrium state.
The eigenvalues of a system describe the relationship between the individual system state variables and their derivatives. The time constants can be derived from the eigenvalues and describe the exponential response of a system after perturbation. The time constant is the time it takes for the systems response to reach 63.2% of its final equilibrium value.

The analysis that is conducted is an open-loop analysis, which means that only the process block of the model will be analysed, and the feedback loop is disregarded. The process and the controller will both add dynamic components to the dynamic behaviour of the full system. It is very difficult to determine what dynamic behaviour is induced by the process and what dynamic behaviour is induced by the controller. This makes interpretation difficult. Therefore, we have chosen to perform an open-loop analysis to identify the properties of the process first.

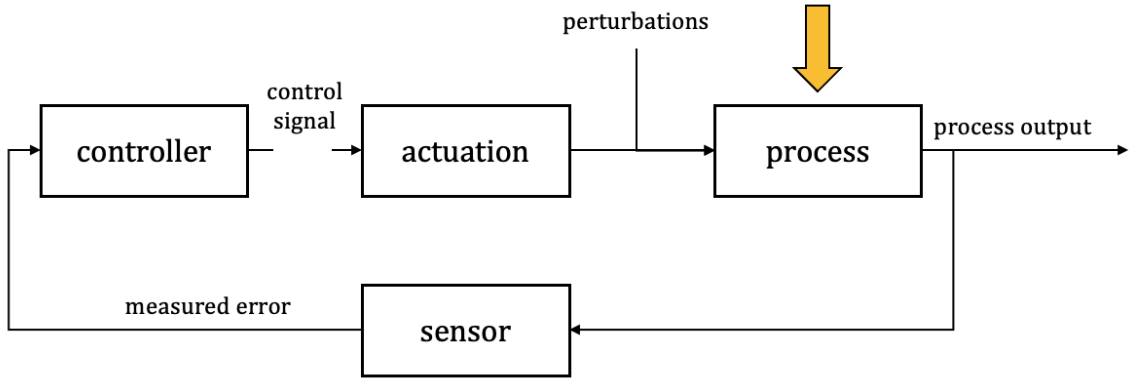

Figure 8 The different components of a closed-loop system. During open-loop analysis, the dynamic behaviour of the process is analysed, and the feedback-loop is disregarded.

The process model can be divided in two subsystems that can be analysed separately: the breathing mechanics and the gas exchange. The first subsystem represents the mechanics of breathing and can be analysed over one breathing cycle. More information about this subsystem can be found in the paragraph 'breathing mechanics' in section 3.1.2. The second subsystem represents the exchange of O_2 and CO_2 and can be analysed over multiple breathing cycles. More information about this subsystem can be found in the paragraphs 'alveolar air' to 'metabolism' in section 3.1.2.

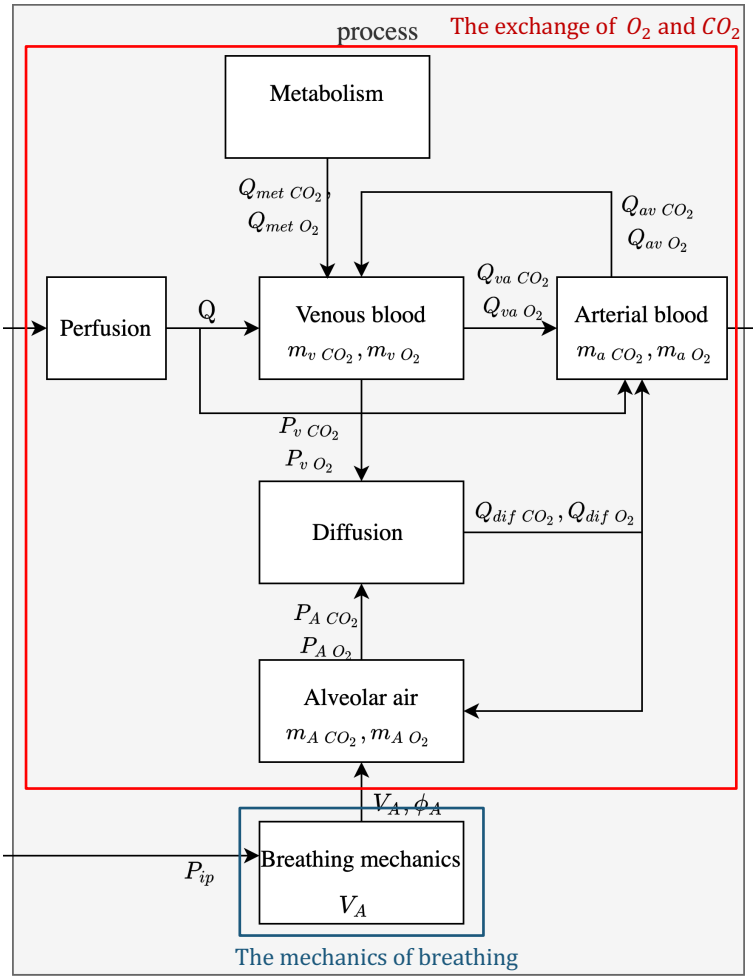

Figure 9 The process block of the model can be divided into two separate subsystems that can be analysed separately.

Both systems will be analysed separately. We will start with the open-loop analysis of the mechanics of breathing. The derivations belonging to the equations described in this section can be found in appendix 2.

3.2.1. Open-loop analysis of the mechanics of breathing

The first step in the analysis is determining the state equations. The state equations express the time derivatives of the state variables in variables and parameters. The subsystem 'mechanics of breathing' only has one state variable, $V_A(t)$. The corresponding state equation is created with the equations from section 3.1.2. and is presented as equation 27.

$$\frac{dV_A(t)}{dt} = \frac{C_{rs} \cdot P_V - C_{rs} \cdot P_{ip} - V_A(t) + V_{FRC}}{C_{rs} \cdot R_{rs}} \tag{27}$$

The second step in the analysis is the expression of the equilibrium state. In equation 28, the equilibrium state of $V_A(t)$ is expressed in model parameters. When these model parameters are known, the exact value of the equilibrium state of $V_A(t)$ can be determined.

$$V_{A\,eq} = C_{rs} \cdot P_{V\,eq} - C_{rs} \cdot P_{lp\,eq} + V_{FRC} \tag{28}$$

The eigenvalues of the system determine the relationship between the individual system state variables. Since this system only has one state variable, the eigenvalue is equal to the factor between this state variable and its derivative.

$$\lambda_1 = \frac{-1}{C_{rs} \cdot R_{rs}} \tag{29}$$

From this eigenvalue, the time constant can be calculated that represents how fast the lungs fill or empty during in- or expiration.

$$\tau_1 = C_{rs} \cdot R_{rs} \tag{30}$$

It is found that the time constant is the product of the respiratory resistance (R_{rs}) and compliance (C_{rs}).

3.2.2. Open-loop analysis of the exchange of O_2 and CO_2

Here, the gas exchange between the lungs and the blood will be described. To avoid repetition, only the equations for CO_2 will be described in this section of the report. In appendix 2 the equations for O_2 can be found.

Unfortunately, full analysis for this subsystem of the original model deemed impossible. The subsystem of the exchange of O_2 and CO_2 is a third order system with three state variables ($m_{A_{CO_2}}(t), m_{a_{CO_2}}(t), m_{b_{CO_2}}(t)$) which makes it complicated to analyse. In appendix 2 the steps of the analysis of the original third order system that were possible are shown.

The third order system can be replaced by a second order system that has one merged blood component instead of two separate compartments for arterial and venous blood. The state variables in this simplified model are the mass of carbon dioxide in the alveolar air ($m_{A_{CO_2}}(t)$) and the mass of carbon dioxide in the blood ($m_{b_{CO_2}}(t)$). The equations belonging to this model are described in the paragraph '*A single blood compartment (simplification)'* in section 3.1.2.

The first step in the analysis is the determination of the state equations. The state equations are created with the equations from section 3.1.2. Equation 31 presents the state equation of the mass of carbon dioxide in the alveolar air compartment. Since the system of the gas exchange is analysed separately from the system of the mechanics of breathing, the term $\phi_{AW}(t)$ is substituted by the term $\phi_{AW\,avg}(t)$. Where $\phi_{AW\,avg}(t)$ is equal to the average outflow and inflow of air per second over multiple cycles. $C_{CO_2\,atm}$ represents the mass carbon dioxide per litre atmospheric air.

$$\frac{dm_{A_{CO_2}}(t)}{dt} = D_L \cdot \left(k_6 \cdot \frac{m_{b_{CO_2}}(t)}{V_b} + k_7 - k_1 \cdot \frac{m_{A_{CO_2}}(t)}{V_{A\,gem}}\right) - \frac{m_{A_{CCO_2}}(t)}{V_{A\,gem}} \cdot \phi_{AW\,avg}(t) + C_{CO_2\,atm} \cdot \phi_{AW\,avg}(t) \tag{31}$$

Equation 32 presents the state equation of the mass of carbon dioxide in the merged blood compartment.

$$\frac{dm_{b_{CO_2}}(t)}{dt} = -D_L \cdot \left(k_6 \cdot \frac{m_{b_{CO_2}}(t)}{V_b} + k_7 - k_1 \cdot \frac{m_{A_{CO_2}}(t)}{V_{A\,gem}} \right) + \phi_{met}(t) \tag{32}$$

The second step in the analysis is the expression of the equilibrium state. In equations 33 and 34, the equilibrium states of $m_{A_{CO_2}}(t)$ and $m_{b_{CO_2}}(t)$ are expressed in model parameters and variables.

$$\frac{m_{A_{CO_2}\,eq}}{V_{A\,gem}} = \frac{\phi_{met}(t)}{\phi_{AW\,avg}(t)} + C_{CO_2\,atm} \tag{33}$$

$$\frac{m_{b_{CO_2}\,eq}}{V_b} = \frac{\left(-D_L \cdot k_7 + D_L \cdot k_1 \cdot \left(\frac{\phi_{met}(t)}{\phi_{AW\,avg}(t)} + C_{CO_2\,atm} \right) \right) + \phi_{met}(t)}{D_L \cdot k_6} \tag{34}$$

The state equations can be notated into the state space form that is represented in equation 35. In this form, the different state variables of the system are represented in the state vector $\mathrm{x}(t)$. The derivatives of the state variables are represented in the vector $\dot{\mathrm{x}}(t)$. The inputs of the system are represented by the vector $\mathrm{u}(t)$. The state-space representation provides a compact way to describe and analyse systems with multiple inputs and outputs. A and B represent the matrices that describe the relations between the vectors.

$$\dot{\mathrm{x}}(t) = \mathrm{A} \cdot \mathrm{x}(t) + \mathrm{B} \cdot \mathrm{u}(t) \tag{35}$$

The state matrix A is of use for determination of the eigenvalues. After filling in the vectors $\dot{\mathrm{x}}(t)$ and $\mathrm{x}(t)$, the state matrix is determined. It is important to note that since our model is not linear, the state matrix contains the variable $\phi_{AW\,avg}(t)$. If we wanted to obtain a numeric value we would have to choose an equilibrium value for $\phi_{AW\,avg}(t)$ and we would have to linearize the state equations around this point. However, since we are only interested in the expressions for the eigenvalues, we can leave the variable in the state matrix.

$$\begin{bmatrix} \dot{m}_{A\,CO_2} \\ \dot{m}_{b\,CO_2} \end{bmatrix} = A \cdot \begin{bmatrix} m_{A\,CO_2} \\ m_{b\,CO_2} \end{bmatrix}$$

$$A = \begin{bmatrix} \frac{-k_1 \cdot D_L - \phi_{AW\,avg}(t)}{V_{A\,gem}} & \frac{D_L \cdot k_6}{V_B} \\ \frac{D_L \cdot k_1}{V_{A\,gem}} & \frac{-D_L \cdot k_6}{V_B} \end{bmatrix}$$

The eigenvalues of the system are determined by taking the determinant of the A-matrix and setting it to zero.

$$|A - \lambda I| = 0$$

After performing the calculations described in appendix 2 the following expressions for the eigenvalues are obtained.

$$\begin{bmatrix}\lambda_1\\ \lambda_2\end{bmatrix}=\begin{bmatrix}-\frac{1}{2}\left(\frac{k_1\cdot D_L+\phi_{AW\,avg}(t)}{V_{A\,gem}}+\frac{D_L\cdot k_6}{V_b}\right)+\frac{1}{2}\sqrt{\left(\frac{k_1\cdot D_L+\phi_{AW\,avg}(t)}{V_{A\,gem}}+\frac{D_L\cdot k_6}{V_b}\right)^2-4\cdot\frac{\phi_{AW\,avg}(t)}{V_{A\,gem}}\cdot\frac{D_L\cdot k_6}{V_b}}\\ -\frac{1}{2}\left(\frac{k_1\cdot D_L+\phi_{AW\,avg}(t)}{V_{A\,gem}}+\frac{D_L\cdot k_6}{V_b}\right)-\frac{1}{2}\sqrt{\left(\frac{k_1\cdot D_L+\phi_{AW\,avg}(t)}{V_{A\,gem}}+\frac{D_L\cdot k_6}{V_b}\right)^2-4\cdot\frac{\phi_{AW\,avg}(t)}{V_{A\,gem}}\cdot\frac{D_L\cdot k_6}{V_b}}\end{bmatrix} \quad (36)$$

The system has two different eigenvalues and the corresponding equations could be expressed in model parameters. Three different terms of aggregated parameters are present in the expressions. These terms are $\frac{k_1\cdot D_L}{V_{A\,gem}}$ (1), $\frac{\phi_{AW\,avg}(t)}{V_{A\,gem}}$ (2) and $\frac{D_L\cdot k_6}{V_b}$ (3). To refer more easily to these terms, each term has an assigned number that is notated in brackets behind the term.

Terms 1 and 2 describes the relation between the current mass of CO_2 and the change of the mass of the CO_2 in the alveolar space. Term 3 describes the relation between the current mass of CO_2 and the change of the mass of CO_2 in the blood.

When we look closely at the expressions of the eigenvalues, it can be seen that the sum of the three different terms occurs both for and under the square root. When looking at the theoretical values of some of the parameters, it is expected that the sum of the three term is large compared to the product of term 2 and 3 that is located under the square root. The eigenvalues can thus be represented as $-\frac{1}{2}a\pm\frac{1}{2}\sqrt{a^2-b}$ with $b<<a$. This results in the expectation of one eigenvalue close to zero and one eigenvalue that is further from zero. Since the time constants are equal to the inverse of the eigenvalues, this results in a small and a large time constant. No expectations can yet be stated about the exact values of these eigenvalues and time constants.

From the expressions of the eigenvalues, the expressions of the time constants are composed.

$$\begin{bmatrix}\tau_1\\ \tau_2\end{bmatrix}=\begin{bmatrix}\frac{2}{\left(\frac{k_1\cdot D_L+\phi_{AW\,avg}(t)}{V_{A\,gem}}+\frac{D_L\cdot k_6}{V_b}\right)-\sqrt{\left(\frac{k_1\cdot D_L+\phi_{AW\,avg}(t)}{V_{A\,gem}}+\frac{D_L\cdot k_6}{V_b}\right)^2-4\cdot\frac{\phi_{AW\,avg}(t)}{V_{A\,gem}}\cdot\frac{D_L\cdot k_6}{V_b}}}\\ \frac{2}{\left(\frac{k_1\cdot D_L+\phi_{AW\,avg}(t)}{V_{A\,gem}}+\frac{D_L\cdot k_6}{V_b}\right)+\sqrt{\left(\frac{k_1\cdot D_L+\phi_{AW\,avg}(t)}{V_{A\,gem}}+\frac{D_L\cdot k_6}{V_b}\right)^2-4\cdot\frac{\phi_{AW\,avg}(t)}{V_{A\,gem}}\cdot\frac{D_L\cdot k_6}{V_b}}}\end{bmatrix} \quad (37)$$

3.2.3. Model simulations

The model was implemented in Simulink and simple simulations were performed. These simulations can provide more insight in the dynamic behaviour of the model. The initial model parameters were estimated from literature and can be found in table 10 in appendix 1. Since the parameters in the model are not yet identified, the model simulations should only be analysed qualitatively. In figure 10 the change of the alveolar volume over time is shown. The shape of this graph is determined by the simple first-order model that was used to describe the breathing mechanics.

In figure 11 the initial responses of the partial pressure of CO_2 in the blood and the alveolar air are shown. As expected, these variables progress exponentially and eventually reach an equilibrium value. Both responses seem to have similar time constants. Which means that if the mass of CO_2 in the alveolar air is in equilibrium, the mass of CO_2 in the blood is also in equilibrium. The responses may be the sum of two exponential responses. Fluctuations can be seen in the response that represent the in- and outflow of CO_2 caused by the breathing cycle.

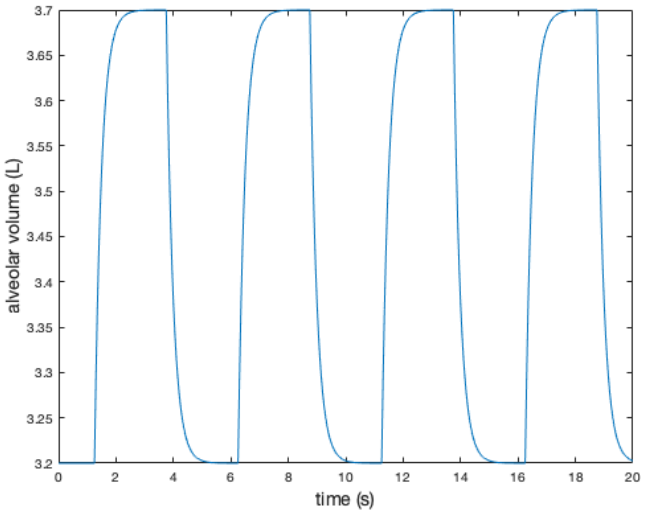

Figure 10 The simulated alveolar volume over time.

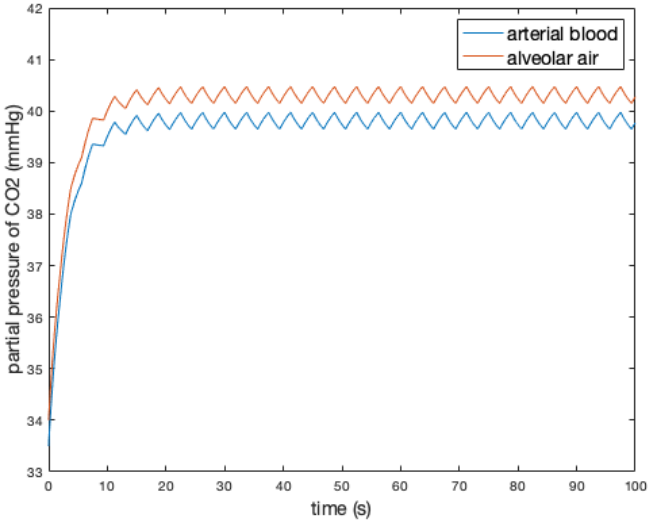

Figure 11 The simulated initial response of the partial pressure of CO2 for the blood and the alveolar air.

In figure 12 the influence of the average in- and outflow of air (minute ventilation/60) on the initial simulated response of the partial pressure in the blood is shown. It is shown that an increase in the average airflow causes a decrease in time constant and a decrease in the equilibrium value of the partial pressure of CO_2 in the blood. This complies with equations 34 and 37. In equation 34 it is shown that when the average airflow $\phi_{AW\ avg}(t)$ increases, the nominator will decrease and the equilibrium value for the mass of CO_2 in the blood ($m_{b_{CO_2\ eq}}$) will therefore decrease.

In equation 37 it can be seen that the large time constant is equal to

$$\frac{2}{\left(\frac{k_1 \cdot D_L + \phi_{AW\ avg}(t)}{V_{A\ gem}} + \frac{D_L \cdot k_6}{V_b}\right) - \sqrt{\left(\frac{k_1 \cdot D_L + \phi_{AW\ avg}(t)}{V_{A\ gem}} + \frac{D_L \cdot k_6}{V_b}\right)^2 - 4 \cdot \frac{\phi_{AW\ avg}(t)}{V_{A\ gem}} \cdot \frac{D_L \cdot k_6}{V_b}}}$$

in section 3.2.2 it was described that it is expected that both $\frac{k_1 \cdot D_L + \phi_{AW\ avg}(t)}{V_{A\ gem}} + \frac{D_L \cdot k_6}{V_b}$ terms (before and under the root) will cancel each other out. Thus, the term $4 \cdot \frac{\phi_{AW\ avg}(t)}{V_{A\ gem}} \cdot \frac{D_L \cdot k_6}{V_b}$ will likely determine the size of the time constant. When $\phi_{AW\ avg}(t)$ increases, this term will increase and since it is located in the denominator, the time constant will decrease.

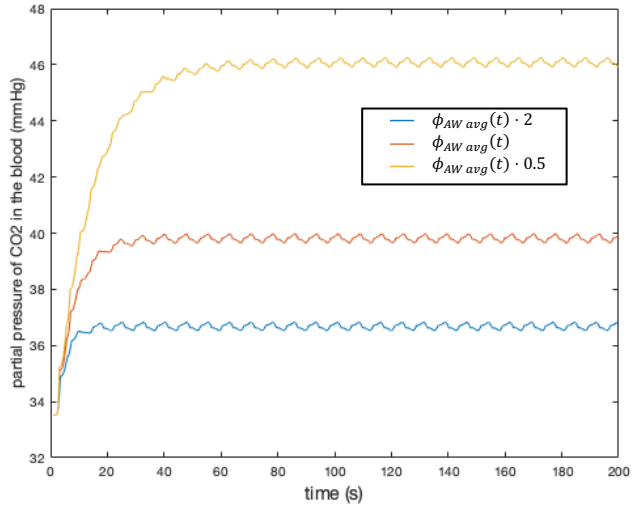

Figure 12 The influence of the average airflow on the simulated initial response of the partial pressure of CO2 in the blood

3.3. Implications of the dynamical analysis for the experiment design

A two-order model with low complexity that encompasses the gas exchange and the respiratory drive was created. Several simplifications of reality were applied in this model. The buffering of carbon dioxide in bicarbonate and the relation between carbon dioxide and the acid-base balance of the blood were not included.

It was not possible to analyse the dynamical behaviour of the original model. For this reason, a slightly simplified model was created that has one blood compartment instead of two. It was possible to analyse the dynamical behaviour of this slightly simplified model.

Expressions for the eigenvalues, time constants and equilibrium values were derived. From these expressions it followed that the model has one eigenvalue that is close to zero and one eigenvalue that is further from zero. As a result, the model response can be described by a fast and a slow exponential response. It is not known what causes these two responses. Our expectation is that directly after the perturbation, the concentration of carbon dioxide in the alveolar air is much higher than the concentration of carbon dioxide in the blood and the atmosphere. During the first few breaths the alveolar air will be almost completely replaced by atmospheric air and the concentration of carbon dioxide will decrease fast (fast response). When the concentration of carbon dioxide in the alveolar air is slightly lower than the concentration of carbon dioxide in the blood, the concentration in the alveolar air will lower more gradually because carbon dioxide molecules will diffuse constantly from the blood to the alveolar air (slow response).

It also followed that the concentrations of O_2 and CO_2 in the alveolar space and blood are dependent on the average airflow, which is dependent on the minute ventilation, and will eventually reach equilibrium value. The eigenvalues, time constants and equilibrium values are expressed in model parameters and no expectations can yet be stated about their exact values. The hypothesis is that the behaviour of the real breathing system will comply with the model's dynamical behaviour.
Experimental measurements should be performed to allow for comparison between the dynamic behaviour of the model and the dynamic behaviour of the real breathing system. If the qualitative behaviour is similar, this would indicate a suitable model structure.

If the dynamic behaviour of the model is similar to that of the real beathing system, it may be possible to identify aggregated parameter groups of the model. We can then try to make predictions with the identified model to show a first application of the model. In section 2 it was described that one of the ways a model could add value to clinical practice was by providing insight in the respiratory parameters and variables and making predictions of patient response to adjustments in ventilator settings. In the next section, the design of the experiment that is used to test the hypothesis that the behaviour of the real breathing system will comply with the model's dynamical behaviour is described. With this experiment it may be possible to perform a first experimental evaluation of the model.

4. Experimental evaluation of the model

The aim of this section is to describe how the experimental measurements and subsequent data analysis should be performed to obtain relevant information about the dynamic behaviour of the breathing system. From the dynamical analysis described in section 3 followed that the model response can be described by the sum of a fast and a slow exponential time constant. It also followed that the concentrations of O_2 and CO_2 in the alveolar space and blood are dependent on the minute ventilation and will eventually reach equilibrium value. The design of the experiment is based on the hypothesis that the real breathing system will present the same dynamic behaviour as the model.

If the dynamic behaviour of the model is similar to that of the real beathing system, it may be possible to identify aggregated parameter groups of the model. We can then try to make predictions with the identified model to show a first application of the model.

Before we will go into detail about the experimental protocol and data analysis, a description about the general process of model identification and validation is given. Adapting the model parameters to a specific person or situation is called model identification. Models are often established on a theoretical basis and the exact values of the model parameters may be unknown. The values of these parameters can be determined from experimental measurements. The response of the model is compared to the experimental measurements (identification measurement set) and the parameters are adapted till the model response is similar to the measured response. The result is an identified model. Then, simulations will be performed with the identified model and the model responses are again compared to experimental measurements (validation measurement set). If the response of the final model is similar to the validation measurement set, this indicates a well-structured and -identified model. It is important that the measurements used for validation are different than the measurements used for identification of the model. Similar datasets may result in an overestimation of the performance of the model.

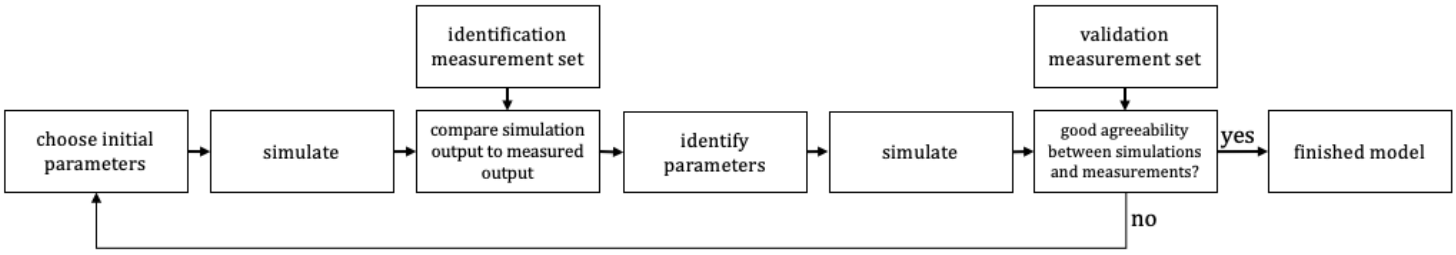

Figure 13 General workflow of model identification and validation.

It is important to keep in mind that the main aim of the experiment is not to identify and validate the model. The main aim is to create a first experimental protocol that is based on the dynamical analysis of the model and to find out what insights can be obtained from this protocol. For this reason, this experiment was only conducted with one subject, being the M-student who performed this research, and no ethics application was yet submitted. In a later stadium, more extensive research with a larger study population may be conducted to improve validity.

4.1. Experimental protocol

4.1.1. general concept

When a person breathes in air with an increased or decreased fraction of inspired carbon dioxide ($F_{insp}CO_2$) for a period of time, this will create perturbation of the equilibrium state of the breathing system. This means that the fractions of O_2 and CO_2 in the alveolar air and the blood will deviate from their equilibrium values.

When the person starts breathing atmospheric air again, the fractions of O_2 and CO_2 in the alveolar air and the blood will return to their original equilibrium state. From the dynamical analysis described in section 3, it is suspected that the initial condition response will consist of the sum of two exponential responses. One response with a fast time constant and one response with a slow time constant. In figure 14 it is presented how such a response may look like. The hypothesis was that these time constants and equilibrium values are dependent on the average in- and outflow of air. For this reason, it is suspected that different time constants and equilibrium values will be obtained when someone is breathing with different minute ventilations.

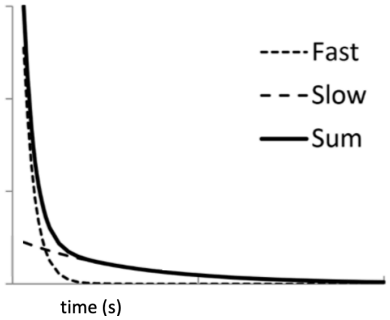

Figure 14 The sum of a fast and a slow exponential response. The response will eventually reach an equilibrium value. This value does not have to be equal to zero.

The hypothesis that followed from the dynamical analysis is that if multiple measurements are conducted and during each measurement the subject breathes with a different constant minute ventilation, different equilibrium values for the concentration of O_2 and CO_2 in the alveolar air and the blood will be reached and different time constants will describe the transient response. This is shown in figure 12 that presents the simulations that were performed with the model. The experimental setup and protocol are based on this principle.

4.1.2. experimental setup

The measurements were conducted in the TechMed centre. During the experiment, the subject was seated in upright position on a chair and was breathing through the mask of the Viasys Oxycon Mobile device. During all measurements, the flow sensor in the Oxycon mobile measured the airflow, tidal volume and the respiratory rate. Oxygen and carbon dioxide sensors in the Oxycon mobile device measured the fraction of inspired carbon dioxide ($F_{insp}CO_2$) and oxygen ($F_{insp}O_2$) and the fraction of expired carbon dioxide ($F_{exp}CO_2$) and oxygen ($F_{exp}O_2$). After every measurement, the obtained data was stored in a designated file for offline analysis.

Elevation of the $F_{insp}CO_2$ and reduction of the $F_{insp}O_2$ (perturbation) was achieved by rebreathing in a balloon that was attached to the Oxycon mobile mask. After the period of perturbation which lasted 180 seconds, the balloon was decoupled manually.

During parts of the measurements, the breathing frequency was controlled by an auditory tone generated from a computer. To maintain a constant inspiratory period-to-respiratory period (IE/II) ratio of 0.5, subjects were instructed to inhale when the first beep was heard and exhale when the second beep was heard. The tidal volume was displayed real-time on the screen and subject was instructed to maintain a constant tidal volume. The measurements were stopped when the subject indicated that this was desirable.

Figure 15 Person wearing the Viasys Oxycon Mobile device

4.1.3. measurement protocol

Four different measurements were performed. All measurements were repeated three times for improved accuracy. During the first 180 seconds of all the measurements, the subject rebreathed in a balloon. This caused the Fi_{CO_2} to increase and this caused the Fi_{O_2} to decrease. After 180 seconds, the balloon was manually decoupled from the mask and the subject was breathing atmospheric air for a period of 600 seconds. This is called the period of recovery.

During all measurements, the subject was breathing with a natural non-imposed frequency during the period of rebreathing. In the first measurement, the subject was also breathing with a natural frequency during the period of recovery. In the second to fourth measurement, the subject was breathing with an imposed breathing frequency and tidal volume, and therefore minute ventilation during the period of recovery. The chosen frequencies were 12, 16 and 20 breaths per minute. The exact measurement protocol can be seen in table 2.

The different imposed frequencies will result in different values for the minute ventilation and are therefore necessary to test our hypothesis. The hypothesis that followed from the dynamical analysis was that if multiple measurements were conducted and during each measurement the subject breathed with a different constant minute ventilation, different equilibrium values for the concentration of O_2 and CO_2 in the alveolar air and the blood would be reached and different time constants would describe the transient response.
We also wanted to perform an open-loop analysis, and therefore it was important that the ventilatory control function of the patient could not influence the minute ventilation by adapting the breathing frequency or the tidal volume.

Table 2 The measurement protocol

Measurement	Task	Breathing frequency (b/m)	Time (s)	repetitions
1	rebreathing	natural	180	3
	recovering	natural	600	
2	rebreathing	natural	180	3
	recovering	12	600	
3	rebreathing	natural	180	3
	recovering	20	600	
4	rebreathing	natural	180	3
	recovering	16	600	

4.2. Data analysis

Due to limited observability, it was not possible to measure the blood gasses during the experiment. It was also not possible to measure the concentrations of O_2 and CO_2 in the alveolar air directly. It was assumed that the fractions of O_2 and CO_2 in the alveolar air could be described by the $F_{exp}CO_2$ and $F_{exp}CO_2$.

Measurement 2 and 3 were used for identification purposes. The measured $F_{exp}CO_2$ and $F_{exp}CO_2$ over time from the measurements were used to identify the time constants and equilibrium values. Since each measurement was repeated three times, the repetitions were averaged to form one graph per measurement. Using the least squares fitting method, an exponential function of the form $y = a \cdot \left(1 - e^{b \cdot x}\right) + c$ was fitted on the slow and the fast component of the graphs belonging to the $F_{exp}CO_2$ and $F_{exp}CO_2$. If the fitting was possible, the time constants could be determined from the found values for b and the equilibrium value could be determined from the found values for a and c.

For reliable identification of the time constants and equilibrium values, the minute ventilation should be constant. To check if this was the case, the minute ventilation was calculated by taking the product of the tidal volume and the respiratory rate every 5 seconds. The result was plotted over time and visually inspected to assess if minute ventilation was constant.

4.2.1. Identification of model parameter aggregates using the time constants and equilibrium values.

Only the identification process of the model parameter aggregates for carbon dioxide is described here. The identification process for oxygen is described in appendix 2.

If it was possible to determine the time constants from the measurements, the found time constants were filled in in equation 38 and 39. Equation 38 contains the expression for the small time constant that was derived during the dynamical analysis.

$$\tau_{small} = \frac{2}{\left(\frac{k_1 \cdot D_{L\,CO2} + \phi_{AW\,avg}(t)}{V_{A\,gem}} + \frac{D_{L\,CO2} \cdot k_6}{V_b}\right) + \sqrt{\left(\frac{k_1 \cdot D_{L\,CO2} + \phi_{AW\,avg}(t)}{V_{A\,gem}} + \frac{D_{L\,CO2} \cdot k_6}{V_b}\right)^2 - 4 \cdot \frac{\phi_{AW\,avg}(t)}{V_{A\,gem}} \cdot \frac{D_{L\,CO2} \cdot k_6}{V_b}}} \quad (38)$$

Equation 39 contains the expression for the large time constant that was derived during the dynamical analysis.

$$\tau_{large} = \frac{2}{\left(\frac{k_1 \cdot D_{L\,CO2} + \phi_{AW\,avg}(t)}{V_{A\,gem}} + \frac{D_{L\,CO2} \cdot k_6}{V_b}\right) - \sqrt{\left(\frac{k_1 \cdot D_{L\,CO2} + \phi_{AW\,avg}(t)}{V_{A\,gem}} + \frac{D_{L\,CO2} \cdot k_6}{V_b}\right)^2 - 4 \cdot \frac{\phi_{AW\,avg}(t)}{V_{A\,gem}} \cdot \frac{D_{L\,CO2} \cdot k_6}{V_b}}} \quad (39)$$

The unknown parameters in both equations were divided into two parameter groups indicated with the capital G. The average airflow ($\phi_{AW\,avg}(t)$) and time constant (τ_{long}) could be determined from the measurements. The parameter $V_{A\,gem}$ was set in advance because it could be reliably estimated from literature. The exact value is presented in table 10 in appendix 1.

$$\tau_{large} = \frac{2}{\left(G_1 + \frac{\phi_{AW\,avg}(t)}{V_{A\,gem}} + G_2\right) \pm \sqrt{\left(G_1 + \frac{\phi_{AW\,avg}(t)}{V_{A\,gem}} + G_2\right)^2 - 4 \cdot \frac{\phi_{AW\,avg}(t)}{V_{A\,gem}} \cdot G_2}} \quad (40)$$

with

$$G_1 = \frac{D_{L\,CO2} \cdot k_1}{V_{A\,gem}}$$

$$G_2 = \frac{D_{L\,CO2} \cdot k_6}{V_B}$$

The least squares fitting method was used to attempt to obtain the optimal combination of values for G_1 and G_2.

If it was possible to determine the equilibrium values of $F_{exp}CO_2$, the found equilibrium values were filled in in equation 41.

$$\frac{m_{A_{CO_2}\,eq}}{V_{A\,gem}} = \frac{\phi_{met}\,(t)}{\phi_{AW\,avg}(t)} + C_{CO_2\,atm} \quad (41)$$

Since, the output that we measured is not the mass concentration of CO_2 $\left(\frac{m_{A_{CO_2}\,eq}}{V_{A\,gem}}\right)$ but the fraction of expired CO_2 $\left(F_{E_{CO_2}\,eq}\right)$, we have to replace $\frac{m_{A_{CO_2}\,eq}}{V_{A\,gem}}$ with $F_{E_{CO_2}\,eq} \cdot k_{13}$. The constant k_{13} is necessary to equalize the units since $F_{E_{CO_2}\,eq}$ has the unit % and the $\frac{m_{A_{CO_2}\,eq}}{V_{A\,gem}}$ has the unit $\frac{g}{L}$.

$$F_{E_{CO_2}\,eq} \cdot k_{13} = \frac{\phi_{met}\,(t)}{\phi_{AW\,avg}(t)} + C_{CO_2\,atm} \tag{42}$$

The unknown parameters k_{13} and $\phi_{met\,avg}$ in the equations were collected into the parameter group indicated with G_3.

$$F_{E_{CO_2}\,eq} = \frac{G_3}{\phi_{AW\,avg}(t)} + C_{CO_2\,atm} \tag{43}$$

with

$$G_3 = \frac{\phi_{met}\,(t)}{k_{13}}$$

4.2.2. Simulations and validation of the identified model

If identification of the parameter groups was possible, simulations were performed with the identified model to compare the model responses to measurement 4. Measurement 4 was not used for model identification to limit the overestimation of the performance of the model. During the simulations, the $F_{insp}CO_2$ was increased for 180 seconds and after this period the $F_{insp}CO_2$ was set to zero to mimic the situation in the experiment. The average airflow in the model was set to the same value used in measurement 4. The time constants and the equilibrium value of Fe_{CO_2} belonging to the simulated response were compared to the time constant and the equilibrium value of Fe_{CO_2} of measurement 4.

4.3 Experimental results

In this section, the findings of the experimental measurements and subsequent analysis are presented. These results give insight into the correspondence between the simulated behaviour of the model and the behaviour of the real breathing system. The results are organized based on the research questions.

4.3.1. What relevant information about the dynamic behaviour of the real breathing system can be obtained from experimental measurements?

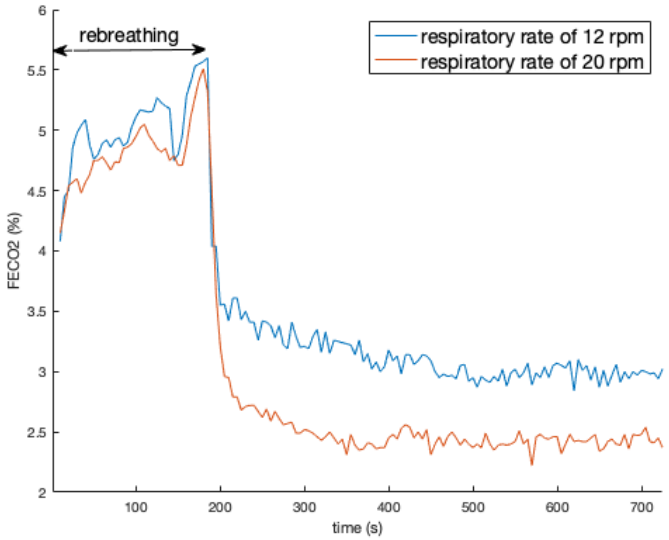

Figure 16 The averaged graphs belonging to measurement 2 and 3. The transient response of the fraction of the expired CO_2 after a period of rebreathing is displayed.

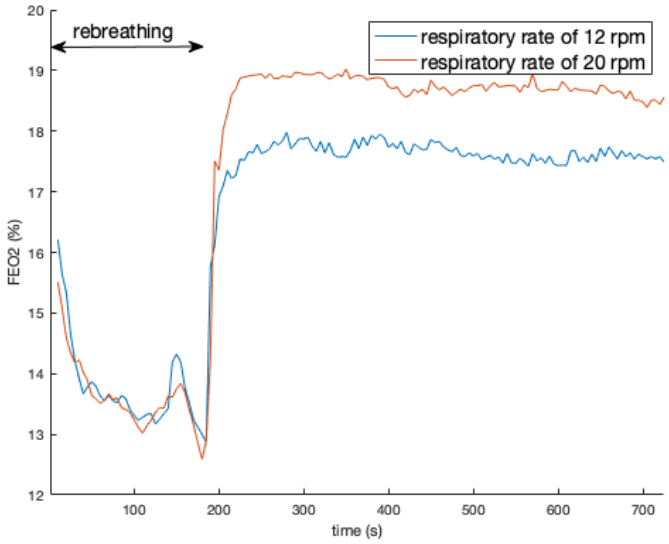

Figure 17 The averaged graphs belonging to measurement 2 and 3. The transient response of the fraction of the expired O_2 after a period of rebreathing is displayed.

In figure 16 and 17 it is shown that the response after a period of rebreathing appears to have two different components. The first is a fast exponential component with a time constant in the order of seconds. The second is a slow exponential component with a time constant in the order of minutes. This complies with the hypothesis that followed from the dynamical analysis in section 3. The total detected response is the sum of the two exponential responses.

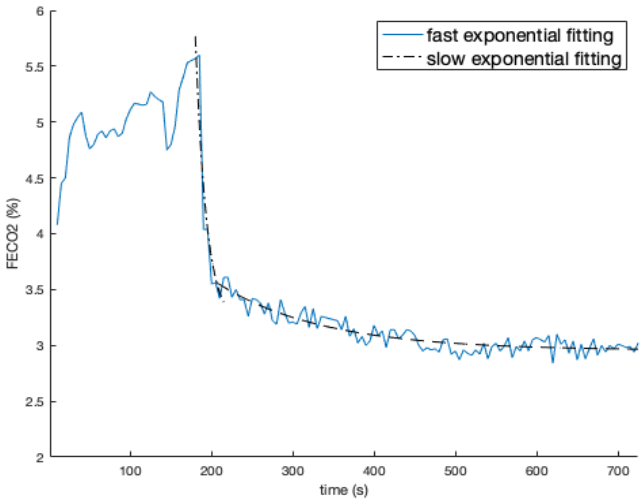

Figure 18 The progression of the fraction of expired CO_2 belonging to measurement 2 (12 rpm) with two fitted exponential fittings belonging to the slow and the fast exponential component.

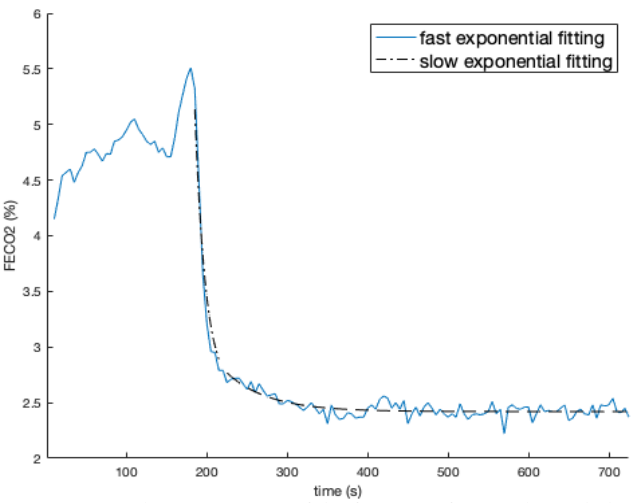

Figure 19 The progression of the fraction of expired CO_2 belonging to measurement 3 (20 rpm) with two fitted exponential fittings belonging to the slow and the fast exponential component.

Figure 18 and 19 show the fits that were found for the fast and slow exponential component of $F_{exp}CO_2$ for measurement 2 (12 rpm) and 3 (20 rpm). The squared norms of the residuals of al fittings are presented in appendix 3.

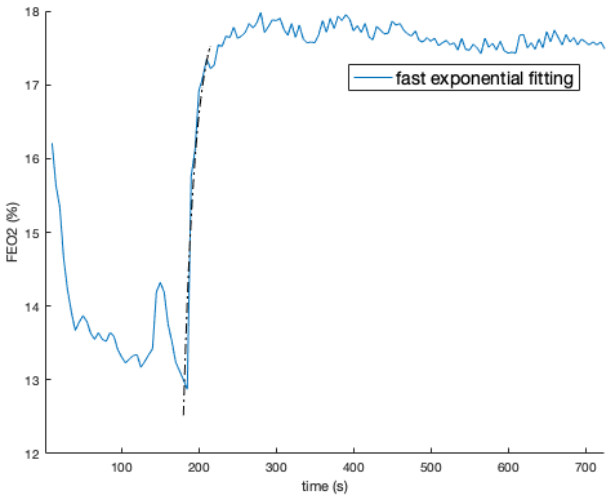

Figure 20 The graph of the progression of the fraction of expired O_2 belonging to measurement 2 (12 rpm) with two fitted exponential functions belonging to a slow and a fast time constant.

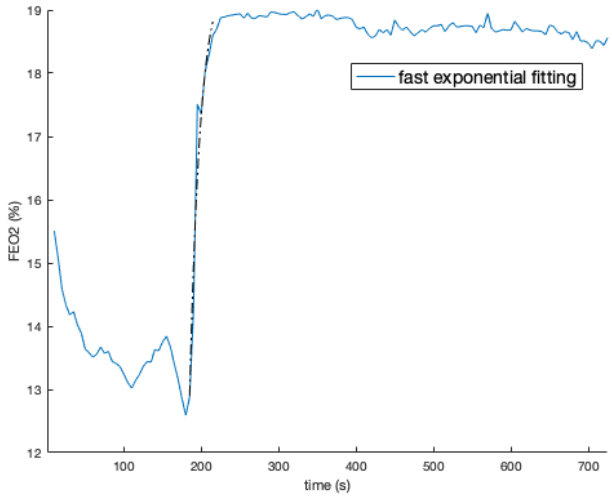

Figure 21 The graph of the progression of the fraction of expired O_2 during measurement 3 (20 rpm) with two fitted exponential functions belonging to a slow and a fast time constant.

Figure 20 and 21 show the fits that were found for the fast exponential component of $F_{exp}O_2$. The squared norms of the residuals of al fittings are presented in appendix 3. No acceptable fit was found for the slow exponential component of $F_{exp}O_2$.

In table 3 it is shown that the when the subject was breathing with a respiratory rate of 20 a lower equilibrium value for the fraction of expired CO_2 and smaller time constants were found compared to when the subject was breathing with a respiratory rate of 12.

Table 3 The equilibrium values and the small and the large time constants belonging to the fitted exponentials of the response of the fraction of expired CO2 are presented for measurement 2 (12 rpm) and 3 (20 rpm).

Respiratory rate	Equilibrium value (%)	Large time constant (s)	small time constant (s)
12	3.0	130.2	13.6
20	2.4	52.5	13.5

In table 4 it is shown that when the subject was breathing with a respiratory rate of 20 a smaller time constant was found for the response of the fraction of the expired O_2 compared to when the subject was breathing with a respiratory rate of 12.

Table 4 The small time constants belonging to the fitted exponentials of the response of the fraction of expired O2 are presented for measurement 2 (12 rpm) and 3 (20 rpm).

Respiratory rate	small time constant (s)
12	15.3
20	13.6

4.2.2. How can this information be used to evaluate the identifiability of the respiratory parameters as well as the model accuracy in predicting ventilatory responses?

Model identification

The model parameter identification method described in section 4.1 can only be conducted when, after rebreathing, the minute ventilation, and therefore the average airflow, is constant during the measurement. The figures in appendix 3 show that during the measurements the minute ventilation was not constant from 180 to 210 seconds. As a result, the fast exponential component cannot be used for model parameter identification purposes. Only the slow exponential component can be used to identify the model parameters. Since the slow exponential component could not be identified for oxygen, only the model that describes carbon dioxide can be identified.

The optimally fitted values of the different parameter groups are stated in table 5.

Table 5 The fitted optimal values for the different parameter group.

Parameter group	**Parameters**	**Identified value**
G_1	$\frac{D_{L\,CO2} \cdot k_1}{V_{A\,gem}}$	20.7
G_2	$\frac{D_{L\,CO2} \cdot k_6}{V_b}$	41.7
G_3	$\frac{\phi_{met\ avg}}{k_{13}}$	0.2

In table 6 it is shown that the large time constant belonging to the measurement 2 (12 rpm) is predicted 20.68 seconds too small by the identified model. The time constant belonging to measurement 3 (20 rpm) is predicted 13.23 seconds too large by the identified model. The model could not be identified to fit both measurement 2 and 3 perfectly.

Table 6 The predicted and the measured time constants and their difference for measurement 2 (12 rpm) and 3 (20 rpm).

Respiratory rate	**Measured time constant (s)**	**Predicted large time constant (s)**	**Error (s)**
12	130.2	109.5	-20.7
20	52.5	65.7	13.2

In table 7 it is shown that the equilibrium value predicted by the identified model and the measured equilibrium value are almost similar.

Table 7 The predicted and the measured equilibrium value for the fraction of expired CO_2 and their difference for measurement 2 (12 rpm) and 3 (20 rpm).

Respiratory rate	**Measured equilibrium value (%)**	**Predicted equilibrium value (%)**	**Error (%)**
12	3.0	2.9	0.0
20	2.4	2.4	0.0

Model validation

In figure 22 it is shown that the response predicted by the identified model is qualitatively similar to the measured response in measurement 4.

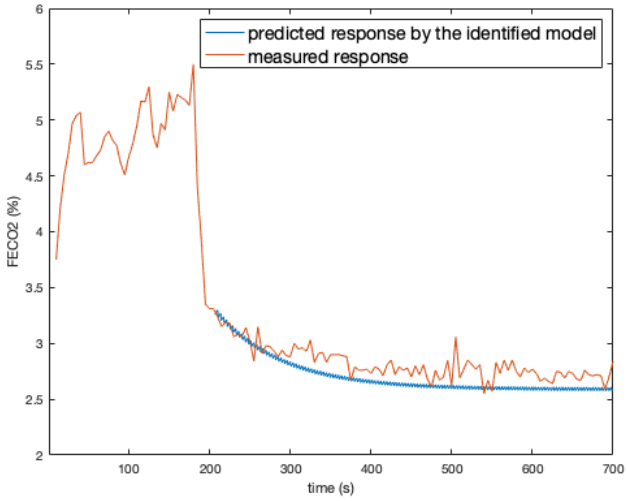

Figure 22 The predicted response of the identified model and the measured response belonging to the breathing frequency of 16 breaths per minute.

In table 8 it is shown that for measurement 4 the identified model predicted an equilibrium of the fraction of expired CO_2 that was 0.13 percent lower than the measured value. The identified model predicted a time constant that was 19.94 seconds smaller than the measured time constant.

Table 8 The predicted and the measured time constant and equilibrium value and their difference for measurement 4.

	predicted	**measured**	**error**
Large time constant (s)	82.38	102.32	-19.94
Equilibrium value (%)	2.59	2.72	-0.13

4.3 Implications of the experimental results for the applicability of the model

The main aim of this section was to create a first experimental protocol that is based on the dynamical analysis of the model and to find out what insights can be obtained from this protocol.

For carbon dioxide, the experimental protocol is suitable for analysis of the dynamic response of the $F_{exp}CO_2$ which is related to the m_ACO_2. One interesting finding from the experimental measurements is that the dynamic response of the $F_{exp}CO_2$ consists of a fast and a slow exponential component. It was also found that the $F_{exp}CO_2$ reaches an equilibrium state when breathing with a constant minute ventilation. The value of this equilibrium state was dependent on the minute ventilation. This complies with the hypothesis that followed from the dynamical analysis of the model described in section 3. This also indicate that the simple model developed in this study may have the right structure to describe the ventilatory response of the exchange of CO_2. A model of this simplicity that can accurately describe the ventilatory response of the exchange of CO_2 has not yet been presented in literature.

These findings give us new insights in the dynamic behavior of the human breathing system. No earlier research has been conducted to find the time constants belonging to the gas exchange after perturbation. Studies have researched the relation between the minute ventilation and the

equilibrium value of $etCO_2$ and etO_2 [63]. However, these studies do not describe the transient response.

For oxygen, the experimental protocol proved not suitable for testing the hypothesis. It was not possible to determine the slow exponential component or the equilibrium value for $F_{exp}O_2$ from the experimental measurements. This outcome is different than expected from the dynamical analysis of the model described in section 3. It is possible, therefore, that the slow exponential component that belongs to oxygen is too fast to be accurately determined from this experimental protocol. A possible improvement may be a larger disruption of the equilibrium state. It was difficult to determine for what time period it was safe to rebreathe. It may be possible to safely rebreathe for a longer time period and disrupt the equilibrium state more in a safe and controlled hospital environment. It may also be useful to assess the $F_{exp}O_2$ in realtime during rebreathing to determine the amount of disruption.

Another important finding is that the found large time constants and equilibrium values for $F_{exp}CO_2$ could be used for rough identification of the aggregated parameter groups of the simplified model. The predictions made with this identified model were qualitatively similar to the experimental measurements. However, they were not quantitatively similar to the experimental measurements. This may indicate the experimental protocol was not optimal for model identification and validation.
This may be due to low observability of certain respiratory variables during the experiment, which could have resulted in suboptimal adaptation of the model to the subject. For example, it would have been useful to assess the concentrations of CO_2 and O_2 in the blood to allow for better adaptation of the model to the subject. In the ICU, continuous transcutaneous measurement of the pH and partial pressures of CO_2 and O_2 in the blood would make constant assessment of these variables possible [50].
Another possible improvement would be to maintain consistent minute ventilation. We have tried to maintain consistent minute ventilation but found that, especially during the first 30 seconds after perturbation, this proved difficult. As a result, it was not possible to determine the fast exponential component. During measurements on patients on mechanical ventilation in the ICU this will be less of a problem since the minute ventilation can be set by the clinician.

It is important to emphasize that this was an orientating experimental study that aimed to find out what insights can be obtained from the experimental protocol that is based on the dynamical analysis of the model. In the future, a study with more participants and approval of the ethics committee could be conducted. The validity of this eventual study should be significantly higher than the validity of this orientating study.

We have shown that a simple model based on the gas exchange and the respiratory drive could provide insight into certain respiratory parameter groups after perturbations and could make predictions that complied qualitatively with experimental measurements. In the next section, it will be described how this may be useful in improving the treatment of in the mechanically ventilated patient on the intensive care.

5. Discussion

In this section, the implications, limitations and suggestions for further research are described. Since the interpretations of the results are presented at the end of each section, these are not included in the discussion.

5.1. Clinical implications

This study aimed to develop a simple but credible model of the physiology of breathing based on the difficulties encountered in current clinical practice. This model should be the initial step towards the use of closed-loop systems based on the physiology of breathing in clinical practice.

This research has presented a first model that is simple and encompasses a limited set of well-chosen aspects of the physiology of breathing. An experiment has been performed and it was shown that model parameter groups could be identified. Predictions could be made with this first model that did qualitatively comply with experimental measurements. The results support the idea that the simple model for carbon dioxide may have a credible structure, which may make it a possible basis for further development.

Since this is an exploratory study and the model is still in the development phase, it is not yet possible to make strong claims about the clinical applicability of the model. The experimental study had low validity and was mainly aimed to find out what insights could be obtained from the experimental protocol. As a result, no statements can yet be made about the accuracy of the model. However, we do want to present our ideas and vision for the potential use of the developed model in the ICU in the future. The coming subparagraphs will discuss the potential clinical applications.

5.1.1. Identification of parameters after application of perturbations

It was shown that after perturbating the fraction of inspired carbon dioxide ($F_{insp}CO_2$) we were able to determine the time constant belonging to the concentration of carbon dioxide in the alveolar air and the blood. The hypothesis that followed from the dynamical analysis was that this time constant is dependent on several parameters, one of them being the efficiency of the gas exchange of carbon dioxide ($D_{L\,CO2}$). If this is the case, the combination of the model and perturbations would provide clinicians with an improved insight into the efficiency of the gas exchange. As described in section 2, the current closed loop systems mainly focus on the breathing mechanics and do not provide insight into the gas exchange. Low insight in this parameter may make it difficult for clinicians to determine the optimal ventilator settings.

It would likely be possible to perform this manoeuvre and obtain an improved insight into the efficiency of the gas exchange in the ICU. The variables that could be perturbated to deviate the gas exchange system from its equilibrium state are the fraction of inspired carbon dioxide or the minute ventilation. After perturbation, the end-tidal carbon dioxide must be measured constantly for several minutes to determine the large time constant.
It may also be possible to determine the time constant from the measurement of the carbon dioxide concentration in the blood using transcutaneous sensors. However, this has yet to be researched. It is important to state that if we want to solely assess the efficiency of the gas exchange, the ventilatory control system of the patient should be impeded, as described in section 4. This can be achieved by letting the patient breathe with an imposed minute ventilation for several minutes after perturbation. In this way, the ventilatory control centre of the patient cannot influence the minute ventilation and does not influence the time constant.

A model-based mechanical ventilation system could automatically and periodically apply perturbations and determine the parameter that describes the efficiency of the gas exchange.

This would be an improvement to current clinical practice, because the clinician could have better insight into the state of the patient without having to perform time-consuming measurements. Constant insight in the efficiency of the gas exchange may make better-substantiated ventilator setting choices possible.

This may mainly be the case towards the end of the second stage described in section 2. In this stage the patient is on assisted ventilation and is preparing to wean of the ventilator. We have described that it is difficult to determine when the patient is ready for weaning. Impaired gas exchange increases the work of breathing and as such also contributes to weaning failure [64]. Most weaning patients still have considerable disturbances in gas exchange at the time of weaning and may develop hypoxemia or hypercapnia or both during a spontaneous breathing trial. Better insight into the efficiency of the gas exchange may therefore improve the clinician's insight into the patient's ability to breathe independently and successfully wean of the ventilator.

Another important factor that determines whether the patient is ready for weaning is the respiratory drive of the patient. Since we have performed an open-loop analysis, the respiratory drive has not yet been integrated in the tested model. When the respiratory drive is integrated, the time constant is expected to be dependent on both the efficiency of the gas exchange and the function of the respiratory drive of the patient. The reason for this is that when the respiratory drive is impaired, the ventilatory response of the patient to disturbance of the equilibrium state will be non-existent or low and it will take longer to reach a new equilibrium state.
To find out if the time constant is indeed dependent on the parameters that have been described, an experiment should be conducted that compares the time constants found in healthy subjects with the time constants found in patients with an impaired gas exchange or respiratory drive.

For diagnostic and prognostic purposes, it may be useful to differentiate between the different causes of impaired gas exchange, e.g. V/Q ratio and alveolar dead space. The simple model only contains one lumped parameter that describes the whole gas exchange function. It is therefore not expected that this first model will allow for the separation of the causes of impaired gas exchange. In further development of the model, it may be useful to also include components that describe the ventilation and the perfusion. It may then be possible to differentiate between the different causes of an impaired gas exchange.

5.1.2. Observation of variables that are not observable in current clinical practice

After we have obtained insight into the patient-specific model parameters, we can tune the model to the individual patient. Through the combination of this tuned model and simple measurements, we may also be able to obtain information that is currently not available in the ICU. The equilibrium equations of the model described in section 3 contain parameters and two variables: the concentration of carbon dioxide in the alveolar air and the concentration of carbon dioxide in the blood. It is suspected that when one of the two variables is known, the other variable could be determined through model calculations. The parameters in these equations can be identified through perturbation as described in the former section.

This means that when the carbon dioxide concentration in the blood is observable through measurements, the carbon dioxide concentration in the alveolar air is observable through model calculations. The carbon dioxide concentration in the alveolar air may be useful for the determination of physiological dead space. In section 2 we have described that physiological dead space is an important parameter to obtain. Determination of the dead space may be especially useful in patients with acute respiratory distress syndrome (ARDS) because it has prognostic value and can be used to guide ventilator settings. However, dead space is seldom calculated in clinical practice because it required the alveolar carbon dioxide concentration,

which is difficult to measure or estimate [38]. Using the model to calculate the alveolar carbon dioxide concentration could therefore be a useful addition to current clinical practice.

Since the state of patients on the ICU changes quickly, it is important to constantly perform perturbations and update the model parameters to make sure the model is always adapted to the current state of the patient.

5.1.3. Prediction of responses to changes in ventilator settings

In the former paragraphs we have described how the model may be able to provide better insight in some important respiratory parameters and variables. In section 2 we have described that in current clinical practice choosing the optimal ventilator settings on the ICU is often challenging. Better insight in the respiratory parameters and variables may make better-substantiated ventilator setting choices possible for the clinician.

Another addition of the model that could be useful when choosing ventilator settings is the ability to predict patient responses on changes in ventilator settings. When the model is adapted to the individual patient, simulations can be performed where certain model inputs (ventilator settings) are changed. The responses of the model variables on these changing ventilator settings are expectations of the actual response in the patient. This model may be able to predict the influence of the fraction of inspired oxygen (FiO_2) and the minute ventilation on the concentrations of carbon dioxide and oxygen in the alveolar air or the blood. In current clinical practice there is a trade-off between enough ventilation and toxicity and nitrogen washout when choosing the optimal fraction of inspired oxygen. The ability to predict patient response to changes in FiO_2 or minute ventilation may therefore be a useful addition to current clinical practice. The mechanical ventilation systems that are currently used do not consider predictions when determining the optimal ventilator settings.

5.1.4. Integrating the model in a closed-loop mechanical ventilation system

In the former paragraphs we have described how the individual model could be a useful addition to current clinical practice. In a future stadium, the further developed model could be integrated in a closed-loop mechanical ventilation system which would impose more benefits.

The model-based closed-loop mechanical ventilation system could then adjust ventilation automatically which is timesaving and may allow for optimized ventilation. It is important that the closed-loop system is aware of the different stages of mechanical ventilation described in section 2 and would know which variables are important to keep at their optimal value during each stage. For example, in the first stage the system should strive to keep the lung volumes and pressures low. In later stages, the system should prioritize the conservation of the breathing function of the patient. This goes beyond the state-of-the-art since the current closed-loop ventilation systems make no distinction in the different stages and therefore are not able to provide optimal settings throughout the whole duration of mechanical ventilation.

The system could also save the value of important respiratory parameters over time to allow for insight into the development of the important respiratory parameters. This may give the clinician and the system insight into the prognosis of the disease and the right treatment choices. In systems that contain and artificial intelligence component, this may even allow for prediction of the expected development of the parameters and the corresponding disease.

5.1.5. Experimental findings and the report

Apart from the model, the experimental findings give us new insights in the dynamic behavior of the human breathing system. No earlier research has been conducted to find the time constants

belonging to the gas exchange after perturbation. The conducted experiment provides expectations for the insights about the dynamics of the human breathing system which can be studied by using a similar experimental design with more participants to improve validity. These insights in the dynamics of the human breathing system should be used when developing new closed-loop mechanical ventilation systems.

This report describes the fundamental concepts of model development and validation. This may give clinicians insight into the development of the models that underlay closed-loop mechanical ventilation systems. This helps to bridge the knowledge-gap between clinicians and engineers and promote communications. Clinicians may be more acceptant of new closed-loop mechanical ventilation when the underlaying models are transparent and understandable to them [65].

In section 5.3. the general suggestions for further research are described. The next step in further research solely related to the development of this model will be specified here. The presented expected improvements of current clinical practice by using the model that are described in this section should be shared with clinicians. It should be discussed whether these stated improvements are indeed desirable in clinical practice.
As described in the former paragraphs, it is expected that the further realization of the addition of the respiratory drive component may be a first relevant step in the development of this particular model. A closed-loop analysis should be conducted to find out what information can be obtained from the addition of this component to the model.

5.2. limitations

The model that was developed in this thesis contains several simplifications of reality that may have influenced the validity. In the breathing mechanics model, the dead space ventilation and pulmonary shunt are assumed non-existent. In the gas exchange model, the CO_2 production and cardiac output are assumed constant. This does not comply with reality and may negatively affect the validity of the model. The acid-base balance was also not considered in this first model to limit complexity. Since the acid-base balance plays an important part in respiratory control addition could provide a more realistic model.

It is beyond the scope of this study to examine the suitability of the model structure for patients on the intensive care. The lungs of the subjects analyzed in this study were healthy. Therefore, the validity of our model in subjects with respiratory pathophysiology has yet to be evaluated. The model may need to be expanded to accurately describe the physiology in patients with lung diseases.

The reader should keep in mind that the main aim of the experiment was not to identify and validate the model, but mainly to find out what insights could be obtained from the experiment whose creation was based on the dynamical analysis of the mode. As a result, the validity of the experiment was of less importance. For this reason, the choice was made to conduct the experiment with one single subject and use a small number of measurements.

Due to practical constraints, the observability of certain relevant state variables during the experiment was low. The partial pressure of carbon dioxide and oxygen in the blood were not observable because the necessary measuring equipment was not available. As a result, identification of the separate model parameters was not possible. It also proved difficult to keep the minute ventilation constant during the 30 seconds after perturbation. As a result, the short time constants belonging to the gas exchange could not be determined. For future studies, more efforts should be exerted to increase the observability.

5.3. Suggestions for further research

Further research should initially focus on developing and comparing different first models of the physiology of breathing with different structures and degrees of complexity. These models should be compared on several levels: accuracy, transparency, clinical applicability etc. Our model could also be included in this research. Afterwards, it is possible to determine the most optimal base structure for further development of a closed-loop mechanical ventilation system based on the physiology of breathing.

Further research should also be conducted to increase our understanding of the dynamics of the breathing system. This will result in better substantiated design choices and model validation. Several different first experiments may be conducted to find out what information can be obtained from different measurement protocols. When these first experiments indicate that useful information can be obtained, experiments with higher validity can be conducted. Since the model should eventually be applied on the ICU, it may also be useful to conduct experiments on the dynamics of the breathing system in patients on mechanical ventilation. Advantages of these experiments is that the controllability and observability of variables is significantly higher on the ICU compared to experimental studies in healthy subjects.

6. Conclusion

The aim of this thesis was to develop a simple but credible model of the physiology of breathing based on the difficulties encountered in current clinical practice that could be the initial step towards the use of a model-based closed-loop mechanical ventilation system in clinical practice and will allow for insight in the clinical applicability.

From the literary review and conversations with clinicians it resulted that the closed-loop mechanical ventilation systems that are used in current clinical practice mainly focus on the respiratory mechanics. A model of the gas exchange and the respiratory drive with low complexity could be of an improvement to current clinical practice by improving the insight in the patient's respiratory parameters and predicting patient responses to changes in ventilator settings.

A two-compartment model aimed to satisfy these requirements was developed. The dynamical behaviour of the model consisted of a slow and a fast exponential component and the model would reach an equilibrium state when ventilating with constant minute ventilation.

An experimental study was conducted that presented relevant information about the dynamical behaviour of carbon dioxide. This behaviour complied with the behaviour expected from the dynamical analysis. Aggregated model parameter groups could be identified, and the predictions of the identified model were qualitatively similar to experimental measurements. While the limited observability and resources limit the possibilities for extensive model validation, this may give an indication that the simple model for carbon dioxide may have the right structure to describe the ventilatory response of the exchange of carbon dioxide.
The experimental protocol did not prove suitable to obtain relevant information about the dynamical behaviour of oxygen.

This research presents an example of a possible model structure for carbon dioxide which may be the initial step towards the use of a simple model of the full physiology of breathing in clinical practice. With the developed model it may be possible to improve the clinician's insight into the efficiency of the gas exchange of patients on mechanical ventilation. This may give the clinician an improved insight into the readiness of the patient for weaning and may make better-substantiated ventilator setting choices possible. Before this model will be clinically applicable, further research is needed to determine the optimal model structure and components and increased testing is necessary.

7. References

1. Rees SE, Karbing DS. Model-based advice for mechanical ventilation: From research (INVENT) to product (Beacon Caresystem). Annu Int Conf IEEE Eng Med Biol Soc. 2015;2015:5331-4.
2. Branson RD, Johannigman JA, Campbell RS, Davis K, Jr. Closed-loop mechanical ventilation. Respir Care. 2002;47(4):427-51; discussion 51-3.
3. Lellouche F, Brochard L. Advanced closed loops during mechanical ventilation (PAV, NAVA, ASV, SmartCare). Best Pract Res Clin Anaesthesiol. 2009;23(1):81-93.
4. Suarez-Sipmann F, Acute Respiratory Failure Working Group of the S. New modes of assisted mechanical ventilation. Med Intensiva. 2014;38(4):249-60.
5. Piquilloud L, Vignaux L, Bialais E, Roeseler J, Sottiaux T, Laterre PF, et al. Neurally adjusted ventilatory assist improves patient-ventilator interaction. Intensive Care Med. 2011;37(2):263-71.
6. Platen PV, Pomprapa A, Lachmann B, Leonhardt S. The dawn of physiological closed-loop ventilation-a review. Crit Care. 2020;24(1):121.
7. Zhang B, Ratano D, Brochard LJ, Georgopoulos D, Duffin J, Long M, et al. A physiology-based mathematical model for the selection of appropriate ventilator controls for lung and diaphragm protection. J Clin Monit Comput. 2020.
8. Chase JG, Preiser JC, Dickson JL, Pironet A, Chiew YS, Pretty CG, et al. Next-generation, personalised, model-based critical care medicine: a state-of-the art review of in silico virtual patient models, methods, and cohorts, and how to validation them. Biomed Eng Online. 2018;17(1):24.
9. Rees SE, Karbing DS. Determining the appropriate model complexity for patient-specific advice on mechanical ventilation. Biomed Tech (Berl). 2017;62(2):183-98.
10. Dasta JF, McLaughlin TP, Mody SH, Piech CT. Daily cost of an intensive care unit day: the contribution of mechanical ventilation. Crit Care Med. 2005;33(6):1266-71.
11. Wilinska M, Bachman T, Swietlinski J, Kostro M, Twardoch-Drozd M. Automated FiO2-SpO2 control system in neonates requiring respiratory support: a comparison of a standard to a narrow SpO2 control range. BMC Pediatr. 2014;14:130.
12. Salverda HH, Oldenburger NJ, Rijken M, Pauws SC, Dargaville PA, Te Pas AB. The effect of automated oxygen control on clinical outcomes in preterm infants: a pre- and post-implementation cohort study. Eur J Pediatr. 2021.
13. Chiari L, Avanzolini G, Ursino M. A comprehensive simulator of the human respiratory system: validation with experimental and simulated data. Ann Biomed Eng. 1997;25(6):985-99.
14. Martinoni EP, Pfister Ch A, Stadler KS, Schumacher PM, Leibundgut D, Bouillon T, et al. Model-based control of mechanical ventilation: design and clinical validation. Br J Anaesth. 2004;92(6):800-7.
15. Hermand E, Lhuissier FJ, Voituron N, Richalet JP. Ventilatory oscillations at exercise in hypoxia: A mathematical model. J Theor Biol. 2016;411:92-101.
16. Otis AB, Fenn WO, Rahn H. Mechanics of breathing in man. J Appl Physiol. 1950;2(11):592-607.
17. Singh PM, Borle A, Trikha A. Newer nonconventional modes of mechanical ventilation. J Emerg Trauma Shock. 2014;7(3):222-7.
18. Jonkman AH, Rauseo M, Carteaux G, Telias I, Sklar MC, Heunks L, et al. Proportional modes of ventilation: technology to assist physiology. Intensive Care Med. 2020.
19. Younes M. Proportional assist ventilation, a new approach to ventilatory support. Theory. Am Rev Respir Dis. 1992;145(1):114-20.
20. Piquilloud L, Tassaux D, Bialais E, Lambermont B, Sottiaux T, Roeseler J, et al. Neurally adjusted ventilatory assist (NAVA) improves patient-ventilator interaction during non-invasive ventilation delivered by face mask. Intensive Care Med. 2012;38(10):1624-31.

21. Vahedi NB, Ramazan-Yousif L, Andersen TS, Jensen HI. Implementation of Neurally Adjusted Ventilatory Assist (NAVA): Patient characteristics and staff experiences. J Healthc Qual Res. 2020;35(4):253-60.
22. Chen CW, Wu CP, Dai YL, Perng WC, Chian CF, Su WL, et al. Effects of implementing adaptive support ventilation in a medical intensive care unit. Respir Care. 2011;56(7):976-83.
23. Jouvet P, Hernert P, Wysocki M. Development and implementation of explicit computerized protocols for mechanical ventilation in children. Ann Intensive Care. 2011;1(1):51.
24. Katayama S, Tonai K, Shima J, Koyama K, Nunomiya S. Predictive factors for successful INTELLiVENT-ASV(R) use: a retrospective observational study. BMC Anesthesiol. 2020;20(1):94.
25. Schwaiberger D, Pickerodt PA, Pomprapa A, Tjarks O, Kork F, Boemke W, et al. Closed-loop mechanical ventilation for lung injury: a novel physiological-feedback mode following the principles of the open lung concept. J Clin Monit Comput. 2018;32(3):493-502.
26. Vizcaychipi MP, Martins L, White JR, Karbing DS, Gupta A, Singh S, et al. Intensive Care Weaning (iCareWean) protocol on weaning from mechanical ventilation: a single-blinded multicentre randomised control trial comparing an open-loop decision support system and routine care, in the general intensive care unit. BMJ Open. 2020;10(9):e042145.
27. Spadaro S, Karbing DS, Dalla Corte F, Mauri T, Moro F, Gioia A, et al. An open-loop, physiological model based decision support system can reduce pressure support while acting to preserve respiratory muscle function. J Crit Care. 2018;48:407-13.
28. Karbing DS, Spadaro S, Dey N, Ragazzi R, Marangoni E, Dalla Corte F, et al. An Open-Loop, Physiologic Model-Based Decision Support System Can Provide Appropriate Ventilator Settings. Crit Care Med. 2018;46(7):e642-e8.
29. Heunks LJ, A. Converstation about closed-loop mechanical ventilation. In: de Jong JI, editor. 2021.
30. Beduneau G, Pham T, Schortgen F, Piquilloud L, Zogheib E, Jonas M, et al. Epidemiology of Weaning Outcome according to a New Definition. The WIND Study. Am J Respir Crit Care Med. 2017;195(6):772-83.
31. Boles JM, Bion J, Connors A, Herridge M, Marsh B, Melot C, et al. Weaning from mechanical ventilation. Eur Respir J. 2007;29(5):1033-56.
32. Grasselli G, Brioni M, Zanella A. Monitoring respiratory mechanics during assisted ventilation. Curr Opin Crit Care. 2020;26(1):11-7.
33. Grinnan DC, Truwit JD. Clinical review: respiratory mechanics in spontaneous and assisted ventilation. Crit Care. 2005;9(5):472-84.
34. Centre de recherches et d'échanges sur la diffusion et l'inculturation du christianisme (France). Colloque (35th : 2014 : Nantes France), Bouron J-M, Salvaing B, Université de Nantes. Les missionnaires : entre identités individuelles et loyautés collectives : XIXe-XXIe siècles. Paris: Éditions Karthala; 2016. 341 pages p.
35. Lucangelo U, Bernabe F, Vatua S, Degrassi G, Villagra A, Fernandez R, et al. Prognostic value of different dead space indices in mechanically ventilated patients with acute lung injury and ARDS. Chest. 2008;133(1):62-71.
36. Matthay MA, Zemans RL, Zimmerman GA, Arabi YM, Beitler JR, Mercat A, et al. Acute respiratory distress syndrome. Nat Rev Dis Primers. 2019;5(1):18.
37. Nuckton TJ, Alonso JA, Kallet RH, Daniel BM, Pittet JF, Eisner MD, et al. Pulmonary dead-space fraction as a risk factor for death in the acute respiratory distress syndrome. N Engl J Med. 2002;346(17):1281-6.
38. Doorduin J, Nollet JL, Vugts MP, Roesthuis LH, Akankan F, van der Hoeven JG, et al. Assessment of dead-space ventilation in patients with acute respiratory distress syndrome: a prospective observational study. Crit Care. 2016;20(1):121.
39. Goligher EC, Fan E, Herridge MS, Murray A, Vorona S, Brace D, et al. Evolution of Diaphragm Thickness during Mechanical Ventilation. Impact of Inspiratory Effort. Am J Respir Crit Care Med. 2015;192(9):1080-8.

40. Brochard L, Slutsky A, Pesenti A. Mechanical Ventilation to Minimize Progression of Lung Injury in Acute Respiratory Failure. Am J Respir Crit Care Med. 2017;195(4):438-42.
41. Goligher EC, Ferguson ND, Brochard LJ. Clinical challenges in mechanical ventilation. Lancet. 2016;387(10030):1856-66.
42. de Vries H, Jonkman A, Shi ZH, Spoelstra-de Man A, Heunks L. Assessing breathing effort in mechanical ventilation: physiology and clinical implications. Ann Transl Med. 2018;6(19):387.
43. Bellani G, Laffey JG, Pham T, Fan E, Brochard L, Esteban A, et al. Epidemiology, Patterns of Care, and Mortality for Patients With Acute Respiratory Distress Syndrome in Intensive Care Units in 50 Countries. JAMA. 2016;315(8):788-800.
44. Jonkman AH, de Vries HJ, Heunks LMA. Physiology of the Respiratory Drive in ICU Patients: Implications for Diagnosis and Treatment. Crit Care. 2020;24(1):104.
45. Barwing J, Pedroni C, Olgemoller U, Quintel M, Moerer O. Electrical activity of the diaphragm (EAdi) as a monitoring parameter in difficult weaning from respirator: a pilot study. Crit Care. 2013;17(4):R182.
46. Whitelaw WA, Derenne JP, Milic-Emili J. Occlusion pressure as a measure of respiratory center output in conscious man. Respir Physiol. 1975;23(2):181-99.
47. Pham T, Telias I, Beitler JR. Esophageal Manometry. Respir Care. 2020;65(6):772-92.
48. Damanhuri NS, Chiew YS, Othman NA, Docherty PD, Pretty CG, Shaw GM, et al. Assessing respiratory mechanics using pressure reconstruction method in mechanically ventilated spontaneous breathing patient. Comput Methods Programs Biomed. 2016;130:175-85.
49. Bou Jawde S, Walkey AJ, Majumdar A, O'Connor GT, Smith BJ, Bates JHT, et al. Tracking respiratory mechanics around natural breathing rates via variable ventilation. Sci Rep. 2020;10(1):6722.
50. Mari A, Nougue H, Mateo J, Vallet B, Vallee F. Transcutaneous PCO2 monitoring in critically ill patients: update and perspectives. J Thorac Dis. 2019;11(Suppl 11):S1558-S67.
51. Sun Q, Zhou, C., Chase, J.G. Parameter updating of a patient-specific lung mechanics model for optimising mechanical ventilation. Biomedical Signal Processing and Control. 2020.
52. Paulus F. Kwaliteit van intensive care-zorg: 'Wij gaan goed voor u zorgen'. Hogeschool van Amsterdam. 2019.
53. Zhou C, Chase JG, Knopp J, Sun Q, Tawhai M, Moller K, et al. Virtual patients for mechanical ventilation in the intensive care unit. Comput Methods Programs Biomed. 2021;199:105912.
54. Morton SE, Dickson J, Chase JG, Docherty P, Desaive T, Howe SL, et al. A virtual patient model for mechanical ventilation. Comput Methods Programs Biomed. 2018;165:77-87.
55. Kuo HJ, Chiu HW, Lee CN, Chen TT, Chang CC, Bien MY. Improvement in the Prediction of Ventilator Weaning Outcomes by an Artificial Neural Network in a Medical ICU. Respir Care. 2015;60(11):1560-9.
56. Tremblay LN, Slutsky AS. Ventilator-induced lung injury: from the bench to the bedside. Intensive Care Med. 2006;32(1):24-33.
57. Allerod C, Karbing DS, Thorgaard P, Andreassen S, Kjaergaard S, Rees SE. Variability of preference toward mechanical ventilator settings: a model-based behavioral analysis. J Crit Care. 2011;26(6):637 e5- e12.
58. Thille AW, Reynaud F, Marie D, Barrau S, Rousseau L, Rault C, et al. Impact of sleep alterations on weaning duration in mechanically ventilated patients: a prospective study. Eur Respir J. 2018;51(4).
59. Spiro SG, Silvestri GA, Agustí A. Clinical respiratory medicine. 4th ed. Philadelphia: Elsevier Saunders; 2012. xxi, 977 p. p.
60. Biscoe TJ, Purves MJ, Sampson SR. The frequency of nerve impulses in single carotid body chemoreceptor afferent fibres recorded in vivo with intact circulation. J Physiol. 1970;208(1):121-31.
61. Nielsen M, Smith H. Studies on the regulation of respiration in acute hypoxia; preliminary report. Acta Physiol Scand. 1951;22(1):44-6.
62. Agur AMR, Grant JCB. Grant's atlas of anatomy. 13th ed. Philadelphia: Wolters Kluwer Health/Lippincott Williams & Wilkins; 2013. xiv, 871 p. p.

63. Mohan R, Duffin J. The effect of hypoxia on the ventilatory response to carbon dioxide in man. Respir Physiol. 1997;108(2):101-15.
64. Heunks LM, van der Hoeven JG. Clinical review: the ABC of weaning failure--a structured approach. Crit Care. 2010;14(6):245.
65. Chatburn RL, Mireles-Cabodevila E. Closed-loop control of mechanical ventilation: description and classification of targeting schemes. Respir Care. 2011;56(1):85-102.
66. Desai JP, Moustarah F. Pulmonary Compliance. StatPearls. Treasure Island (FL)2021.
67. Guerin C, Richard JC. Measurement of respiratory system resistance during mechanical ventilation. Intensive Care Med. 2007;33(6):1046-9.
68. Boron WF, Boulpaep EL. Medical physiology. Third edition. ed. Philadelphia, PA: Elsevier; 2017. xii, 1297 pages p.
69. VERKERK G. Binas; Informatieboek voor natuurwetenschappen en wiskunde. 2004.
70. Ellis AC, Hyatt TC, Hunter GR, Gower BA. Respiratory quotient predicts fat mass gain in premenopausal women. Obesity (Silver Spring). 2010;18(12):2255-9.
71. Lahiri S, DeLaney RG. Relationship between carotid chemoreceptor activity and ventilation in the cat. Respir Physiol. 1975;24(3):267-86.

Appendix 1: Model development

1.1. Overview of the model parameters and variables

Table 9 Overview of the model variables for carbon dioxide

	full name	**abbr.**	**unit**
Input variables	Ventilator induced pressure	$P_V(t)$	cmH_2O
	Velocity of blood flow	$Q(t)$	L/s
	CO_2-flow through airways	$\phi_{AW\,CO_2}(t)$	g/s
	Metabolic CO_2-flow	$\phi_{met\,CO_2}(t)$	g/s
	Concentration of CO_2 in the inspired air	$C_{atm_{CO_2}}(t)$	g/L
State variables	Alveolar volume	$V_A(t)$	mL
	Alveolar pressure	$P_A(t)$	cmH_2O
	Mass of CO_2 in alveolar space	$m_{A\,CO_2}(t)$	g
	Mass of CO_2 in arterial blood	$m_{a\,CO_2}(t)$	g
	Mass of CO_2 in venous blood	$m_{v\,CO_2}(t)$	g
	Mass of CO_2 in total blood	$m_{b\,CO_2}(t)$	g
General variable	Intrapleural pressure	$P_{IP}(t)$	cmH_2O
	Transpulmonary pressure	$P_{TP}(t)$	cmH_2O
	Airway pressure	$P_{AW}(t)$	cmH_2O
	Partial pressure of CO_2 in alveolar air	$P_{A_{CO_2}}(t)$	$mmHg$
	Partial pressure of CO_2 in venous blood	$P_{v_{CO_2}}(t)$	$mmHg$
	Partial pressure of CO_2 in arterial blood	$P_{a_{CO_2}}(t)$	$mmHg$
	Partial pressure of CO_2 in total blood	$P_{b_{CO_2}}(t)$	$mmHg$
	Diffusion flow of CO_2 between alveolar air and capillaries	$\phi_{dif\,CO_2}(t)$	g/s
	CO_2-flow from the arterial blood to the venous blood	$\phi_{av_{CO_2}}(t)$	g/s
	CO_2-flow from the venous blood to the arterial blood	$\phi_{va_{CO_2}}(t)$	g/s
	Concentration of CO_2 in the alveolar air	$C_{A_{CO_2}}(t)$	g/L
	Activity of the central chemoreceptors	$a_{ccr}(t)$	$1/s$
	Activity of the central pattern generator	a_{cpg}	$1/s$

Table 10 Overview of the model parameters for carbon dioxide

full name	**abbr.**	**unit**	**initial value**	**source**
Respiratory compliance	C_{rs}	mL/cmH_2O	$2 \cdot 10^2$	[66]
Respiratory resistance	R_{rs}	$(cmH_2O \cdot s)/mL$	$3.7 \cdot 10^{-3}$	[67]
Functional residual capacity	V_{FRC}	mL	$2.8 \cdot 10^3$	[68]
Density carbon dioxide STP	ρ_{CO_2}	g/mL	$2.0 \cdot 10^{-3}$	[69]
Molar volume at BTPS	V_M	L	22.4	[69]
Diffusion capacity co2	$D_{L_{CO_2}}$	g/s	$1.66 \cdot 10^{-3}$	[68]
Arterial blood volume	V_a	L	1.11	[68]
Venous blood volume	V_v	L	3.51	[68]
Total blood volume	V_b	L	4.60	[68]
Respiratory quotient	RQ	-	0.8	[70]
Setpoint partial pressure CO_2	$P_{a_{CO_2}\,dsetpoint}$	$mmHg$	40	[71]
Constant 1	k_1	$L/g \cdot mmHg$	-	-
Constant 2	k_2	$L/g \cdot mmHg$	-	-
Constant 3	k_3	$L/g \cdot mmHg$	-	-
Constant 4	k_4	$mmHg$	-	-

Constant 5	k_5	$mmHg$	-	-
Constant 6	k_6	$L/g \cdot mmHg$	-	-
Constant 7	k_7	$mmHg$	-	-
Constant 8	k_8	$1/mmHg \cdot s$	-	-
Constant 9	k_9	$1/s$	-	-
Constant 10	k_{10}	$1/s$	-	-
Constant 10	k_{11}	s/cmH_2O	-	-

Table 11 Overview of the model variables for oxygen

	full name	**abbr.**	**unit**
input variables	Ventilator induced pressure	$P_V(t)$	cmH_2O
	Velocity of blood flow	$Q(t)$	L/s
	O_2-flow through airways	$\phi_{AW\,O_2}(t)$	g/s
	Metabolic O_2-flow	$\phi_{met\,O_2}(t)$	g/s
	Concentration of O_2 in the inspired air	$C_{atm\,O_2}(t)$	g/L
State variables	Alveolar volume	$V_A(t)$	mL
	Mass of O_2 in alveolar space	$m_{A\,O_2}(t)$	g
	Mass of O_2 in arterial blood	$m_{a\,O_2}(t)$	g
	Mass of O_2 in venous blood	$m_{v\,O_2}(t)$	g
	Mass of O_2 in total blood	$m_{b\,O_2}(t)$	g
	Partial pressure of O_2 in alveolar air	$P_{A_{O_2}}(t)$	$mmHg$
	Partial pressure of O_2 in venous blood	$P_{v_{O_2}}(t)$	$mmHg$
	Partial pressure of O_2 in arterial blood	$P_{a_{O_2}}(t)$	$mmHg$
	Partial pressure of O_2 in total blood	$P_{b_{O_2}}(t)$	$mmHg$
	Diffusion flow of O_2 between alveolar air and capillaries	$\phi_{dif\,O_2}(t)$	g/s
	O_2-flow from the arterial blood to the venous blood	$\phi_{av\,O_2}(t)$	g/s
	O_2-flow from the venous blood to the arterial blood	$\phi_{va\,O_2}(t)$	g/s
	Dissolved mass of O_2 in arterial blood	$C_{a_{O_2}\,dissolved}(t)$	g/L
	Dissolved mass of O_2 in venous blood	$C_{v_{O_2}\,dissolved}(t)$	g/L
	Activity of the central chemoreceptors	$a_{ccr}(t)$	$1/s$
	Activity of the central pattern generator	a_{cpg}	$1/s$

Table 12 Overview of the model parameters for oxygen

full name	**abbr.**	**unit**	**initial value**	**source**
Diffusion capacity o2	$D_{L_{O_2}}$	g/s	$2 \cdot 10^2$	[66]
Haemoglobin	Hb	$Mmol/L$	10	[67]
Saturation haemoglobin	SpO_2	%	99	[68]
Arterial blood volume	V_a	L	1.11	[68]
Venous blood volume	V_v	L	3.51	[68]
Respiratory quotient	RQ	-	0.8	[70]
Constant 1	k_1	$L/g \cdot mmHg$	-	-
Constant 2	k_2	$L/\% \cdot mmol$	-	-
Constant 3	k_3	$L/g \cdot mmHg$	-	-
Constant 4	k_4	$L/\% \cdot mmol$	-	-
Constant 5	k_5	$L/g \cdot mmHg$	-	-
Constant 6	k_6	$L/\% \cdot mmol$	-	-
Constant 7	k_7	$L/g \cdot mmHg$	-	-

1.2. Overview of the equations for oxygen

Alveolar air

The change in the number of O_2 molecules in the alveolar air ($m_{A\,O_2}(t)$) depends on the diffusion flow from the alveolar air to the capillaries ($\phi_{dif\,O_2}(t)$) and the flow of O_2 in and out of the body ($\phi_{AW\,O_2}(t)$).

$$\frac{dm_{A\,O_2}(t)}{dt} = \phi_{AW\,O_2}(t) - \phi_{dif\,O_2}(t) \tag{44}$$

The partial pressure of O_2 ($P_{A\,O_2}$) depends on the mass of O_2 in the alveolar air, the volume of the alveolar air and the total pressure of the alveolar air.

$$P_{A\,O_2}(t) = k_1 \cdot \frac{m_{A\,O_2}(t)}{V_A(t)} \tag{45}$$

The flow of O_2 in and out of the lungs ($\phi_{AW\,O_2}(t)$) is dependent on the airflow ($\phi_{AW}(t)$) and during exhalation on the concentration of O_2 in the lungs ($C_{A_{O_2}}(t)$) or during inhalation on the concentration of O_2 in the inspired air ($C_{atm_{O_2}}(t)$).

Inhalation

$$\phi_{AW\,O_2}(t) = C_{atm_{O_2}}(t) \cdot \phi_{AW}(t) \tag{46}$$

Exhalation

$$\phi_{AW\,O_2}(t) = C_{A_{O_2}}(t) \cdot \phi_{AW}(t) \tag{47}$$

Diffusion of oxygen between alveolar air and the pulmonary capillaries

The movements of both O_2 and CO_2 across the alveolar blood-gas barrier occur by simple diffusion. Fick law describes that the net flow is proportional to the difference in partial pressures of O_2 and CO_2 in the alveolar air and the blood. The diffusion coefficient (D_L) is dependent on the properties of both the barrier and the gas. If we assume that the alveolar air, blood-gas barrier and pulmonary capillary blood are uniform in space and time, then the net diffusion of O_2 from alveolar air to pulmonary capillary blood is described by equation 46.

$$\phi_{dif\,O_2}(t) = D_{L_{O_2}}\left(P_{A_{O_2}}(t) - P_{v_{O_2}}(t)\right) \tag{48}$$

Arterial blood

The flow of O_2 molecules in the arterial blood is equal to the flow of O_2 molecules in the venous blood minus the diffusion flow of O_2 molecules to the alveolar air. The flow of O_2 molecules in the blood is equal to the change in number of O_2 molecules in the blood.

$$\frac{dm_{a_{O_2}}(t)}{dt} = \phi_{va\,O_2}(t) + \phi_{dif\,O_2}(t) - \phi_{av\,O_2}(t) \tag{49}$$

The flow of O_2 from the venous to the arterial compartment ($\phi_{va\,O_2}(t)$) and the flow of O_2 from the arterial to the venous compartment ($\phi_{av\,O_2}(t)$) are equal to the product of the blood flow in the compartment ($Q(t)$) and the concentration of O_2 in the sending compartment.

$$\phi_{va\,O_2}(t) = Q(t) \cdot \frac{m_{v_{O_2}}(t)}{V_v} \tag{50}$$

$$\phi_{av\,O_2}(t) = Q(t) \cdot \frac{m_{a_{O_2}}(t)}{V_a} \tag{51}$$

The mass concentration of O_2 in the arterial blood can be calculated by dividing the mass of O_2 in the blood ($m_{a_{O_2}}$ with the volume (V_a). The dissolved mass of O_2 is dependent on the number of haemoglobin molecules (Hb) and the fraction of haemoglobin molecule that have bound oxygen (SpO_2).

$$\frac{m_{a_{O_2}\,dissolved}(t)}{V_a} = \frac{m_{a_{O_2}}(t)}{V_a} \cdot (1 - k_2 \cdot SpO_2 \cdot Hb) \tag{52}$$

The partial pressure of oxygen in the arterial blood ($P_{a_{O_2}}$) is linearly related to the mass concentration of dissolved oxygen. The constant k_3 is used to describe the linear relation.

$$P_{a_{O_2}} = k_3 \cdot \frac{m_{a_{O_2}\,dissolved}(t)}{V_a} \tag{53}$$

Venous blood

The flow of O_2 molecules in the venous blood is equal to the flow of O_2 molecules in the arterial blood minus the diffusion flow of O_2 molecules to the metabolism ($\phi_{met\,O_2}$). The flow of O_2 molecules in and out of the venous blood is equal to the change in number of O_2 molecules in the venous blood.

$$\frac{dm_{v_{O_2}}(t)}{dt} = \phi_{av\,O_2}(t) - \phi_{met\,O_2}(t) - \phi_{va\,O_2}(t) \tag{54}$$

The mass concentration of O_2 in the venous blood can be calculated by dividing the mass of O_2 in the blood ($m_{a_{O_2}}$ with the volume (V_v). The dissolved mass of O_2 is dependent on the number of haemoglobin molecules (Hb) and the fraction of haemoglobin molecule that have bound oxygen (SpO_2).

$$\frac{m_{v_{O_2}\,dissolved}(t)}{V_v} = \frac{m_{v_{O_2}}(t)}{V_v} \cdot (1 - k_4 \cdot SpO_2 \cdot Hb) \tag{55}$$

The partial pressure of oxygen in the venous blood ($P_{v_{O_2}}$) is linearly related to the mass concentration of dissolved oxygen. The constant k_5 is used to describe the linear relation.

$$P_{v_{O_2}}(t) = k_5 \cdot \frac{m_{v_{O_2}\,dissolved}(t)}{V_v} \tag{56}$$

A single blood compartment (simplification)

If the dynamical analysis of the original model proves impossible, a simplification should be applied. A simplification of the model is described here that turns the third order model in a second order model. The block for the arterial and the venous blood are merged into one single block that describes the total blood volume.

The change of the total O_2 mass in the blood ($m_{b_{o_2}}(t)$) is equal to the sum of the flows that carry O_2 in and out of the compartment. The outgoing flow is the flow of O_2 molecules that diffuse to the lungs and the ingoing flow is the metabolic flow of O_2 molecules.

$$\frac{dm_{b_{o_2}}(t)}{dt} = \phi_{dif\ O_2}(t) - \phi_{met\ O_2}(t) \tag{57}$$

The mass concentration of O_2 in the blood can be calculated by dividing the mass of O_2 in the blood ($m_{b_{O_2}}$ with the volume (V_b). The dissolved mass of O_2 is dependent on the number of haemoglobin molecules (Hb) and the fraction of haemoglobin molecule that have bound oxygen (SpO_2).

$$\frac{m_{b_{O_2}\,dissolved}(t)}{V_b} = \frac{m_{b_{O_2}}(t)}{V_b} \cdot (1 - k_6 \cdot SpO_2 \cdot Hb) \tag{58}$$

The partial pressure of O_2 in the blood ($P_{b_{O_2}}(t)$) is dependent on the mass concentration of O_2 in the arterial blood. The constant k_7 is used to describe the linear relation.

$$P_{b_{O_2}}(t) = k_7 \cdot \frac{m_{b_{O_2}\,dissolved}(t)}{V_b} \tag{59}$$

Metabolism

The metabolism encompasses all the chemical processes involved in energy production, energy release and growth. The metabolism requires a supply of O_2 and produces CO_2. The respiratory quotient (RQ) is the ratio of moles of CO_2 produced per mole of O_2 consumed at the tissue level. For people eating a typical western diet the RQ is approximately 0.8.

$$\phi_{met\ O_2}(t) = \frac{\phi_{met\ CO_2}(t)}{RQ} \tag{60}$$

For description of 'prefusion', 'Central and peripheral chemoreceptors', 'central pattern generator' and 'breathing muscles' see section 2.

Perfusion

Perfusion ($Q(t)$) is the input variable for the subsystems 'arterial blood' and 'venous blood'. It represents the convective movement of blood that carries the dissolved gasses to and from the lung.

Central and peripheral chemoreceptors

See section 3.1.2.

1.3. Overview of Simulink model

Full Simulink model

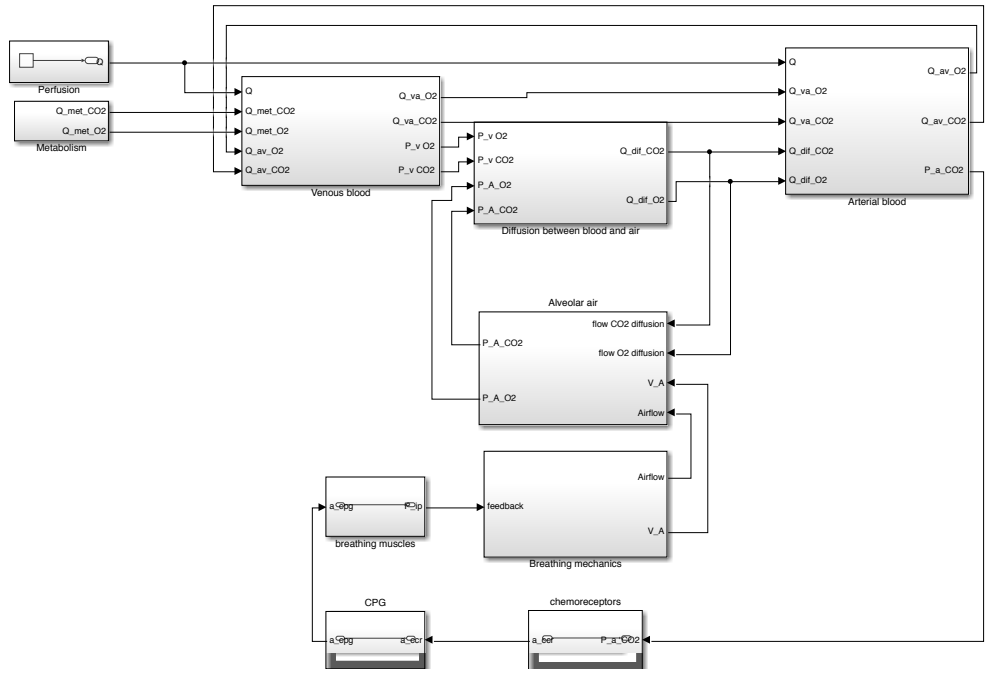

Breathing mechanics

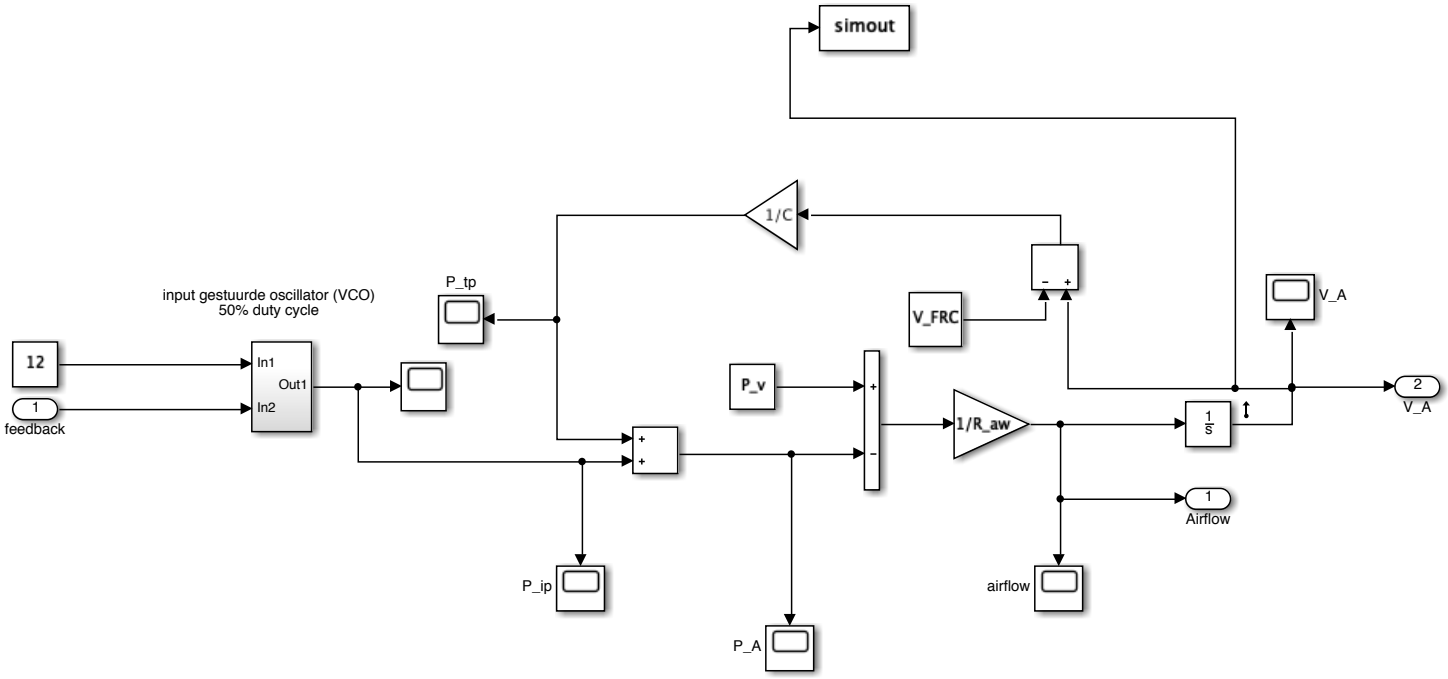

Arterial blood

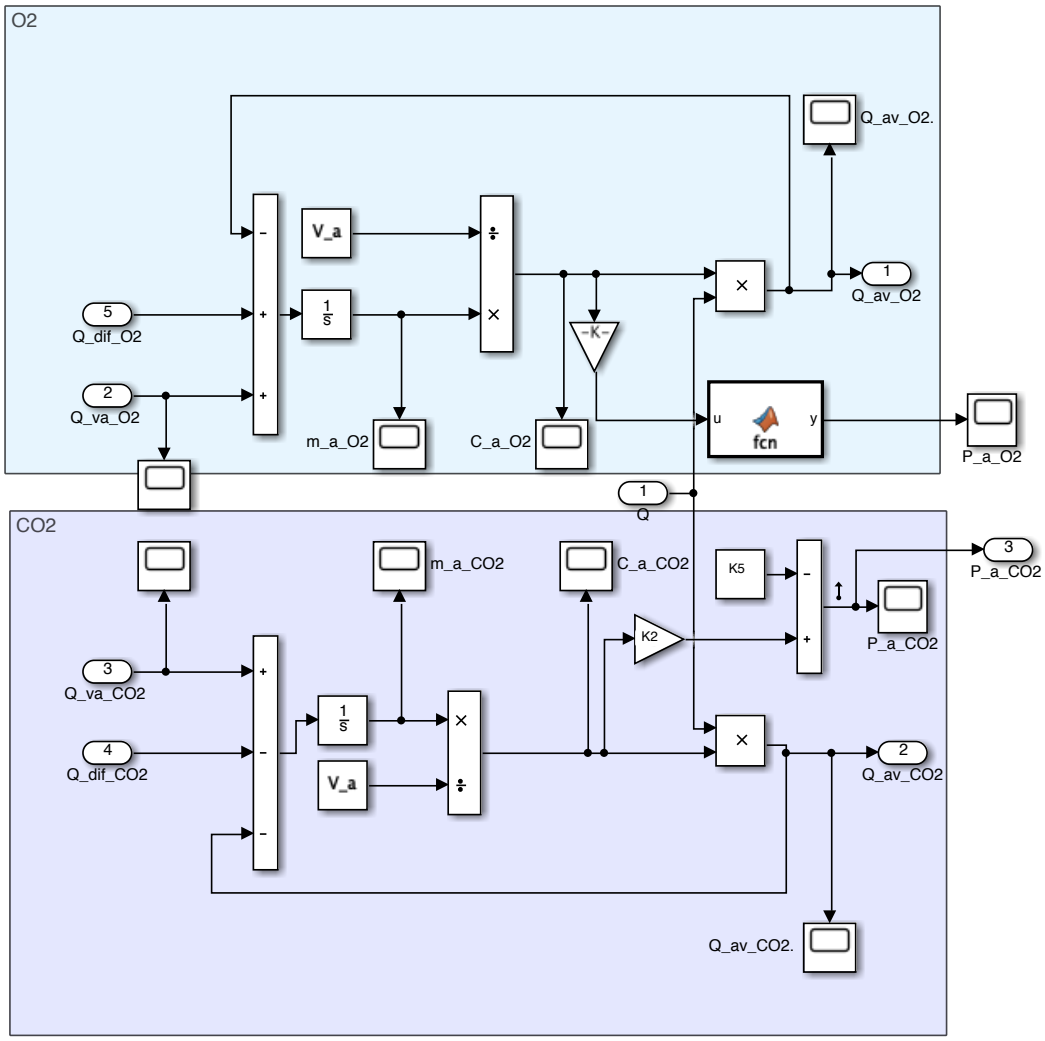

alveolar air

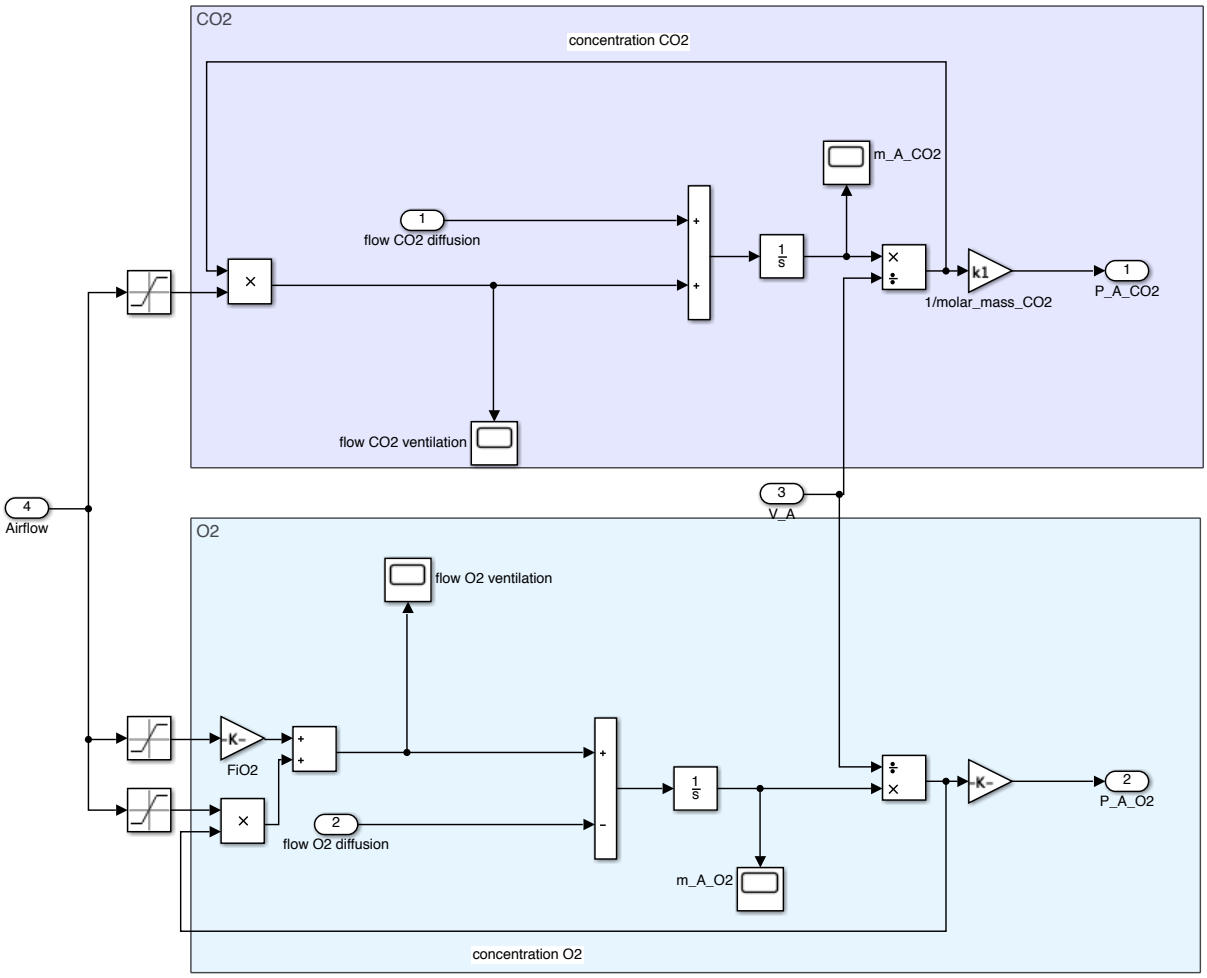

Appendix 2: Dynamical analysis

2.1. Dynamical analysis of the original third order gas exchange model (carbon dioxide)

The first step in the analysis is the determination of the state equations. The state equations are created with the equations from section 3.1 and

$$\frac{dm_{A_{CO_2}}(t)}{dt} = D_{L\,CO2} \cdot \left(k_3 \cdot \frac{m_{v_{CO_2}}(t)}{V_v} - k_4 - k_1 \cdot \frac{m_{A\,CO_2}(t)}{V_{A\,gem}}\right) - \phi_{AW\,avg}(t) \cdot \frac{m_{A_{CO_2}}(t)}{V_{A\,gem}} + C_{CO_2\,atm} \cdot \phi_{AW\,avg}(t)$$

$$\frac{dm_{a_{CO_2}}(t)}{dt} = Q\left(\frac{m_{v\,CO_2}}{V_v} - \frac{m_{a\,CO_2}}{V_a}\right) - D_{L\,CO2} \cdot \left(k_3 \cdot \frac{m_{v_{CO_2}}(t)}{V_v} - k_4 - k_1 \cdot \frac{m_{A\,CO_2}(t)}{V_{A\,gem}}\right)$$

$$\frac{dm_{v_{CO_2}}(t)}{dt} = Q \cdot \left(\frac{m_{a\,CO_2}}{V_a} - \frac{m_{v\,CO_2}}{V_v}\right) + Q_{met\,CO_2}$$

The state equations can be notated into the state space form.

$$\begin{bmatrix} \dot{m}_{A\,CO_2} \\ \dot{m}_{a\,CO_2} \\ \dot{m}_{v\,CO_2} \end{bmatrix} = A \begin{bmatrix} m_{A\,CO_2} \\ m_{a\,CO_2} \\ m_{v\,CO_2} \end{bmatrix}$$

$$\text{A=} \begin{vmatrix} \frac{-D_{L\,CO2} \cdot k_1 - \phi_{AW\,avg}(t)}{V_{A\,gem}} & 0 & \frac{D_{L\,CO2} \cdot K_3}{V_v} \\ D_{L\,CO2} \cdot \frac{k_1}{V_{A\,gem}} & -\frac{Q}{V_a} & \frac{Q - D_{L\,CO2} \cdot K_3}{V_v} \\ 0 & \frac{Q}{V_a} & -\frac{Q}{V_v} \end{vmatrix}$$

The eigenvalues of the system are determined by taking the determinant of the A-matrix minus the identity matrix with the eigenvalues x on the diagonal and setting it to zero.

$$\text{A=} \begin{vmatrix} \frac{-D_{L\,CO2} \cdot k_1 - \phi_{AW\,avg}(t)}{V_{A\,gem}} - x & 0 & \frac{D_{L\,CO2} \cdot K_3}{V_v} \\ D_{L\,CO2} \cdot \frac{k_1}{V_{A\,gem}} & -\frac{Q}{V_a} - x & \frac{Q - D_{L\,CO2} \cdot K_3}{V_v} \\ 0 & \frac{Q}{V_a} & -\frac{Q}{V_v} - x \end{vmatrix}$$

$$\left(\frac{-k_1 \cdot D_{L\,CO2} - \phi_{AW\,avg}(t)}{V_{A\,gem}} - x\right) \cdot \left(\left(-\frac{Q}{V_a} - x\right) \cdot \left(-\frac{Q}{V_v} - x\right) - \left(\frac{Q - D_{L\,CO2} \cdot k_3}{V_v}\right) \cdot \left(\frac{Q}{V_a}\right)\right) + \left(\frac{D_{L\,CO2} \cdot k_3}{V_v}\right) \cdot \left(\frac{D_{L\,CO2} \cdot k_1}{V_{A\,(t)}}\right) \cdot \left(\frac{Q}{V_a}\right)$$

$$\left(\frac{-k_1 \cdot D_{L\,CO2} - \phi_{AW\,avg}(t)}{V_{A\,gem}}\right) \cdot \left(\left(-\frac{Q}{V_a} - x\right) \cdot \left(-\frac{Q}{V_v} - x\right) - \left(\frac{Q - D_{L\,CO2} \cdot k_3}{V_v}\right) \cdot \left(\frac{Q}{V_a}\right)\right) - x \cdot \left(\left(-\frac{Q}{V_a} - x\right) \cdot \left(-\frac{Q}{V_v} - x\right) - \left(\frac{Q - D_{L\,CO2} \cdot k_3}{V_v}\right) \cdot \left(\frac{Q}{V_a}\right)\right) + \left(\frac{D_{L\,CO2} \cdot k_3}{V_v}\right) \cdot \left(\frac{D_{L\,CO2} \cdot k_1}{V_{A\,(t)}}\right) \cdot \left(\frac{Q}{V_a}\right)$$

$$\left(\frac{-k_1 \cdot D_{L\,CO2} - \phi_{AW\,avg}(t)}{V_{A\,gem}}\right) \cdot \left(\left(\frac{Q}{V_a}\frac{Q}{V_v} + x\left(\frac{Q}{V_a} + \frac{Q}{V_v}\right) + x^2\right) - \left(\frac{Q - D_{L\,CO2} \cdot k_3}{V_v}\right) \cdot \left(\frac{Q}{V_a}\right)\right) - x \cdot \left(\left(\frac{Q}{V_a}\frac{Q}{V_v} + x\left(\frac{Q}{V_a} + \frac{Q}{V_v}\right) + x^2\right) - \left(\frac{Q - D_{L\,CO2} \cdot k_3}{V_v}\right) \cdot \left(\frac{Q}{V_a}\right)\right) + \left(\frac{D_{L\,CO2} \cdot k_3}{V_v}\right) \cdot \left(\frac{D_{L\,CO2} \cdot k_1}{V_{A\,(t)}}\right) \cdot \left(\frac{Q}{V_a}\right)$$

$$\left(\frac{-k_1 \cdot D_{L\,CO2} - \phi_{AW\,avg}(t)}{V_{A\,gem}}\right) \cdot \left(\left(\frac{Q}{V_a}\frac{Q}{V_v} + x\left(\frac{Q}{V_a} + \frac{Q}{V_v}\right) + x^2\right) - \left(\frac{Q - D_{L\,CO2} \cdot k_3}{V_v}\right) \cdot \left(\frac{Q}{V_a}\right)\right) + \left(\left(-\frac{Q}{V_a}\frac{Q}{V_v}x - x^2\left(\frac{Q}{V_a} + \frac{Q}{V_v}\right) - x^3\right) + x\left(\frac{Q - D_{L\,CO2} \cdot k_3}{V_v}\right) \cdot \left(\frac{Q}{V_a}\right)\right) + \left(\frac{D_{L\,CO2} \cdot k_3}{V_v}\right) \cdot \left(\frac{D_{L\,CO2} \cdot k_1}{V_{A\,(t)}}\right) \cdot \left(\frac{Q}{V_a}\right)$$

$$\left(\frac{-k_1 \cdot D_{L\,CO2} - \phi_{AW\,avg}(t)}{V_{A\,gem}}\right) \cdot \frac{Q}{V_a}\frac{Q}{V_v} + x\left(\frac{-k_1 \cdot D_{L\,CO2} - \phi_{AW\,avg}(t)}{V_{A\,gem}}\right) \cdot \left(\frac{Q}{V_a} + \frac{Q}{V_v}\right) + x^2\left(\frac{-k_1 \cdot D_{L\,CO2} - \phi_{AW\,avg}(t)}{V_{A\,gem}}\right) - \left(\frac{Q - D_{L\,CO2} \cdot k_3}{V_v}\right) \cdot \left(\frac{Q}{V_a}\right)\left(\frac{-k_1 \cdot D_{L\,CO2} - \phi_{AW\,avg}(t)}{V_{A\,gem}}\right) - \frac{Q}{V_a}\frac{Q}{V_v}x - x^2\left(\frac{Q}{V_a} + \frac{Q}{V_v}\right)$$
$$- x^3 + x\left(\frac{Q - D_{L\,CO2} \cdot k_3}{V_v}\right) \cdot \left(\frac{Q}{V_a}\right) + \left(\frac{D_{L\,CO2} \cdot k_3}{V_v}\right) \cdot \left(\frac{D_{L\,CO2} \cdot k_1}{V_{A\,(t)}}\right) \cdot \left(\frac{Q}{V_a}\right)$$

$$-x^3 + x^2\left(\frac{-k_1 \cdot D_{L\,CO2} - \phi_{AW\,avg}(t)}{V_{A\,gem}} - \left(\frac{Q}{V_a} + \frac{Q}{V_v}\right)\right) + x\left(\left(\frac{-k_1 \cdot D_{L\,CO2} - \phi_{AW\,avg}(t)}{V_{A\,gem}}\right) \cdot \left(\frac{Q}{V_a} + \frac{Q}{V_v}\right) - \frac{Q}{V_a}\frac{Q}{V_v} + \left(\frac{Q - D_{L\,CO2} \cdot k_3}{V_v}\right) \cdot \left(\frac{Q}{V_a}\right)\right) + \left(\frac{-k_1 \cdot D_{L\,CO2} - \phi_{AW\,avg}(t)}{V_{A\,gem}}\right) \cdot \frac{Q}{V_a}\frac{Q}{V_v} - \left(\frac{Q - D_{L\,CO2} \cdot k_3}{V_v}\right)$$
$$\cdot \left(\frac{Q}{V_a}\right)\left(\frac{-k_1 \cdot D_{L\,CO2} - \phi_{AW\,avg}(t)}{V_{A\,gem}}\right) + \left(\frac{D_{L\,CO2} \cdot k_3}{V_v}\right) \cdot \left(\frac{D_{L\,CO2} \cdot k_1}{V_{A\,gem}}\right) \cdot \left(\frac{Q}{V_a}\right)$$

$$-x^3+x^2\left(\frac{-k_1\cdot D_{L\,CO2}-\phi_{AW\,avg}(t)}{V_{A\,gem}}-\left(\frac{Q}{V_a}+\frac{Q}{V_v}\right)\right)+x\left(\left(\frac{-k_1\cdot D_{L\,CO2}-\phi_{AW\,avg}(t)}{V_{A\,gem}}\right)\cdot\left(\frac{Q}{V_a}+\frac{Q}{V_v}\right)-\frac{Q}{V_a}\frac{Q}{V_v}+\left(\frac{Q-D_{L\,CO2}\cdot k_3}{V_v}\right)\cdot\left(\frac{Q}{V_a}\right)\right)+\left(\frac{-k_1\cdot D_{L\,CO2}-\phi_{AW\,avg}(t)}{V_{A\,gem}}\right)\cdot\frac{Q}{V_a}\frac{Q}{V_v}-\left(\frac{Q}{V_v}\right)\cdot\left(\frac{Q}{V_a}\right)\left(\frac{-k_1\cdot D_{L\,CO2}-\phi_{AW\,avg}(t)}{V_{A\,gem}}\right)-\left(\frac{-D_{L\,CO2}\cdot k_3}{V_v}\right)\cdot\left(\frac{Q}{V_a}\right)\left(\frac{-k_1\cdot D_{L\,CO2}-\phi_{AW\,avg}(t)}{V_{A\,gem}}\right)+\left(\frac{D_{L\,CO2}\cdot k_3}{V_v}\right)\cdot\left(\frac{D_{L\,CO2}\cdot k_1}{V_{A\,gem}}\right)\cdot\left(\frac{Q}{V_a}\right)$$

$$-x^3+x^2\left(\frac{-k_1\cdot D_{L\,CO2}-\phi_{AW\,avg}(t)}{V_{A\,gem}}-\left(\frac{Q}{V_a}+\frac{Q}{V_v}\right)\right)+x\left(\left(\frac{-k_1\cdot D_{L\,CO2}-\phi_{AW\,avg}(t)}{V_{A\,gem}}\right)\cdot\left(\frac{Q}{V_a}+\frac{Q}{V_v}\right)-\frac{Q}{V_a}\frac{Q}{V_v}+\left(\frac{Q-D_{L\,CO2}\cdot k_3}{V_v}\right)\cdot\left(\frac{Q}{V_a}\right)\right)-\left(\frac{-D_{L\,CO2}\cdot k_3}{V_v}\right)\cdot\left(\frac{Q}{V_a}\right)\left(\frac{-k_1\cdot D_{L\,CO2}-\phi_{AW\,avg}(t)}{V_{A\,gem}}\right)+\left(\frac{D_{L\,CO2}\cdot k_3}{V_v}\right)\cdot\left(\frac{D_{L\,CO2}\cdot k_1}{V_{A\,gem}}\right)\cdot\left(\frac{Q}{V_a}\right)$$

$$-x^3+x^2\left(\frac{-k_1\cdot D_{L\,CO2}-\phi_{AW\,avg}(t)}{V_{A\,gem}}-\left(\frac{Q}{V_a}+\frac{Q}{V_v}\right)\right)+x\left(\left(\frac{-k_1\cdot D_{L\,CO2}-\phi_{AW\,avg}(t)}{V_{A\,gem}}\right)\cdot\left(\frac{Q}{V_a}+\frac{Q}{V_v}\right)-\frac{Q}{V_a}\frac{Q}{V_v}+\left(\frac{Q-D_{L\,CO2}\cdot k_3}{V_v}\right)\cdot\left(\frac{Q}{V_a}\right)\right)-\left(\frac{-D_{L\,CO2}\cdot k_3}{V_v}\right)\cdot\left(\frac{Q}{V_a}\right)\left(\frac{-\phi_{AW\,avg}(t)}{V_{A\,gem}}\right)$$

$$-x^3+x^2\left(\frac{-k_1\cdot D_{L\,CO2}-\phi_{AW\,avg}(t)}{V_{A\,gem}}-\left(\frac{Q}{V_a}+\frac{Q}{V_v}\right)\right)+x\left(\left(\frac{-k_1\cdot D_{L\,CO2}-\phi_{AW\,avg}(t)}{V_{A\,gem}}\right)\cdot\left(\frac{Q}{V_a}+\frac{Q}{V_v}\right)+\left(\frac{-D_{L\,CO2}\cdot k_3}{V_v}\right)\cdot\left(\frac{Q}{V_a}\right)\right)-\left(\frac{-D_{L\,CO2}\cdot k_3}{V_v}\right)\cdot\left(\frac{Q}{V_a}\right)\left(\frac{-\phi_{AW\,avg}(t)}{V_{A\,gem}}\right)$$

$$-x^3+x^2\left(\frac{-k_1\cdot D_{L\,CO2}-\phi_{AW\,avg}(t)}{V_{A\,gem}}-\frac{Q}{V_a}-\frac{Q}{V_v}\right)+x\left(\frac{-k_1\cdot D_{L\,CO2}}{V_{A\,gem}}\frac{Q}{V_a}+\frac{-k_1\cdot D_{L\,CO2}}{V_{A\,gem}}\frac{Q}{V_v}+\frac{-\phi_{AW\,avg}(t)}{V_{A\,gem}}\frac{Q}{V_a}+\frac{-\phi_{AW\,avg}(t)}{V_{A\,gem}}\frac{Q}{V_v}+\left(\frac{-D_{L\,CO2}\cdot k_3}{V_v}\right)\cdot\left(\frac{Q}{V_a}\right)\right)-\left(\frac{-D_{L\,CO2}\cdot k_3}{V_v}\right)\cdot\left(\frac{Q}{V_a}\right)\left(\frac{-\phi_{AW\,avg}(t)}{V_{A\,gem}}\right)$$

$$-x^3+x^2\left(\frac{-k_1\cdot D_{L\,CO2}-\phi_{AW\,avg}(t)}{V_{A\,gem}}-\frac{Q}{V_a}-\frac{Q}{V_v}\right)+x\left(\frac{-k_1\cdot D_{L\,CO2}}{V_{A\,gem}}\frac{Q}{V_a}+\frac{-k_1\cdot D_{L\,CO2}}{V_{A\,gem}}\frac{Q}{V_v}+\frac{-\phi_{AW\,avg}(t)}{V_{A\,gem}}\frac{Q}{V_a}+\frac{-\phi_{AW\,avg}(t)}{V_{A\,gem}}\frac{Q}{V_v}\cdot\right)+\left(\frac{-D_{L\,CO2}\cdot k_3}{V_v}\right)\left(\frac{Q}{V_a}\right)\left(x-\left(\frac{-\phi_{AW\,avg}(t)}{V_{A\,gem}}\right)\right)$$

$$x^2\left(\frac{-k_1\cdot D_{L\,CO2}-\phi_{AW\,avg}(t)}{V_{A\,gem}}-\frac{Q}{V_a}-\frac{Q}{V_v}-x\right)+\left(\frac{Q}{V_v}+\frac{Q}{V_a}\right)x\left(\left(\frac{-\phi_{AW\,avg}(t)}{V_{A\,gem}}\right)+\frac{-k_1\cdot D_{L\,CO2}}{V_{A\,gem}}\right)+\left(\frac{-D_{L\,CO2}\cdot k_3}{V_v}\right)\left(\frac{Q}{V_a}\right)\left(x-\left(\frac{-\phi_{AW\,avg}(t)}{V_{A\,gem}}\right)\right)$$

$$x^2\left(\frac{-k_1\cdot D_{L\,CO2}-\phi_{AW\,avg}(t)}{V_{A\,gem}}-2\frac{Q}{V_a}-x\right)+\left(2\frac{Q}{V_a}\right)x\left(\left(\frac{-\phi_{AW\,avg}(t)}{V_{A\,gem}}\right)+\frac{-k_1\cdot D_{L\,CO2}}{V_{A\,gem}}\right)+\left(\frac{-D_{L\,CO2}\cdot k_3}{V_v}\right)\left(\frac{Q}{V_a}\right)\left(x-\left(\frac{-\phi_{AW\,avg}(t)}{V_{A\,gem}}\right)\right)$$

Unfortunately, this equation proves unsolvable. We have tried solving the equation algebraically and by using Matlab.

2.2. Dynamical analysis of the second order gas exchange model (carbon dioxide)

We start with composing the equations for the state variables.

$$\frac{dm_{A_{CO_2}}(t)}{dt} = \phi_{diffusion} - \phi_{airflow\ out} + \phi_{airflow\ in} \tag{61}$$

$$\frac{dm_{A_{CO_2}}(t)}{dt} = D_L \cdot \left(k_6 \cdot \frac{m_{b_{CO_2}}(t)}{V_b} + k_7 - k_1 \cdot \frac{m_{A_{CO_2}}(t)}{V_{A\,gem}}\right) - \frac{m_{A_{CO_2}}(t)}{V_{A\,gem}} \cdot \phi_{AW\ avg}(t) + C_{CO_2\,atm} \cdot \phi_{AW\ avg}(t) \tag{62}$$

$$\frac{dm_{b_{CO_2}}(t)}{dt} = -\phi_{diffusion} + \phi_{metabolism} \tag{63}$$

$$\frac{dm_{b_{CO_2}}(t)}{dt} = -D_L \cdot \left(k_6 \cdot \frac{m_{b_{CO_2}}(t)}{V_b} + k_7 - k_1 \cdot \frac{m_{A_{CO_2}}(t)}{V_{A\,gem}}\right) + \phi_{met}(t) \tag{64}$$

From the state equations, the equilibrium values can be determined. When the system is in equilibrium, the state derivatives are equal to zero. The system is in equilibrium, so

$$0 = D_L \cdot \left(k_6 \cdot \frac{m_{b_{CO_2}}(t)}{V_b} + k_7 - k_1 \cdot \frac{m_{A_{CO_2}}(t)}{V_{A\,gem}}\right) - \frac{m_{A_{CO_2}}(t)}{V_{A\,gem}} \cdot \phi_{AW\ avg}(t) + C_{CO_2\,atm} \cdot \phi_{AW\ avg}(t) \tag{65}$$

$$\frac{m_{A_{CO_2}}(t)}{V_{A\,gem}} \cdot (D_L \cdot k_1 + \phi_{AW\ avg}(t)) = D_L \cdot \left(k_6 \cdot \frac{m_{b_{CO_2}}(t)}{V_b} + k_7\right) + C_{CO_2\,atm} \cdot \phi_{AW\ avg}(t) \tag{66}$$

$$\frac{m_{A_{CO_2}}(t)}{V_{A\,gem}} = \frac{D_L \cdot \left(k_6 \cdot \frac{m_{b_{CO_2}}(t)}{V_b} + k_7\right) + C_{CO_2\,atm} \cdot \phi_{AW\ avg}(t)}{(D_L \cdot k_1 + \phi_{AW\ avg}(t))} \tag{67}$$

If we want to express $\frac{m_{A_{CO_2}}(t)}{V_{A\,gem}}$ in parameters, we need to find an expression for $\frac{m_{b_{CO_2}}(t)}{V_b}$ when the system is in equilibrium.

$$\frac{dm_{b_{CO_2}}(t)}{dt} = -D_L \cdot \left(k_6 \cdot \frac{m_{b_{CO_2}}(t)}{V_b} + k_7 - k_1 \cdot \frac{m_{A_{CO_2}}(t)}{V_{A\,gem}} + \right) + \phi_{met}(t) \tag{68}$$

$$0 = -D_L \cdot \left(k_6 \cdot \frac{m_{b_{CO_2}}(t)}{V_b} + k_7 - k_1 \cdot \frac{m_{A_{CO_2}}(t)}{V_{A\,gem}}\right) + \phi_{met}(t) \tag{69}$$

$$D_L \cdot k_6 \cdot \frac{m_{b_{CO_2}}(t)}{V_b} = \left(-D_L \cdot k_7 + D_L \cdot k_1 \cdot \frac{m_{A_{CO_2}}(t)}{V_{A\,gem}}\right) + \phi_{met}(t) \tag{70}$$

$$\frac{m_{b_{CO_2}}(t)}{V_b} = \frac{\left(-D_L \cdot k_7 + D_L \cdot k_1 \cdot \frac{m_{A_{CO_2}}(t)}{V_{A\,gem}}\right) + \phi_{met}(t)}{D_L \cdot k_6} \tag{71}$$

Now we can fill in the expression for $\frac{m_{b_{CO_2}}(t)}{V_b}$ in the equilibrium equation for the alveolar air.

$$\frac{m_{A_{CO_2}}(t)}{V_{A\,gem}} = \frac{D_L \cdot \left(k_6 \cdot \frac{\left(-D_L \cdot k_7 + D_L \cdot k_1 \cdot \frac{m_{A_{CO_2}}(t)}{V_{A\,gem}}\right) + \phi_{met}(t)}{D_L \cdot k_6} + k_7 \right) + C_{CO_2\,atm} \cdot \phi_{AW\,avg}(t)}{(D_L \cdot k_1 + \phi_{AW\,avg}(t))} \tag{72}$$

$$\frac{m_{A_{CO_2}}(t)}{V_{A\,gem}} = \frac{-D_L \cdot k_7 + D_L \cdot k_1 \cdot \frac{m_{A_{CO_2}}(t)}{V_{A\,gem}} + D_L \cdot k_7 + \phi_{met}(t) + C_{CO_2\,atm} \cdot \phi_{AW\,avg}(t)}{(D_L \cdot k_1 + \phi_{AW\,avg}(t))} \tag{73}$$

$$\frac{m_{A_{CO_2}}(t)}{V_{A\,gem}} = \frac{D_L \cdot k_1 \cdot \frac{m_{A_{CO_2}}(t)}{V_{A\,gem}} + \phi_{met}(t) + C_{CO_2\,atm} \cdot \phi_{AW\,avg}(t)}{(D_L \cdot k_1 + \phi_{AW\,avg}(t))} \tag{74}$$

$$\frac{m_{A_{CO_2}}(t)}{V_{A\,gem}} \cdot \left(1 - \frac{D_L \cdot k_1}{D_L \cdot k_1 + \phi_{AW\,avg}(t)}\right) = \frac{\phi_{met}(t) + C_{CO_2\,atm} \cdot \phi_{AW\,avg}(t)}{(D_L \cdot k_1 + \phi_{AW\,avg}(t))} \tag{75}$$

$$\frac{m_{A_{CO_2}}(t)}{V_{A\,gem}} \left(-D_L \cdot k_1 + \phi_{AW\,avg}(t) + D_L \cdot k_1\right) = \phi_{met}(t) + C_{CO_2\,atm} \cdot \phi_{AW\,avg}(t) \tag{76}$$

$$\frac{m_{A_{CO_2}}(t)}{V_{A\,gem}} = \frac{\phi_{met}(t) + C_{CO_2\,atm} \cdot \phi_{AW\,avg}(t)}{\phi_{AW\,avg}(t)} \tag{77}$$

$$\frac{m_{A_{CO_2}}(t)}{V_{A\,gem}} = \frac{\phi_{met}(t)}{\phi_{AW\,avg}(t)} + C_{CO_2\,atm} \tag{78}$$

Now we can fill in the expression for $\frac{m_{A_{CO_2}}(t)}{V_{A\,gem}}$ in the equilibrium equation for the blood.

$$\frac{m_{b_{CO_2}}(t)}{V_b} = \frac{\left(-D_L \cdot k_7 + D_L \cdot k_1 \cdot \frac{m_{A_{CO_2}}(t)}{V_{A\,gem}}\right) + \phi_{met}(t)}{D_L \cdot k_6} \tag{79}$$

$$\frac{m_{b_{CO_2}}(t)}{V_b} = \frac{\left(-D_L \cdot k_7 + D_L \cdot k_1 \cdot \left(\frac{\phi_{met}(t)}{\phi_{AW\,avg}(t)} + C_{CO_2\,atm}\right)\right) + \phi_{met}(t)}{D_L \cdot k_6} \tag{80}$$

Now can derive the expressions for the eigenvalues.

$$A = \begin{bmatrix} \frac{-k_1 \cdot D_L - \phi_{AW\,avg}(t)}{V_{A\,gem}} & \frac{D_L \cdot k_6}{V_b} \\ \frac{D_L \cdot k_1}{V_{A\,gem}} & \frac{-D_L \cdot k_6}{V_b} \end{bmatrix}$$

For determination of the eigenvalues, the determinant of the A-matrix minus the similar-sized identity matrix multiplied by the eigenvalues is set to zero.

$$A = \begin{bmatrix} \frac{-k_1 \cdot D_L - \phi_{AW\,avg}(t)}{V_{A\,gem}} - \lambda & \frac{D_L \cdot k_6}{V_B} \\ \frac{D_L \cdot k_1}{V_{A\,gem}} & \frac{-D_L \cdot k_6}{V_B} - \lambda \end{bmatrix}$$

$$\left(\frac{-k_1 \cdot D_L - \phi_{AW\,avg}(t)}{V_{A\,gem}} - \lambda\right) \cdot \left(\frac{-D_L \cdot k_6}{V_B} - \lambda\right) - \left(\frac{D_L \cdot k_6}{V_B}\right) \cdot \left(\frac{D_L \cdot k_1}{V_{A\,gem}}\right) = 0 \quad (81)$$

$$\frac{-k_1 \cdot D_L - \phi_{AW\,avg}(t)}{V_{A\,gem}} \cdot \frac{-D_L \cdot k_6}{V_b} - \lambda \cdot \frac{-k_1 \cdot D_L - \phi_{AW\,avg}(t)}{V_{A\,gem}} - \lambda \cdot \frac{-D_L \cdot k_6}{V_b} + \lambda^2 - \frac{D_L \cdot k_6}{V_b} \cdot \frac{D_L \cdot k_1}{V_{A\,gem}} = 0 \quad (82)$$

$$\lambda^2 + \lambda\left(\frac{k_1 \cdot D_L + \phi_{AW\,avg}(t)}{V_{A\,gem}} + \frac{D_L \cdot k_6}{V_b}\right) + \frac{-k_1 \cdot D_L - \phi_{AW\,avg}(t)}{V_{A\,gem}} \cdot \frac{-D_L \cdot k_6}{V_b} - \frac{D_L \cdot k_6}{V_b} \cdot \frac{D_L \cdot k_1}{V_{A\,gem}} = 0 \quad (83)$$

$$\lambda^2 + \lambda\left(\frac{k_1 \cdot D_L + \phi_{AW\,avg}(t)}{V_{A\,gem}} + \frac{D_L \cdot k_6}{V_b}\right) + \frac{-k_1 \cdot D_L}{V_{A\,gem}} \cdot \frac{-D_L \cdot k_6}{V_b} + \frac{-\phi_{AW\,avg}(t)}{V_{A\,gem}} \cdot \frac{-D_L \cdot k_6}{V_b} - \frac{D_L \cdot k_6}{V_b} \cdot \frac{D_L \cdot k_1}{V_{A\,gem}} = 0 \quad (84)$$

$$\lambda^2 + \lambda\left(\frac{k_1 \cdot D_L + \phi_{AW\,avg}(t)}{V_{A\,gem}} + \frac{D_L \cdot k_6}{V_b}\right) + \frac{\phi_{AW\,avg}(t)}{V_{A\,gem}} \cdot \frac{D_L \cdot k_6}{V_b} = 0 \quad (85)$$

$$\lambda = \frac{-\left(\frac{k_1 \cdot D_L + \phi_{AW\,avg}(t)}{V_{A\,gem}} + \frac{D_L \cdot k_6}{V_b}\right) \pm \sqrt{\left(\frac{k_1 \cdot D_L + \phi_{AW\,avg}(t)}{V_{A\,gem}} + \frac{D_L \cdot k_6}{V_b}\right)^2 - 4 \cdot \frac{\phi_{AW\,avg}(t)}{V_{A\,gem}} \cdot \frac{D_L \cdot k_6}{V_b}}}{2} \quad (86)$$

Two different eigenvalues are found.

$$\begin{bmatrix} \lambda_1 \\ \lambda_2 \end{bmatrix} = \begin{bmatrix} -\frac{1}{2}\left(\frac{k_1 \cdot D_L + \phi_{AW\,avg}(t)}{V_{A\,gem}} + \frac{D_L \cdot k_6}{V_b}\right) + \frac{1}{2}\sqrt{\left(\frac{k_1 \cdot D_L + \phi_{AW\,avg}(t)}{V_{A\,gem}} + \frac{D_L \cdot k_6}{V_b}\right)^2 - 4 \cdot \frac{\phi_{AW\,avg}(t)}{V_{A\,gem}} \cdot \frac{D_L \cdot k_6}{V_b}} \\ -\frac{1}{2}\left(\frac{k_1 \cdot D_L + \phi_{AW\,avg}(t)}{V_{A\,gem}} + \frac{D_L \cdot k_6}{V_b}\right) - \frac{1}{2}\sqrt{\left(\frac{k_1 \cdot D_L + \phi_{AW\,avg}(t)}{V_{A\,gem}} + \frac{D_L \cdot k_6}{V_b}\right)^2 - 4 \cdot \frac{\phi_{AW\,avg}(t)}{V_{A\,gem}} \cdot \frac{D_L \cdot k_6}{V_b}} \end{bmatrix}$$

The associated time constants can be determined by taking the absolute value of the inverse of the eigenvalues.

$$\begin{bmatrix} \tau_1 \\ \tau_2 \end{bmatrix} = \begin{bmatrix} \frac{2}{\left|-\left(\frac{k_1 \cdot D_L + \phi_{AW\,avg}(t)}{V_{A\,gem}} + \frac{D_L \cdot k_6}{V_b}\right) + \sqrt{\left(\frac{k_1 \cdot D_L + \phi_{AW\,avg}(t)}{V_{A\,gem}} + \frac{D_L \cdot k_6}{V_b}\right)^2 - 4 \cdot \frac{\phi_{AW\,avg}(t)}{V_{A\,gem}} \cdot \frac{D_L \cdot k_6}{V_b}}\right|} \\ \frac{2}{\left|-\left(\frac{k_1 \cdot D_L + \phi_{AW\,avg}(t)}{V_{A\,gem}} + \frac{D_L \cdot k_6}{V_b}\right) - \sqrt{\left(\frac{k_1 \cdot D_L + \phi_{AW\,avg}(t)}{V_{A\,gem}} + \frac{D_L \cdot k_6}{V_b}\right)^2 - 4 \cdot \frac{\phi_{AW\,avg}(t)}{V_{A\,gem}} \cdot \frac{D_L \cdot k_6}{V_b}}\right|} \end{bmatrix}$$

2.3. Dynamical analysis of the second order gas exchange model (oxygen)

We start with composing the equations for the state variables.

$$\frac{dm_{A_{O_2}}(t)}{dt} = -\phi_{diffusion} - \phi_{airflow\ out} + \phi_{airflow\ in} \tag{87}$$

$$\frac{dm_{A_{O_2}}(t)}{dt} = -D_L \cdot \left(k_1 \cdot \frac{m_{A\,O_2}(t)}{V_{A\,gem}} - k_7 \cdot \frac{m_{b_{O_2}}(t)}{V_b} \cdot (1 - k_6 \cdot SpO_2 \cdot Hb)\right) - \frac{m_{A_{O_2}}(t)}{V_{A\,gem}} \cdot \phi_{AW\,avg}(t) + C_{O_2\,atm} \cdot \phi_{AW\,avg}(t) \tag{88}$$

$$\frac{dm_{b_{O_2}}(t)}{dt} = \phi_{diffusion} - \phi_{metabolism} \tag{89}$$

$$\frac{dm_{b_{O_2}}(t)}{dt} = D_L \cdot \left(k_1 \cdot \frac{m_{A\,O_2}(t)}{V_{A\,gem}} - k_7 \cdot \frac{m_{b_{O_2}}(t)}{V_b} \cdot (1 - k_6 \cdot SpO_2 \cdot Hb)\right) - \phi_{met}\,(t) \tag{90}$$

From the state equations, the equilibrium values can be determined. When the system is in equilibrium, the state derivatives are equal to zero. The system is in equilibrium, so

$$0 = -D_L \cdot \left(k_1 \cdot \frac{m_{A\,O_2}(t)}{V_{A\,gem}} - k_7 \cdot \frac{m_{b_{O_2}}(t)}{V_b} \cdot (1 - k_6 \cdot SpO_2 \cdot Hb)\right) - \frac{m_{A_{O_2}}(t)}{V_{A\,gem}} \cdot \phi_{AW\,avg}(t) + C_{O_2\,atm} \cdot \phi_{AW\,avg}(t) \tag{91}$$

$$\frac{m_{A_{O_2}}(t)}{V_{A\,gem}} \cdot (D_L \cdot k_1 + \phi_{AW\,avg}(t)) = -D_L \cdot \left(-k_7 \cdot \frac{m_{b_{O_2}}(t)}{V_b} \cdot (1 - k_6 \cdot SpO_2 \cdot Hb)\right) + C_{O_2\,atm} \cdot \phi_{AW\,avg}(t) \tag{92}$$

$$\frac{m_{A_{O_2}}(t)}{V_{A\,gem}} = \frac{-D_L \cdot \left(-k_7 \cdot \frac{m_{b_{O_2}}(t)}{V_b} \cdot (1 - k_6 \cdot SpO_2 \cdot Hb)\right) + C_{O_2\,atm} \cdot \phi_{AW\,avg}(t)}{(D_L \cdot k_1 + \phi_{AW\,avg}(t))} \tag{93}$$

If we want to express $\frac{m_{A_{CO_2}}(t)}{V_{A\,gem}}$ in parameters, we need to find an expression for $\frac{m_{b_{CO_2}}(t)}{V_b}$ when the system is in equilibrium.

$$\frac{dm_{b_{CO_2}}(t)}{dt} = D_L \cdot \left(k_1 \cdot \frac{m_{A\,O_2}(t)}{V_{A\,gem}} - k_7 \cdot \frac{m_{b_{O_2}}(t)}{V_b} \cdot (1 - k_6 \cdot SpO_2 \cdot Hb)\right) - \phi_{met}\,(t) \tag{94}$$

$$0 = D_L \cdot \left(k_1 \cdot \frac{m_{A\,O_2}(t)}{V_{A\,gem}} - k_7 \cdot \frac{m_{b_{O_2}}(t)}{V_b} \cdot (1 - k_6 \cdot SpO_2 \cdot Hb)\right) - \phi_{met}\,(t) \tag{95}$$

$$D_L \cdot k_7 \cdot \frac{m_{b_{O_2}}(t)}{V_b} \cdot (1 - k_6 \cdot SpO_2 \cdot Hb) = D_L \cdot k_1 \cdot \frac{m_{A_{O_2}}(t)}{V_{A\,gem}} - \phi_{met}\,(t) \tag{96}$$

$$\frac{m_{b_{O_2}}(t)}{V_b} = \frac{D_L \cdot k_1 \cdot \frac{m_{A_{O_2}}(t)}{V_{A\,gem}} - \phi_{met}\,(t)}{D_L \cdot k_7 \cdot (1 - k_6 \cdot SpO_2 \cdot Hb)} \tag{97}$$

Now we can fill in the expression for $\frac{m_{b_{CO_2}}(t)}{V_b}$ in the equation

$$\frac{m_{A_{O_2}}(t)}{V_{A\,gem}} = \frac{-D_L \cdot \left(-k_7 \cdot \left(\frac{D_L \cdot k_1 \cdot \frac{m_{A_{O_2}}(t)}{V_{A\,gem}} - \phi_{met}(t)}{D_L \cdot k_7 \cdot (1 - k_6 \cdot SpO_2 \cdot Hb)} \right) \cdot (1 - k_6 \cdot SpO_2 \cdot Hb) \right) + C_{O_2\,atm} \cdot \phi_{AW\,avg}(t)}{(D_L \cdot k_1 + \phi_{AW\,avg}(t))} \quad (98)$$

$$\frac{m_{A_{O_2}}(t)}{V_{A\,gem}} = \frac{D_L \cdot k_1 \cdot \frac{m_{A_{O_2}}(t)}{V_{A\,gem}} - \phi_{met}(t) + C_{O_2\,atm} \cdot \phi_{AW\,avg}(t)}{(D_L \cdot k_1 + \phi_{AW\,avg}(t))} \quad (99)$$

$$\frac{m_{A_{O_2}}(t)}{V_{A\,gem}}\left(1 - \frac{D_L \cdot k_1}{D_L \cdot k_1 + \phi_{AW\,avg}(t)}\right) = \frac{-\phi_{met}(t) + C_{O_2\,atm} \cdot \phi_{AW\,avg}(t)}{(D_L \cdot k_1 + \phi_{AW\,avg}(t))} \quad (100)$$

$$\frac{m_{A_{O_2}}(t)}{V_{A\,gem}} = \frac{\left(\frac{-\phi_{met}(t) + C_{O_2\,atm} \cdot \phi_{AW\,avg}(t)}{\left(D_L \cdot k_1 + \phi_{AW\,avg}(t)\right)} \right)}{\left(1 - \frac{D_L \cdot k_1}{D_L \cdot k_1 + \phi_{AW\,avg}(t)}\right)} \quad (101)$$

$$\frac{m_{A_{O_2}}(t)}{V_{A\,gem}} = \frac{-\phi_{met}(t) + C_{O_2\,atm} \cdot \phi_{AW\,avg}(t)}{D_L \cdot k_1 + \phi_{AW\,avg}(t) - D_L \cdot k_1} \quad (102)$$

$$\frac{m_{A_{O_2}}(t)}{V_{A\,gem}} = \frac{-\phi_{met}(t) + C_{O_2\,atm} \cdot \phi_{AW\,avg}(t)}{\phi_{AW\,avg}(t)} \quad (103)$$

$$\frac{m_{A_{O_2}}(t)}{V_{A\,gem}} = -\frac{\phi_{met}(t)}{\phi_{AW\,avg}(t)} + C_{O_2\,atm} \quad (104)$$

Determination of the expressions for the eigenvalues

$$A = \begin{bmatrix} \frac{-k_1 \cdot D_L - \phi_{AW\,avg}(t)}{V_{A\,gem}} & \frac{D_L \cdot k_7}{V_b} \\ \frac{D_L \cdot k_1}{V_{A\,gem}} & \frac{-D_L \cdot k_7}{V_b} \end{bmatrix}$$

$$A = \begin{bmatrix} \frac{-k_1 \cdot D_L - \phi_{AW\,avg}(t)}{V_{A\,gem}} - \lambda & \frac{D_L \cdot k_7}{V_b} \\ \frac{D_L \cdot k_1}{V_{A\,gem}} & \frac{-D_L \cdot k_7}{V_b} - \lambda \end{bmatrix}$$

$$\left(\frac{-k_1 \cdot D_L - \phi_{AW\,avg}(t)}{V_{A\,gem}} - \lambda\right) \cdot \left(\frac{-D_L \cdot k_7}{V_B} - \lambda\right) - \left(\frac{D_L \cdot k_7}{V_B}\right) \cdot \left(\frac{D_L \cdot k_1}{V_{A\,gem}}\right) = 0 \quad (105)$$

$$\frac{-k_1 \cdot D_L - \phi_{AW\,avg}(t)}{V_{A\,gem}} \cdot \frac{-D_L \cdot k_7}{V_b} - \lambda \cdot \frac{-k_1 \cdot D_L - \phi_{AW\,avg}(t)}{V_{A\,gem}} - \lambda \cdot \frac{-D_L \cdot k_7}{V_b} + \lambda^2 - \frac{D_L \cdot k_7}{V_b} \cdot \frac{D_L \cdot k_1}{V_{A\,gem}} = 0 \quad (106)$$

$$\lambda^2 + \lambda\left(\frac{k_1 \cdot D_L + \phi_{AW\,avg}(t)}{V_{A\,gem}} + \frac{D_L \cdot k_7}{V_b}\right) + \frac{-k_1 \cdot D_L - \phi_{AW\,avg}(t)}{V_{A\,gem}} \cdot \frac{-D_L \cdot k_7}{V_b} - \frac{D_L \cdot k_7}{V_b} \cdot \frac{D_L \cdot k_1}{V_{A\,gem}} = 0 \quad (107)$$

$$\lambda^2 + \lambda\left(\frac{k_1 \cdot D_L + \phi_{AW\,avg}(t)}{V_{A\,gem}} + \frac{D_L \cdot k_7}{V_b}\right) + \frac{-k_1 \cdot D_L}{V_{A\,gem}} \cdot \frac{-D_L \cdot k_7}{V_b} + \frac{-\phi_{AW\,avg}(t)}{V_{A\,gem}} \cdot \frac{-D_L \cdot k_7}{V_b} - \frac{D_L \cdot k_7}{V_b} \cdot \frac{D_L \cdot k_1}{V_{A\,gem}} = 0 \quad (108)$$

$$\lambda^2 + \lambda\left(\frac{k_1 \cdot D_L + \phi_{AW\,avg}(t)}{V_{A\,gem}} + \frac{D_L \cdot k_7}{V_b}\right) + \frac{\phi_{AW\,avg}(t)}{V_{A\,gem}} \cdot \frac{D_L \cdot k_7}{V_b} = 0 \quad (109)$$

$$\lambda = \frac{-\left(\frac{k_1 \cdot D_L + \phi_{AW\,avg}(t)}{V_{A\,gem}} + \frac{D_L \cdot k_7}{V_b}\right) \pm \sqrt{\left(\frac{k_1 \cdot D_L + \phi_{AW\,avg}(t)}{V_{A\,gem}} + \frac{D_L \cdot k_7}{V_b}\right)^2 - 4 \cdot \frac{\phi_{AW\,avg}(t)}{V_{A\,gem}} \cdot \frac{D_L \cdot k_7}{V_b}}}{2} \quad (110)$$

Two different eigenvalues are found.

$$\begin{bmatrix}\lambda_1 \\ \lambda_2\end{bmatrix} = \begin{bmatrix} -\frac{1}{2}\left(\frac{k_1 \cdot D_L + \phi_{AW\,avg}(t)}{V_{A\,gem}} + \frac{D_L \cdot k_7}{V_b}\right) + \frac{1}{2}\sqrt{\left(\frac{k_1 \cdot D_L + \phi_{AW\,avg}(t)}{V_{A\,gem}} + \frac{D_L \cdot k_7}{V_b}\right)^2 - 4 \cdot \frac{\phi_{AW\,avg}(t)}{V_{A\,gem}} \cdot \frac{D_L \cdot k_7}{V_b}} \\ -\frac{1}{2}\left(\frac{k_1 \cdot D_L + \phi_{AW\,avg}(t)}{V_{A\,gem}} + \frac{D_L \cdot k_7}{V_b}\right) - \frac{1}{2}\sqrt{\left(\frac{k_1 \cdot D_L + \phi_{AW\,avg}(t)}{V_{A\,gem}} + \frac{D_L \cdot k_7}{V_b}\right)^2 - 4 \cdot \frac{\phi_{AW\,avg}(t)}{V_{A\,gem}} \cdot \frac{D_L \cdot k_7}{V_b}} \end{bmatrix}$$

The associated time constants can be determined by taking the absolute value of the inverse of the eigenvalues.

$$\begin{bmatrix}\tau_1 \\ \tau_2\end{bmatrix} = \begin{bmatrix} \left|\frac{2}{-\left(\frac{k_1 \cdot D_L + \phi_{AW\,avg}(t)}{V_{A\,gem}} + \frac{D_L \cdot k_7}{V_b}\right) + \sqrt{\left(\frac{k_1 \cdot D_L + \phi_{AW\,avg}(t)}{V_{A\,gem}} + \frac{D_L \cdot k_7}{V_b}\right)^2 - 4 \cdot \frac{\phi_{AW\,avg}(t)}{V_{A\,gem}} \cdot \frac{D_L \cdot k_7}{V_b}}}\right| \\ \left|\frac{2}{-\left(\frac{k_1 \cdot D_L + \phi_{AW\,avg}(t)}{V_{A\,gem}} + \frac{D_L \cdot k_7}{V_b}\right) - \sqrt{\left(\frac{k_1 \cdot D_L + \phi_{AW\,avg}(t)}{V_{A\,gem}} + \frac{D_L \cdot k_7}{V_b}\right)^2 - 4 \cdot \frac{\phi_{AW\,avg}(t)}{V_{A\,gem}} \cdot \frac{D_L \cdot k_7}{V_b}}}\right| \end{bmatrix}$$

Appendix 3: Experimental figures

Table 13 Squared norm of the residuals

	fitting	**Squared norm of the residual**
Carbon dioxide	Measurement 2 fast fitting	0.68
	Measurement 2 slow fitting	0.56
	Measurement 3 fast fitting	0.21
	Measurement 3 slow fitting	0.32
oxygen	Measurement 2 fast fitting	2.23
	Measurement 3 fast fitting	1.90

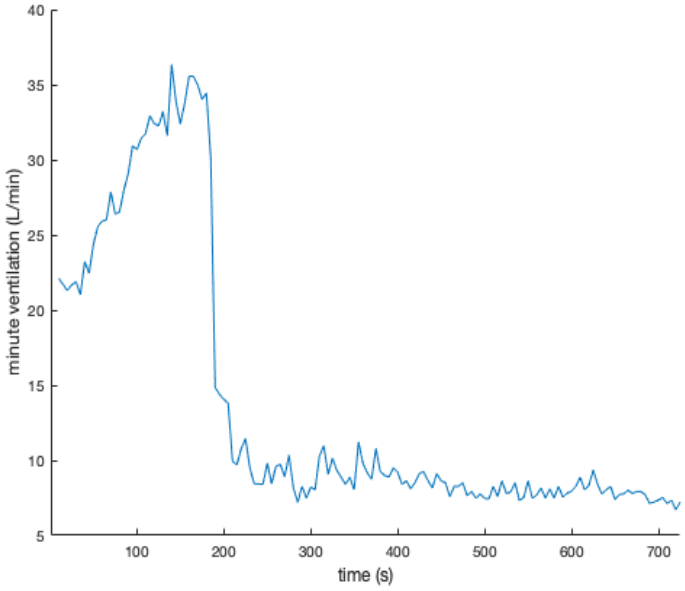

Figure 23 minute ventilation during measurement 2 (12 rpm)

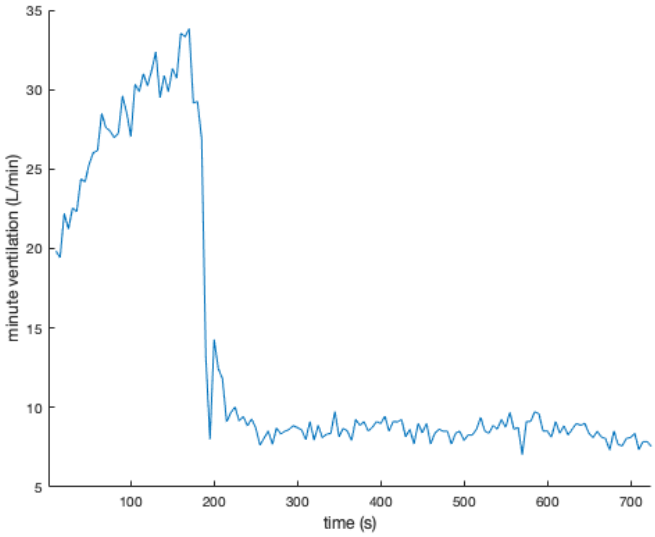

Figure 24 minute ventilation during measurement 3 (20 rpm)

Appendix 4: Conversations with clinicians

-What are the different stages of mechanical ventilation?
-What are the variables that are important to control during each stage?
-What are the variables that are important to observe during each stage?
-How and how often are these variables measured during each stage?
-What difficulties arise in measuring these variables?
-What are the parameters that are important to identify during each stage?
-How and how often are these parameters identified during each stage?
-What difficulties arise in identifying these parameters?
-What are the important ventilator settings the need to be chosen during each stage?
-What difficulties arise in choosing these ventilator settings?
-How does the clinician determine when a patient can move to the next stage?
-What other difficulties arise during each stage?
-What role could a model of the physiology of breathing play in alleviating these difficulties?
-What part of the physiology of breathing are important to include in the model?